Adding multi-objective optimisation capability to an electricity utility energy flow simulator

Ryno Ockert Brits

Department of Industrial Engineering

Stellenbosch University

Study leader: James Bekker

Thesis presented in partial fulfilment of the requirements for the degree of Master of Engineering in the Faculty of Engineering at Stellenbosch University

M. Eng Industrial (Research)

March 2016

Declaration

By submitting this thesis electronically, I declare that the entirety of the work contained therein is my own, original work, that I am the sole author thereof (save to the extent explicitly otherwise stated), that reproduction and publication thereof by Stellenbosch University will not infringe any third party rights and that I have not previously in its entirety or in part submitted it for obtaining any qualification.

Date: March 2016

Abstract

The energy flow simulator (EFS) is a strategic decision support tool that was developed for the South African national electricity utility Eskom. The advanced set of algorithms incorporated into the EFS enables various departments within Eskom to simulate and analyse the Eskom value chain from primary energy to end-use over a certain study horizon. The research in this thesis is aimed at determining whether multi-objective optimisation (MOO) capability can be added to the EFS. The study forms part of a series of research projects. This project builds on the work of Hatton (2015) in which the focus was on single-objective optimisation capability for the EFS. Inventory management at Eskom's coal-fired power stations was identified as the most suitable area for the formulation of an MOO model. It was also identified that certain modifications to the existing EFS architecture can possibly improve its potential as an optimisation tool.

The architecture of the EFS is studied and modifications to it are proposed. A multi-objective inventory model is then formulated for Eskom's network of coal-fired power stations using the simulation outputs of the EFS. The model is based on the movement of coal between the various power stations in an attempt to maintain an optimal inventory level at each station as far as possible. To solve the model, a suitable MOO algorithm is selected and integrated with the simulation component of the EFS. Several experiments are conducted to validate the MOO model and test the effectiveness of the algorithm in solving the optimisation problem.

Opsomming

Die energievloei-simulator (EVS) is 'n strategiese besluitondersteuningsinstrument wat ontwikkel is vir die Suid-Afrikaanse nasionale elektrisiteitsverskaffer, Eskom. Die gevorderde stel algoritmes waaruit die EVS bestaan stel verskeie departemente binne Eskom in staat om die Eskom-waardeketting te simuleer en te analiseer, vanaf primêre energie tot eindgebruik, oor 'n sekere studie tydperk. Die navorsing in hierdie tesis is daarop gemik om te bepaal of meerdoelige optimeringsvermoë tot die EVS bygevoeg kan word. Die studie vorm deel van 'n reeks navorsingsprojekte. Hierdie projek bou voort op die werk van Hatton (2015) waarin die fokus op enkeldoel-optimeringsvermoë vir die EVS was. Voorraadbestuur by Eskom se steenkoolaangedrewe kragstasies is geïdentifiseer as die mees geskikte gebied vir die formulering van 'n meerdoelige optimeringsmodel. Daar is ook geïdentifiseer dat sekere veranderinge aan die bestaande argitektuur van die EVS moontlik die model se potensiaal as 'n optimeringsinstrument kan verbeter.

Die argitektuur van die EVS word bestudeer en veranderinge daaraan word voorgestel. 'n Meerdoelige voorraadbestuursmodel word daarna vir Eskom se netwerk van steenkoolaangedrewe kragstasies geformuleer deur die simulasie-uitsette van die EVS te gebruik. Die model is gebaseer op die beweging van steenkool tussen die verskillende kragstasies om 'n optimale voorraadvlak by elke stasie the probeer handhaaf. Om die model op te los word 'n geskikte meerdoelige optimeringsalgoritme gekies en met die EVS se simulasie komponent geïntegreer. Verskeie eksperimente word uitgevoer om te bevestig dat die meerdoelige optimeringsmodel korrek is en om die doeltreffendheid van die algoritme as oplossingsmetode vir die probleem te toets.

Contents

Declaration ii

Abstract iii

Opsomming iv

1 Introduction 1

1.1 Background to the study . . . 1
1.2 Problem statement . . . 3
1.3 Research objectives . . . 3
1.4 Structure of the document . . . 4

2 Literature: Modelling in the electricity generation industry 5

2.1 Background to Chapter 2 . . . 5
2.1.1 An introduction to electricity generation, transmission and distribution . . . 6
2.2 Electricity markets . . . 7
2.2.1 Modelling trends and techniques . . . 8
2.2.1.1 One-firm optimisation models . . . 8
2.2.1.2 Equilibrium models . . . 10
2.2.1.3 Simulation models . . . 11
2.3 Power station logistics systems . . . 12
2.3.1 Coal suppliers . . . 13
2.3.2 Coal transportation systems . . . 13
2.3.3 Coal inventory management at power stations . . . 15
2.4 Summary: Chapter 2 . . . 16

3 The energy flow simulator **17**
3.1 Background to Chapter 3 . . . 17
3.1.1 An introduction to the South African electricity generation sector . . . 17
3.1.2 Eskom's generation mix . . . 18
3.1.3 Eskom's coal supply chain . . . 20
3.2 An introduction to the energy flow simulator . . . 23
3.3 Architecture of the energy flow simulator . . . 23
3.3.1 Load forecasting . . . 24
3.3.2 Production planning . . . 25
3.3.3 Fuel planning . . . 30
3.3.4 Primary energy . . . 32
3.4 Order of simulation . . . 35
3.5 Analysis capability of the energy flow simulator . . . 36
3.6 Proposed modifications to the energy flow simulator . . . 37
3.7 Modifications to the architecture of the energy flow simulator . . . 38
3.7.1 Production planning . . . 39
3.7.2 Fuel planning . . . 43
3.7.3 Primary energy . . . 44
3.8 Verification and validation of the modified primary energy module 46
3.8.1 Verification . . . 46
3.8.2 Validation . . . 46
3.9 Summary: Chapter 3 . . . 48

4 Literature: Simulation optimisation **50**
4.1 An introduction to simulation optimisation . . . 51
4.2 Simulation optimisation techniques . . . 52
4.2.1 Classical approaches . . . 53
4.2.1.1 Discrete input parameters . . . 53
4.2.1.2 Continuous input parameters . . . 53
4.2.2 Metaheuristics . . . 54
4.3 Multi-objective simulation optimisation . . . 55
4.3.1 The multi-objective optimisation problem . . . 56

4.3.2 Approaches to multi-objective optimisation 57
4.3.3 Pareto terminology 58
4.3.4 Metaheuristics for multi-objective optimisation 59
4.4 Summary: Chapter 4 61

5 Multi-objective model formulation and solution approach 62
5.1 Background to Chapter 5 62
5.1.1 Inventory models 63
5.1.2 Why manage coal stockpiles? 65
5.1.3 Inventory management at Eskom's coal-fired power stations 66
5.2 Model formulation 68
5.2.1 Decision variables 68
5.2.2 Objective functions 74
5.3 Solution approach 75
5.3.1 The cross-entropy method for multi-objective optimisation 77
5.3.2 Existing research and applications of the cross-entropy method for multi-objective optimisation 83
5.3.3 The cross-entropy method for multi-objective optimisation applied to this study 84
5.3.3.1 Integration with the primary energy module . . . 84
5.3.3.2 Parameter settings 86
5.4 Summary: Chapter 5 86

6 Experiments and results 88
6.1 Baseline inputs to the energy flow simulator 88
6.2 Simulation settings for the primary energy module 92
6.3 Overview of experiments 92
6.4 Testing the two model formulations with both coal transfer policies 94
6.4.1 Experimental design 94
6.4.2 Results for the first model formulation 95
6.4.3 Results for the second model formulation 100
6.5 Adding additional constraints to the model 105
6.5.1 Experimental design 105
6.5.2 Results 107

6.6 Varying the coal transfer matrix . . . 110
6.6.1 Experimental design . . . 110
6.6.2 Results . . . 112
6.7 Varying input parameters of the primary energy module . . . 113
6.7.1 Experimental design . . . 113
6.7.2 Results . . . 115
6.8 Findings made from the experimental results . . . 117
6.9 Summary: Chapter 6 . . . 118

7 Summary and conclusions **120**
7.1 Project summary . . . 120
7.2 Value of the study . . . 122
7.3 Suggestions for future research . . . 122
7.4 Value gained by the researcher . . . 124

References **136**

A Additional experimental results **137**
A.1 Experiment 1 . . . 138
A.2 Experiment 2 . . . 148
A.3 Experiment 3 . . . 160

List of Figures

3.1 Distribution of power stations in South Africa. 21
3.2 Major coalfields in South Africa. 22
3.3 Existing EFS structure and primary information flows. 24
3.4 Conceptual diagram of the PE module. 35
3.5 Monthly compared to daily simulation resolution. 38
3.6 Variation exhibited by the modified PE module. 48

4.1 Integration of a simulation model and optimisation technique. . . . 52
4.2 MOO mapping. 57
4.3 Pareto front explained for two minimised objectives. 59

5.1 Characteristics of the (s, S) inventory process. 65
5.2 The monetary value of coal inventory on hand. 68
5.3 Two hypothetical scenarios for extreme variation between coal delivery and burn. 70
5.4 Hypothetical scenario for typical variation between coal delivery and burn. 70
5.5 Characteristics of the coal transfer functions. 73
5.6 Example of a histogram for the decision variable x_i. 79
5.7 Example of an inverted histogram. 80
5.8 Integration of the PE module and the MOO CEM algorithm. . . . 85

6.1 Pareto fronts achieved for model 1 with the two transfer policies, expected value as output statistic. 95

6.2 A comparison of the Pareto fronts achieved for model 1 with (a) the closest first transfer policy and (b) the most urgent transfer policy when different output statistics are used. 96
6.3 Ranges of the T_s values achieved for model 1 with (a) the closest first transfer policy and (b) the most urgent transfer policy, expected value as output statistic. 97
6.4 Pareto fronts achieved for model 2 with the two transfer policies, expected value as output statistic 100
6.5 A comparison of the Pareto fronts achieved for model 2 with (a) the closest first transfer policy and (b) the most urgent transfer policy when different output statistics are used. 101
6.6 Ranges of the T_s values achieved for model 2 with (a) the closest first transfer policy and (b) the most urgent transfer policy, expected value as output statistic. 102
6.7 Pareto fronts achieved for Experiment 2.1 and Experiment 2.2. . . 107
6.8 Pareto fronts achieved for Experiment 2.3 and Experiment 2.4. . . 107
6.9 Pareto fronts achieved for Experiment 2.5 and Experiment 2.6. . . 108
6.10 Pareto fronts achieved for Experiment 3.1 and Experiment 3.2. . . 112
6.11 Pareto fronts achieved for Experiment 4.1 and Experiment 4.2. . . 115
6.12 Pareto fronts achieved for Experiment 4.3 and Experiment 4.4. . . 116

A.1 Progression of the values of $\hat{\mu}_i$ for the variables $x_i = L_s$, model 1 with the closest first transfer policy. 138
A.2 Progression of the values of $\hat{\sigma}_i$ for the variables $x_i = L_s$, model 1 with the closest first transfer policy. 138
A.3 Progression of the values of $\hat{\mu}_i$ for the variables $x_i = T_s - L_s$, model 1 with the closest first transfer policy. 139
A.4 Progression of the values of $\hat{\sigma}_i$ for the variables $x_i = T_s - L_s$, model 1 with the closest first transfer policy. 139
A.5 Progression of the values of $\hat{\mu}_i$ for the variables $x_i = U_s - T_s$, model 1 with the closest first transfer policy. 140
A.6 Progression of the values of $\hat{\sigma}_i$ for the variables $x_i = U_s - T_s$, model 1 with the closest first transfer policy. 140

A.7 Progression of the values of $\hat{\mu}_i$ for the variables $x_i = L_s$, model 2 with the closest first transfer policy. 141
A.8 Progression of the values of $\hat{\sigma}_i$ for the variables $x_i = L_s$, model 2 with the closest first transfer policy. 141
A.9 Progression of the values of $\hat{\mu}_i$ for the variables $x_i = T_s - L_s$, model 2 with the closest first transfer policy. 142
A.10 Progression of the values of $\hat{\sigma}_i$ for the variables $x_i = T_s - L_s$, model 2 with the closest first transfer policy. 142
A.11 Progression of the values of $\hat{\mu}_i$ for the variables $x_i = U_s - T_s$, model 2 with the closest first transfer policy. 143
A.12 Progression of the values of $\hat{\sigma}_i$ for the variables $x_i = U_s - T_s$, model 2 with the closest first transfer policy. 143

List of Tables

3.1 Eskom's base load power stations. 19
3.2 Eskom's peak demand power stations. 20
3.3 Index values for the power stations. 26
3.4 Units of measurement for the parameters in the PP module. 28
3.5 Units of measurement for the parameters in the FP module. 31
3.6 Analysis capability of the EFS. 36

5.1 Working matrix of the MOO CEM algorithm. 85
5.2 Parameter settings for the MOO CEM algorithm. 86

6.1 Baseline variation for the PE module. 89
6.2 Baseline coal transfer matrix. 90
6.3 Distance matrix for the coal-fired power stations (km). 91
6.4 Approximation of the objective function values for a good solution of model 1 with both transfer policies, expected value as output statistic. 98
6.5 Approximation of the decision variable values for a good solution of model 1 with both transfer policies, expected value as output statistic. 99
6.6 Approximation of the objective function values for a good solution of model 2 with both transfer policies, expected value as output statistic. 103
6.7 Approximation of the decision variable values for a good solution of model 2 with both transfer policies, expected value as output statistic. 104

6.8 Experimental design for Experiment 2. 106
6.9 Modified coal transfer matrix for Experiment 3. 111
6.10 Experimental design for Experiment 3. 112
6.11 Sampling distribution ranges for Experiment 4. 114
6.12 Experimental design for Experiment 4. 114

A.1 Coal transfers recorded for a good solution of model 1 with the closest first coal transfer policy, expected value as output statistic (ktonnes). 144
A.2 Coal transfers recorded for a good solution of model 1 with the most urgent coal transfer policy, expected value as output statistic (ktonnes). 145
A.3 Coal transfers recorded for a good solution of model 2 with the closest first coal transfer policy, expected value as output statistic (ktonnes). 146
A.4 Coal transfers recorded for a good solution of model 2 with the most urgent coal transfer policy, expected value as output statistic (ktonnes). 147
A.5 Approximation of the objective function values for a good solution of Experiment 2.1. 148
A.6 Approximation of the decision variable values for a good solution of Experiment 2.1. 148
A.7 Coal transfers recorded for a good solution of Experiment 2.1 (ktonnes). 149
A.8 Approximation of the objective function values for a good solution of Experiment 2.2. 150
A.9 Approximation of the decision variable values for a good solution of Experiment 2.2. 150
A.10 Coal transfers recorded for a good solution of Experiment 2.2 (ktonnes). 151
A.11 Approximation of the objective function values for a good solution of Experiment 2.3. 152

A.12 Approximation of the decision variable values for a good solution of Experiment 2.3. . . . 152
A.13 Coal transfers recorded for a good solution of Experiment 2.3 (ktonnes). . . . 153
A.14 Approximation of the objective function values for a good solution of Experiment 2.4. . . . 154
A.15 Approximation of the decision variable values for a good solution of Experiment 2.4. . . . 154
A.16 Coal transfers recorded for a good solution of Experiment 2.4 (ktonnes). . . . 155
A.17 Approximation of the objective function values for a good solution of Experiment 2.5. . . . 156
A.18 Approximation of the decision variable values for a good solution of Experiment 2.5. . . . 156
A.19 Coal transfers recorded for a good solution of Experiment 2.5 (ktonnes). . . . 157
A.20 Approximation of the objective function values for a good solution of Experiment 2.6. . . . 158
A.21 Approximation of the decision variable values for a good solution of Experiment 2.6. . . . 158
A.22 Coal transfers recorded for a good solution of Experiment 2.6 (ktonnes). . . . 159
A.23 Approximation of the objective function values for a good solution of Experiment 3.1. . . . 160
A.24 Approximation of the decision variable values for a good solution of Experiment 3.1. . . . 160
A.25 Coal transfers recorded for a good solution of Experiment 3.1 (ktonnes). . . . 161
A.26 Approximation of the objective function values for a good solution of Experiment 3.2. . . . 162
A.27 Approximation of the decision variable values for a good solution of Experiment 3.2. . . . 162

A.28 Coal transfers recorded for a good solution of Experiment 3.2 (ktonnes). 163

Nomenclature

Roman Symbols

$\bar{R}$	Total average coal inventory outside the warning limits
$\bar{S}$	Total average coal stockpile level
CV_s	Calorific value of the coal at power station s
EAF_{sd}	Energy availability factor for power station s on day d
EAF_{sm}	Energy availability factor for power station s during month m
$\mathrm{EUF}_s^{(\max)}$	Maximum energy utilisation factor for power station s
$\mathrm{EUF}_s^{(\min)}$	Minimum energy utilisation factor for power station s
OCLF_{sd}	Other capability loss factor for power station s on day d
OCLF_{sm}	Other capability loss factor for power station s during month m
PCLF_{sd}	Planned capability loss factor for power station s on day d

PCLF_{sm}	Planned capability loss factor for power station s during month m
$\text{UCLF}_{sd}^{(\text{s})}$	Stochastic unplanned capability loss factor for power station s on day d
UCLF_{sd}	Unplanned capability loss factor for power station s on day d
UCLF_{sm}	Unplanned capability loss factor for power station s during month m
a_i	Decision variable lower limit
A_{sq}	Available generation capacity of power station s during time period q
$B_{sd}^{(\text{a})}$	Actual coal burnt at power station s on day d
$B_{sm}^{(\text{a})}$	Actual coal burnt at power station s during month m
$B_{sd}^{(\text{p})}$	Planned coal to be burnt at power station s on day d
$B_{sm}^{(\text{p})}$	Planned coal to be burnt at power station s during month m
b_i	Decision variable upper limit
C_s	Generation cost for power station s
D	Number of decision variables in an optimisation problem
d	Index for days
$D_{sd}^{(\text{a})}$	Actual coal delivery to power station s on day d

$D_{sm}^{(\mathrm{a})}$	Actual coal delivery to power station s during month m
$D_{sm}^{(\mathrm{p})}$	Planned coal delivery to power station s during month m
$D_{s}^{(\mathrm{p})}$	Planned daily coal delivery to power station s
d_m	Number of days in month m
E_r	Number of rows in elite vector
f	Mathematical function
F_q	Forecast demand during time period q
$G_{sd}^{(\mathrm{p})}$	Planned electricity generation at power station s on day d
$G_{sd}^{(\mathrm{a})}$	Actual electricity generation at power station s on day d
$G_{sm}^{(\mathrm{a})}$	Actual electricity generation at power station s during month m
$G_{sm}^{(\mathrm{p})}$	Planned electricity generation at power station s during month m
g_i	Mathematical function
G_{pq}	Planned electricity generation at power station s during time period q
h_j	Mathematical function
H_s	Heat rate for power station s
I_s	Installed generation capacity of power station s
K	Number of objectives in an optimisation problem

$l_s^{(\max_{\mathrm{d}})}$	Maximum daily load for power station s
$l_s^{(\max_{\mathrm{w}})}$	Maximum weekly load for power station s
$l_s^{(\min_{\mathrm{d}})}$	Minimum daily load for power station s
$l_s^{(\min_{\mathrm{w}})}$	Minimum weekly load for power station s
$l_s^{(\mathrm{req}_{\mathrm{d}})}$	Daily load requirement for power station s
$l_s^{(\mathrm{req}_{\mathrm{w}})}$	Weekly load requirement for power station s
L_s	Decision variable for the lower warning limit of power station s
M	Number of inequality constraints
m	Index for months
N	Population size for the MOO CEM algorithm
p_h	Probability of inverting MOO CEM histogram counts
Q	Number of equality constraints
q	Index for time periods in the PP module
r	Number of classes of the elite vector of the MOO CEM algorithm
s	Index for power stations
$S_{sm}^{(\mathrm{corr})}$	Stockpile correction for power station s during month m
$S_s^{(\mathrm{i})}$	Initial coal stockpile level at power station s
$S_{s,d}$	Coal stockpile level at power station s at the end of day d

$S_{s,m}$	Coal stockpile level at power station s at the end of month m
T_s	Decision variable for the target coal stockpile level of power station s
U_s	Decision variable for the upper warning limit of power station s
X_{sd}	Total distance of coal transfers from power station s on day d
$Y_{s,d}$	Coal transferred from power station s on day d
Z	Total coal transfers

Greek Symbols

α	Smoothing parameter for the MOO CEM algorithm
ϵ	Common termination threshold for the MOO CEM algorithm
κ	Histogram class index of the MOO CEM algorithm
μ_i	Mean of a distribution
Ω	Feasible region of an optimisation problem
ω	Stochastic component of a simulation model
ϕ_i	Truncated normal distribution
ρ	Rank value of multi-objective solution vector
ρ_E	Ranking threshold of the MOO CEM algorithm
$\sigma_s^{(\mathrm{CV})}$	Standard deviation for the calorific value of the coal at power station s

$\sigma_s^{(\mathrm{D})}$	Standard deviation of the coal delivery to power station s
$\sigma_s^{(\mathrm{UCLF})}$	Standard deviation of the unplanned capability loss factor for power station s
σ_i	Standard deviation of a distribution
Θ	The complete input domain of an optimisation problem
θ	Input vector to an optimisation problem

Other Symbols

$\mathbb{E}$	Mathematical expectation
$\mathbb{Z}$	Set of all integers
$\mathcal{D}$	Set of indices for days
$\mathcal{M}$	Set of indices for months
$\mathcal{Q}$	Set of indices for time periods in the PP module
$\mathcal{S}$	Set of indices for power stations
τ_{ij}	MOO CEM histogram frequency count, decision variable i, class j
$\mathbf{C}_i$	MOO CEM algorithm histogram class boundaries of decision variable x_i
$\mathbf{W}$	Working matrix of the MOO CEM algorithm

Acronyms

CEM	Cross-entropy method
CV	Calorific value

EFS	Energy flow simulator
ELD	Economic load dispatch
EOQ	Economic order quantity
FP	Fuel planning
GDP	Gross domestic product
IPP	Independent power producer
ISO	Independent system operator
kg	kilogram
km	kilometre
ktonnes	kilotonnes
LF	Load forecasting
LP	Linear program
MCP	Market clearing price
MJ	Megajoule
MOO	Multi-objective optimisation
MOO CEM	Multi-objective optimisation using the cross-entropy method
MW	Megawatt
MWh	Megawatt-hours
OCGT	Open-cycle gas turbine
pdf	probability density function
PE	Primary energy

PP	Production planning
R	R programming language
RTS	return-to-service
SDB	Standard daily burn
SFE	Supply function equilibrium
SO	Simulation optimisation
UC	Unit commitment
USA	United States of America
VRP	Vehicle routing problem
ZAR	South African rand

Chapter 1

Introduction

This chapter serves as an introduction to the research problem being addressed in this thesis. A background to the study is provided, followed by a formal problem statement and the research objectives. The chapter is concluded with a summary of the document structure.

1.1 Background to the study

The continued evolution of civilizations is highly dependent on a secure and accessible supply of energy and, as the human population continues to grow, global energy demand will continue to increase (Asif & Muneer, 2007). Electricity utilities are at the forefront of global energy supply. Successful planning in and operation of these utilities are essential to sustain economies all over the world.

In South Africa, approximately 95% of the country's electricity is provided by the state-owned electricity utility Eskom (Eskom Holdings SOC Ltd, 2014d). The utility is vertically integrated and performs generation, transmission and distribution functions. South Africa's electricity supply sector is currently confronted with serious challenges. A very tight demand/supply balance exists and the distribution segment is facing serious financial difficulties.

However, this was not always the case. A massive capacity expansion programme during the 1970s and 1980s led to a period of electricity surplus and in the two decades that followed, Eskom could supply some of the lowest priced

electricity in the world. In the years following the end of apartheid, the country carried out a national electrification programme which more than doubled the percentage of South African residents connected to electricity supply. No capacity expansion during that period and a failed attempt by government to decentralise the country's electricity sector in the late 1990s resulted in a tremendous amount of pressure on Eskom by the turn of the century (Baker, 2011; Kessides *et al.*, 2007).

In 2005 Eskom embarked on another capacity expansion programme which included the construction of two large coal-fired power stations (Kusile in Mpumalanga and Medupi in Limpopo province) and one hydroelectric pumped storage scheme (Ingula on the border of KwaZulu-Natal and the Free State). The programme also included the recommissioning of three coal-fired power stations that had previously been taken out of operation (Baker, 2011). The pressure on the already constrained system intensified rapidly, however, and, regardless of several demand-side management programmes, the country reached an electricity crisis in 2008. Eskom was forced to introduce load shedding and in the subsequent years, the system remained heavily constrained.

The problems that the South African electricity supply sector is currently experiencing have placed an even greater emphasis on effective operations planning within Eskom. In an attempt to assist with this, an energy flow simulator (EFS) was developed by an industry partner of Eskom. The EFS is a strategic decision support tool in which the Eskom value chain is modelled. The advanced set of algorithms incorporated into the EFS enables various departments within Eskom to simulate and analyse the Eskom value chain from primary energy to end-use over a certain study horizon. The *what-if* analysis that the EFS allows for, provides a way of planning for unexpected events and disturbances.

Even though the EFS incorporates an optimisation component, the values of many variables chosen by the Eskom management are known to be sub-optimal. The EFS is thus not an optimisation tool. This lack of optimisation capability is the foundation of this study. The research in this thesis forms part of a series of research projects. This project builds on the work of Hatton (2015) in which the focus was on *single-objective optimisation* capability for the EFS. He identi-

fied that inventory management at Eskom's coal-fired power stations is the most suitable area for the formulation of an optimisation model within the EFS.

1.2 Problem statement

The ability of a coal-fired power station to meet its generation targets is influenced by the bottleneck that is created during periods of coal shortage. The simulation outputs of the EFS allow for the formulation of a multi-objective coal inventory model. By successfully formulating such a model and integrating an optimisation algorithm with the EFS to solve the model, a significant contribution can possibly be made to a problem that Eskom has faced for many years, namely establishing an optimal inventory management policy.

1.3 Research objectives

The main objective of this study is to determine whether *multi-objective optimisation* (MOO) capability can be added to the EFS through the formulation of a coal inventory model. As this study forms part of the bigger EFS project, which is currently still a work-in-progress, a secondary objective is to propose modifications to the existing EFS architecture to improve its potential as an optimisation tool.

The following research tasks need to be performed to achieve the research objectives:

1. Study relevant literature on modelling in the electricity generation industry.
2. Study the existing architecture of the EFS, propose modifications to it and subsequently modify it.
3. Study literature on *simulation optimisation* (SO) and MOO.
4. Formulate a multi-objective coal inventory model for the EFS and identify a suitable MOO algorithm to solve the model.
5. Integrate the MOO algorithm with the EFS.

6. Perform experiments to validate the multi-objective SO model and test the effectiveness of the MOO algorithm in solving the model.

7. Document the findings made from the experimental results and provide recommendations for future research.

8. Master the R programming language and the document preparation system LaTeX.

1.4 Structure of the document

This chapter is an introduction to the research study. It provides a background to the study and gives the formal problem statement and the research objectives.

In **Chapter 2**, an introductory literature study on modelling in the electricity generation industry is presented. The focus is on electricity markets and power station logistics systems.

Chapter 3 introduces the South African electricity generation sector as well as Eskom's generation mix and coal supply chain. This is followed by detailed descriptions of the existing EFS architecture and the proposed modifications to it.

Chapter 4 is a literature study on SO. The aim of the study is to gain sufficient knowledge of SO, specifically in the MOO context, in order to proceed to the formulation of the MOO model.

The background to **Chapter 5** includes literature on inventory models, a discussion of the importance of managing coal stockpiles and an overview of Eskom's inventory management policy. Thereafter, the proposed multi-objective inventory model is presented and the solution approach is discussed.

The experimental design and subsequent experimental results are documented in **Chapter 6**.

Chapter 7 is a summary of the thesis in which all concluding remarks are presented.

Additional experimental results are included in **Appendix A**.

Chapter 2

Literature: Modelling in the electricity generation industry

Chapter 1 was an introduction to the problem being addressed in this thesis, namely to determine whether multi-objective optimisation (MOO) capability can be added to Eskom's energy flow simulator (EFS) through the formulation of a coal inventory model. This chapter is a literature study on modelling in the electricity generation industry.

Many studies have been conducted on the modelling of operations related to electricity supply. A short background to the chapter introduces the concepts of electricity generation, transmission and distribution. Thereafter, the focus is on electricity markets and power station logistics systems.

The aim of this chapter is not only to survey some past studies but also to gain a broad understanding of how electricity markets and power station logistics systems work.

2.1 Background to Chapter 2

The aim of this section is to introduce the concepts of electricity generation, transmission and distribution and also to provide an overview of the electricity generation technologies that will be referred to throughout the document.

2.1.1 An introduction to electricity generation, transmission and distribution

The majority of global electricity generation takes place at *thermal* and *hydroelectric* power stations. Both operate on the same principle. The electrical current is produced by wires in a coil that cuts the lines of force between the two poles of a rotating magnet. The magnet and the coil are referred to as the rotor and the stator respectively (Eskom Holdings SOC Ltd, 2014e). The rotor is coupled to a turbine that is driven by steam at thermal power stations and by water at hydroelectric power stations.

The steam used to drive a turbine at a thermal power station is produced by heating water to very high temperatures. The water is heated either by burning fossil fuels such as *coal*, *oil* and *gas*, or by the *nuclear* fission process (Eskom Holdings SOC Ltd, 2015a). Currently, more than 40% of the world's electricity is generated at coal-fired power stations. This figure does not seem that high but many countries such as South Africa (93%), Poland (92%), China (79%), India (69%) and the USA (49%) rely primarily on coal for electricity generation (Sarker *et al.*, 2014).

With regard to hydroelectric power stations, there are two types, namely *conventional hydroelectric* power stations and *pumped storage schemes*. At a conventional hydroelectric station water is conveyed through waterways from a river or from a dam in a river. The water then flows through the turbine runner to spin the shaft that is coupled to the rotor. After running through the turbine, the water is discharged back into the river to continue its course. At a pumped storage scheme, on the other hand, the water that drives the turbine is reused. Water is stored in an *upper reservoir* and, after running through the turbine, is discharged into a *lower reservoir* from where it is pumped back to the upper reservoir. Pumping usually takes place during offpeak periods in order to have maximum generation capability during peak periods (Eskom Holdings SOC Ltd, 2015b).

Most thermal and hydroelectric power stations typically have more than one *generating unit* that make up the station's *installed generation capacity*. This

installed generation capacity, measured in Megawatt (MW), can be defined as the maximum output of a power station at every moment in time while in operation.

Finding ways to generate electricity from renewable sources is becoming increasingly important all over the world. The most popular example is that of *wind turbines*. The problem, however, is that wind is not reliable because it cannot be controlled. In addition, many generating units are required for a wind energy farm to have a significant installed capacity. Another renewable, completely different approach is to convert solar radiation into direct current electricity using semiconducters. See Eskom Holdings SOC Ltd (2015c) for more detail.

From the power stations, the electricity is *transmitted* along power lines to substations and distribution stations. Before the generated electricity is fed into the transmission network, the voltage is increased using step-up transformers. Transmission happens at high voltages to make up for losses that occur over long distances and to limit the number and size of power lines required. At the substations and distribution stations, the voltage is decreased again using step-down transformers before being *distributed* to consumers (Eskom Holdings SOC Ltd, 2014f).

2.2 Electricity markets

Over the past 30 years, significant changes in the electricity industry have led to less regulated markets in many industrialised countries. Deregulation has led to more competion among electricity suppliers, each with the goal of maximising its own profits (Otero-Novas *et al.*, 2000; Ventosa *et al.*, 2005). The first country to introduce supplier competition into its electricity market was Chile, in 1982. England, Wales and Norway followed in 1990 (Anuta *et al.*, 2014). Prior to this, electricity markets were characterised by regional monopolies run either by public utilities or by private enterprises (Boom, 2003).

Electricity markets are complex for three main reasons, namely electricity cannot be stored on a large scale; a physical link is required for its transportation; and an electricity market is, similar to many other markets, characterised by an uncertain demand. Suppliers competing in the same market must use the same transmission and distribution network, and all supply flowing into the network

and all demand flowing out of the network must be balanced at all times. Failing to preserve the balance will cause the entire network to collapse (Boom, 2003; Möst & Keles, 2010).

2.2.1 Modelling trends and techniques

Researchers have for many years attempted to use models to solve problems releted to electricity markets. By surveying the most relevant publications on electricity market modelling, Ventosa *et al.* (2005) identified three major trends, namely *one-firm optimisation models*, *equilibrium models* and *simulation models*. One-firm optimisation models typically focus on maximising profit for one participant competing in the market while considering a set of technical and economic constraints. These models, which are well suited to short-term studies, are able to deal with difficult and detailed problems. In many cases the other participants competing in the market are not considered. In contrast, equilibrium models generally focus on simultaneously maximising profit for each participant competing in the market. In these models, overall market behaviour is modelled and competition among participants is taken into account. Equilibrium models are well suited to long-term studies because there is a lower demand for detailed modelling capability while the response of all competing participants is more significant. When electricity markets are too complex to address with equilibrium models, simulation models can be used as an alternative.

2.2.1.1 One-firm optimisation models

Optimisation as a modelling tool is often used by electricity market participants to determine *optimal bidding strategies*. In many deregulated electricity markets, pool trading takes place in which each competing supplier is faced with the challenge of submitting a supply bid to an independent system operator (ISO). The role of the ISO is to determine the winning bid as well as a uniform market clearing price (MCP) (David & Wen, 2000; Zhang *et al.*, 1999). There are typically three approaches that suppliers can follow to determine optimal bidding strategies. The first approach involves estimating the MCP and offering a price that is a little cheaper than the MCP. The second approach is based on estimations

of the bidding behaviour of rival participants. The third approach is based on methods and techniques from game theory.

In most deregulated markets, strategic bidding initially took place mainly on the supply side but in recent years, demand-side bidding has also gained importance. The structure of some electricity markets has evolved to the extent that large consumers and electricity distributors can also submit bids (David & Wen, 2000). Several publications are available on strategic bidding in electricity markets. Mielczarski *et al.* (1999) give a good overview of bidding strategies by analysing the typical bidding behaviour of electricity suppliers in the Australian market. David & Wen (2000) presented a literature survey of strategic bidding in competitive electricity markets based on more than 30 research publications. García *et al.* (1999) describe a general methodology for bidding in deregulated markets. Also see Fleten & Pettersen (2005), Kazempour *et al.* (2015) and Sarkhani *et al.* (2014) for practical examples related to strategic bidding in recent publications.

Another application of optimisation models in electricity markets is related to *unit commitment* (UC) (Marcovecchio *et al.*, 2014; Rahman *et al.*, 2014). Electricity suppliers encounter the UC problem when they have to decide which generating units to commit or decommit over a study horizon. This can include generating units in a single power station or in multiple power stations, typically of the same type (e.g. thermal). The objective of the UC problem is to, within generation limits, meet the expected demand and provide a specific margin of operating reserve at the minimum operating cost. Depending on the formulation of the problem, the cost function can include fuel costs, maintenance costs, and startup and shutdown costs (Dogra *et al.*, 2014; Hao *et al.*, 1997; Rahman *et al.*, 2014). The UC problem has been studied for several decades. Padhy (2004) presented an in-depth survey of the different optimisation approaches that have been proposed for the problem since the 1960s.

An extension of the UC problem is the *economic load dispatch* (ELD) problem (Roy *et al.*, 2014; Singh *et al.*, 2014; Subathra *et al.*, 2014). It involves solving the UC problem and then scheduling the outputs of the committed generating units in order to meet the total expected demand plus transmission losses at a

minimum operating cost. This must be done in such a way that all the unit and system equality and inequality constraints are satisfied (Dogra *et al.*, 2014).

A more complicated version of the ELD problem is the *short-term hydrothermal coordination* problem (Beltran & Heredia, 1999; Ramirez & Oñate, 2006). It differs from the ELD problem in that the supplier's generation mix includes thermal and hydroelectric power stations. The objective of minimising the total operating cost remains the same. However, the challenge arises from the fact that hydroelectric power stations present additional, and different, constraints to thermal power stations. The study horizon is typically between one day and one week (Farhat & El-Hawary, 2009).

2.2.1.2 Equilibrium models

In deregulated electricity markets, equilibrium models, which have a close relation to game theory, seek to explain the behaviour of each participant competing in the market. In these models, market participants are mostly suppliers. Searching for market equilibrium is essential for participants and for the ISO. Each participant is concerned with setting its own strategies and goals while the ISO is concerned with security of supply to the market (Alikhanzadeh *et al.*, 2011). Ventosa *et al.* (2005) mention a few major uses for electricity market equilibruim models, namely market power analysis, market design, yearly economic planning, long-term hydrothermal coordination, capacity expansion planning and congestion management.

Several theoretical equilibrium models such as the *Stackelberg*, *Cournot*, *Bertrand*, *Supply Function Equilibrium* (SFE) and *Conjectural Variation* models are available (Abeygunawardana *et al.*, 2008). The Stackelberg model is appropriate for conditions in which smaller firms can only follow the behaviour of a large dominant firm. The Bertrand, Cournot, SFE and Conjectural Variation models, on the other hand, are appropriate when a market is more competitive (Alikhanzadeh *et al.*, 2011).

In the Cournot model, suppliers compete on supply quantity strategies as opposed to the Bertrand model where they compete on supply price strategies.

The Cournot model is a popular choice because, owing to its simplicity, computation is easy in many cases. However, the model assumes that competitors do not respond to price changes. In the Bertrand model, each supplier first sets its supply price and then supply whatever quantity is required. The model gives any supplier the opportunity to capture the entire market by setting its price below that of the competitors. This seems unrealistic in view of increasing marginal costs and the limited installed capacity of electricity suppliers. In markets where suppliers submit a supply function bid for each generating unit, the assumptions of the Cournot and Bertrand models may not be appropriate. SFE models, where suppliers compete on offer curve strategies, have thus been selected as the basis of many electricity market models (Abeygunawardana *et al.*, 2008; Alikhanzadeh *et al.*, 2011; Ventosa *et al.*, 2005). The SFE model is an evolution of the Cournot model (see Baldick (2002) for a comparison of the Cournot and SFE models of bid-based electricity markets). The Conjectural Variation model is an extension to the Cournot model. In comparison, it is more accurate and flexible. The model expects future reactions of competitors and its estimates are based on unilateral changes in output (Alikhanzadeh *et al.*, 2011).

2.2.1.3 Simulation models

The equilibrium models discussed in 2.2.1.2 are all based on the formal definition of equilibrium, which is mathematically expressed as a set of algebraic and/or differential equations. This holds two major disadvantages when very complex markets are modelled. First, the representation of competition among participants is limited and secondly, the set of equations is often too hard to solve. In cases where these problems occur, simulation models can be used as an alternative. Simulation models typically involve setting sequential rules to represent each participant's strategic decision dynamics. The flexibility of being able to implement almost any kind of strategic behaviour is a great advantage of the simulation approach (Ventosa *et al.*, 2005).

According to Otero-Novas *et al.* (2000) the simulation of an electricity market must consider the market structure as well as the strategies of the market participants. It should go beyond a simple optimisation that is based on the operating costs of the generating units.

Ventosa *et al.* (2005) mention that electricity market simulation models are often closely related to equilibrium models. Two examples are the models proposed by Otero-Novas *et al.* (2000) and Day & Bunn (2001). These models are based on the Cournot and the SFE schemes respectively.

Another simulation approach used for electricity markets is that of agent-based simulation models (Rastegar *et al.*, 2009; Zhou *et al.*, 2011). In these models, market participants learn from past experience, which then enables them to make improved decisions going forward (Ventosa *et al.*, 2005).

2.3 Power station logistics systems

Logistics plays a significant role in the operation of thermal power stations. Several simulation and optimisation studies have been conducted on the logistics systems and supply chains of coal-fired power stations in particular. These studies vary in that some incorporate the entire coal supply chain while others only focus on a particular part of it. Throughout this section, the terms 'power station logistics system' and 'coal supply chain' will be used interchangeably. The reason for this is that many electricity suppliers are responsible for their coal supply from the moment it leaves the suppliers. Others only take ownership of the coal upon delivery to their power stations. This section focuses on the logistics involved from the moment the coal leaves the ground until it is stored at the power station.

In their paper, Li & Li (2008) proposed a simulation and optimisation model for the logistics system of a coal-fired power station using WITNESS software. The objective was to minimise the total cost of the logistics system. The model, which was applied to a power station in China, included the coal suppliers, the coal transportation system and the power station itself. These researchers regard these as the three major components of a power station's logistics system. The selection of suppliers is critical in guaranteeing the quantity and quality of coal supply. The transportation system has many requirements and constraints that must be considered, while at the power station the coal storage systems, the coal conveying systems and the human resources must be managed.

The remainder of this section includes a discussion of coal suppliers, coal transportation systems and coal inventory management at power stations. Past studies are referred to throughout.

2.3.1 Coal suppliers

When modelling an entire coal supply chain, complexity can arise when multiple suppliers supply to a single power station. Different suppliers will almost always offer coal at different prices. The quality of the coal will also vary from supplier to supplier (Yucekaya, 2013).

Coal is extracted at either open-cast or underground mines. After extraction, the coal is processed before being stored on large stockpiles. Processing can include crushing, washing and sometimes blending, depending on the needs of the client (West, 2011). In some cases, the coal is processed at separate coal-handling facilities or even at the power stations themselves. Several studies have been conducted on the processing of coal. These include studies on coal washing (Zhang & Xia, 2014), coal blending (Jian & Shi-xin, 2013; Xi-jin *et al.*, 2009) and machine scheduling at coal-handling facilities (Conradie *et al.*, 2008; Hanoun *et al.*, 2013).

Another, completely different, type of problem encountered by coal suppliers is that of inventory management. According to West (2011) ensuring security of coal supply is the most critical factor driving the optimisation of coal supply chains. The optimisation model proposed by West (2011) demonstrates that the principal costs incurred from high coal inventory levels include working capital, holding costs and double handling costs. The uncertainty of coal demand is a major problem for coal suppliers. There is thus a need to determine optimal inventory levels at coal mines in order for them to reduce costs while still being able to always meet demand.

2.3.2 Coal transportation systems

From the mines, the coal is transported to the power stations. Depending on the terms of the supply contract, the transportation of the coal can either be the

responsibility of the mines or of the power stations. In many cases external transportation companies are used. The complexity of a coal transportation system lies in the fact that multiple transportation methods are usually involved. These typically include transportation by rail, road and conveyor systems. Transportation costs are usually dependent on the method of transportation and on the distance between supplier and client. In an ideal world, a power station should be located close to a coal mine. However, this is not usually the case since the generation and demand points should also be in close proximity of one another (Yucekaya, 2013).

Due to a lack of coal resources, many countries are forced to import coal. When this is the case, even more complexity is added to the supply chain due to the handling and storage of the coal at ports. Yabin (2010) proposed a simulation model of a coal ocean-shipping logistics system using WITNESS software. The main focus of the study was the operation of the transshipment port and the objective was to minimise the logistics cost.

Several other studies on coal transportation systems are available in scholarly literature. Two examples are the papers by Fang *et al.* (2011) and Yucekaya (2013). Fang *et al.* (2011) proposed a regional coal transportation and storage optimisation model for a coal-fired power station in China. The objective was to minimise regional transportation and storage costs. In their model, coal is transported from logistics centres or freight centres in the region to the coal-fired power station. The coal goes through the following three steps in the transportation system: storage at the logistics centres, transportation to the power station and storage at the power station. Yucekaya (2013) developed a model to minimise coal purchasing and transportation costs for a power company with more than one power station in the USA. The model considers multimode transportation alternatives, multiple products, multiple suppliers, capacity limitations on transportation routes, supplier capacity for a particular product and power station burn capability constraints.

2.3.3 Coal inventory management at power stations

While, in a typical coal supply chain, the coal suppliers and transportation companies are responsible for managing inventory levels at the mines and throughout the transportation network, the electricity suppliers are responsible for managing the coal stockpiles at their power stations. According to Zhanwu *et al.* (2011) the survival and development of coal-fired power stations are seriously influenced by the bottleneck that is created by a coal shortage. Compared to other enterprises, inventory management at coal-fired power stations has its own features and requirements due to the nature of the goods being stored. Zhanwu *et al.* (2011) mention the following as the four main features of coal inventory management:

1. **The uncertainty of coal demand:** The uncertain demand for coal at power stations is triggered by the uncertain demand for electricity. In many countries, coal demand for electricity generation varies from season to season. There are two reasons for this. First, consumers tend to use more electricity during very hot or very cold periods and secondly, hydroelectirc power stations can typically produce more electricity during wet seasons, which reduces the load placed on coal-fired power stations.

2. **The uncertainty of coal prices:** The price of coal varies over time. Similar to any other market, high demand means high prices, and vice versa.

3. **The uncertainty of inventory replenishment:** Due to weather conditions and other uncertainties within coal transportation networks, the inventory replenishment of coal is inconsistent.

4. **The requirement of safety stock:** Each of the abovementioned uncertainties emphasises the need to stockpile coal because coal shortages will result in an electricity shortage. Safety stock is an effective management tool for protecting an electricity supplier against uncertainty. However, there is a trade-off between having the ability to always provide customers with the promised service level and the costs involved in storing large amounts of coal at a power station (Ma & Lin, 2008).

Studies related to inventory management at power stations mostly involve the determination of a safety stock level. Zhanwu *et al.* (2011) proposed a practical inventory model to minimise the loss of profit. Through solving the model, reasonable safety stock could be determined. Ma & Lin (2008) presented two models, one to determine the optimal service level for a coal-fired power station and one to determine the optimal safety stock.

2.4 Summary: Chapter 2

This chapter was an introductory literature study on modelling in the electricity generation industry. The background to the chapter introduced the concepts of electricity generation, transmission and distribution. Thereafter, a section on electricity markets was included to gain some knowledge from existing literature before studying the architecture of Eskom's energy flow simulator (EFS). The section on power station logistics systems was included with an eye on the main research objective, namely to determine whether multi-objective optimisation (MOO) capability can be added to the EFS through the formulation of a coal inventory model.

A detailed description of the existing EFS as well as the proposed modifications to it follows in Chapter 3.

Chapter 3

The energy flow simulator

Chapter 2 was a literature study on modelling in the electricity generation industry. The aim of this chapter is to describe the energy flow simulator (EFS) in its current form and also to propose modifications to the EFS that can possibly improve its potential as an optimisation tool.

Background is provided on the South African electricity generation sector and on Eskom's generation mix and coal supply chain. This is followed by an introduction to the EFS and a detailed description of its existing architecture. Short sections follow in which the order of simulation and the analysis capability of the EFS are summarised. Thereafter, the proposed modifications to the EFS are described. The chapter is concluded with a section in which the modifications are verified and validated.

3.1 Background to Chapter 3

In this section, the South African electricity generation sector is briefly introduced and Eskom's generation mix and coal supply chain are described.

3.1.1 An introduction to the South African electricity generation sector

Unlike most global electricity markets, the South African electricity market is not deregulated. The state-owned electricity utility Eskom, which is the 11th largest

electricity generator in the world, provides approximately 95% of the country's electricity (Eskom Holdings SOC Ltd, 2014b,d). The other 5% is provided by municipalities and *independent power producers* (IPPs).

Eskom is also the sole transmitter of electricity in South Africa (Baker, 2011). From Eskom's power stations, electricity is fed into the national transmission grid. This high-voltage grid links the power stations to substations and distribution stations in the cities, towns and rural areas throughout the country. From there, Eskom is responsible for 60% of the distribution to consumers. The balance is distributed by municipalities after being purchased from Eskom (Baker, 2011; Eskom Holdings SOC Ltd, 2014f).

3.1.2 Eskom's generation mix

Eskom's generation mix includes a variety of power stations, all of which are classified into two categories: **base load** power stations which supply electricity around the clock, and **peak demand** power stations which can react quickly to changes in demand (Eskom Holdings SOC Ltd, 2014a).

Base load power stations are designed to operate continuously at a steady load and are generally only shut down for planned maintenance or in the case of emergency maintenance. Eskom's base load power stations include 13 coal-fired stations, which generate 93% of the electricity produced by Eskom, and one nuclear station. Three of the coal-fired stations (Camden, Grootvlei and Komati) are *return-to-service* (RTS) stations which were recommissioned in 2005 to meet the country's growing electricity demand. Two new, very large coal-fired power stations (Kusile and Medupi) are currently under construction. The introduction of this additional generation capacity will relieve the pressure on Eskom's base load stations in the near future (Eskom Holdings SOC Ltd, 2014a,d). Details of all the base load power stations are provided in Table 3.1.

Peak demand power stations are responsible for generating the additional demand placed on the system over and above the base demand. Peak demand periods in South Africa are typically in the early mornings and early evenings (Eskom Holdings SOC Ltd, 2014a). Eskom's peak demand power stations include

Table 3.1: Eskom's base load power stations.

Type	Name	Location	Installed capacity (MW)
Coal	Arnot	Middelburg, Mpumalanga	2 352
	Duvha	Witbank, Mpumalanga	3 600
	Hendrina	Hendrina, Mpumalanga	1 965
	Kendal	Witbank, Mpumalanga	4 116
	Kriel	Kriel, Mpumalanga	3 000
	Lethabo	Sasolburg, Free State	3 708
	Majuba	Volksrust, Mpumalanga	4 110
	Matimba	Lephalale, Limpopo	3 990
	Matla	Kriel, Mpumalanga	3 600
	Tutuka	Standerton, Mpumalanga	3 654
	Camden (RTS)	Ermelo, Mpumalanga	1 510
	Grootvlei (RTS)	Balfour, Mpumalanga	1 200
	Komati (RTS)	Middelburg, Mpumalanga	940
	Kusile (new)	Witbank, Mpumalanga	4 800
	Medupi (new)	Lephalale, Limpopo	4 764
Nuclear	Koeberg	Melkbosstrand, Western Cape	1 910

two conventional hydroelectric stations (Gariep and Vanderkloof), two hydroelectric pumped storage schemes (Drakensberg and Palmiet) and four *open-cycle gas turbine* (OCGT) stations (Acacia, Port Rex, Ankerlig and Gourikwa). Water as a source for electricity generation is only used for peak demand periods due to South Africa's inconsistent rainfall and limited water resources. A new pumped storage scheme (Ingula) is currently under construction and will be added to the system in the near future. The four OCGT stations are, due to their high operating cost, only employed in periods when the other stations cannot meet the demand. Acacia and Port Rex use kerosene to power their engines whereas Ankerlig and Gourikwa run on diesel (Eskom Holdings SOC Ltd, 2014a,d). Details of all the peak demand power stations are provided in Table 3.2.

Table 3.2: Eskom's peak demand power stations.

Type	Name	Location	Installed capacity (MW)
Hydro-electric	Gariep	Norvalspoort, Border of Eastern Cape and Free State	360
	Vanderkloof	Petrusville, Northern Cape	240
Pumped storage	Drakensberg	Bergville, KwaZulu-Natal	1 000
	Palmiet	Grabouw, Western Cape	400
	Ingula (new)	Border of Free State and KwaZulu-Natal	1 332
OCGT	Acacia	Cape Town, Western Cape	171
	Port Rex	East London, Eastern Cape	171
	Ankerlig	Atlantis, Western Cape	1 338
	Gourikwa	Mossel Bay, Western Cape	746

The map of South Africa shown in Figure 3.1 shows the distribution of the base load and peak demand power stations in the country. In addition to these stations, Eskom also has an experimental wind energy farm at Klipheuwel in the Western Cape. Its capacity is 3 MW. Another wind energy farm is currently under construction at Vredendal in the Western Cape. Its capacity will eventually be 100 MW (Eskom Holdings SOC Ltd, 2014d).

3.1.3 Eskom's coal supply chain

South Africa's very high reliance on coal for electricity generation is unlikely to change in the near future for two reasons, namely the lack of suitable alternatives and the country's large coal reserves (Eberhard, 2011; Eskom Holdings SOC Ltd, 2014b,d). South Africa is the fifth highest producer of hard coal in the world and also one of the five largest coal users in the world behind China, the USA, India and Japan. Altogether 53% of the coal produced by the country is used for electricity generation. The coal reserves in South Africa are estimated at

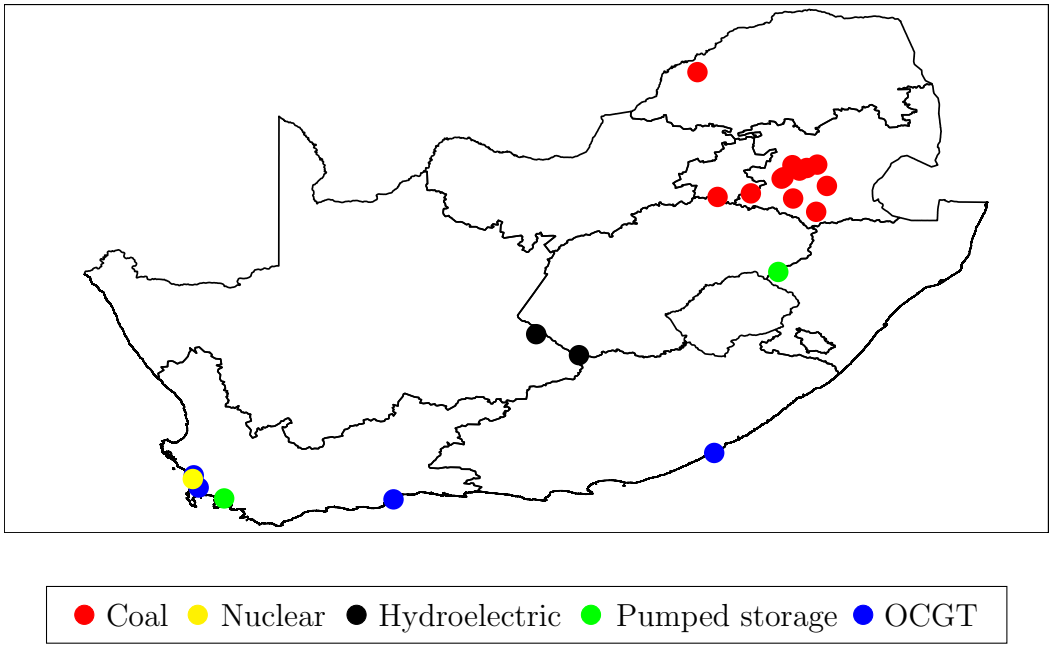

Figure 3.1: Distribution of power stations in South Africa.

53 billion tonnes and, at the current production rate, there are approximately 200 years of coal supply left in the country (Eskom Holdings SOC Ltd, 2014b).

From Figure 3.1 one can see that all Eskom's coal-fired power stations are situated in the northern parts of the country. This is no coincidence. The locations of these power stations were strategically selected to be in close proximity of South Africa's coal fields, which are mainly in the Central Basin. This includes the Witbank, Highveld and Ermelo coalfields. The Waterberg coalfield and other coalfields in Limpopo have in recent years also been explored (Eberhard, 2011). Figure 3.2 shows South Africa's major coalfields.

Eskom does not own its own mines and therefore rely on private mines for coal supply. The majority of the coal used by Eskom is produced by eight mega-mines that each produces more than 10 million tonnes per annum. Seven of these mines are in the Central Basin while the other one is in the Waterberg (Eberhard, 2011).

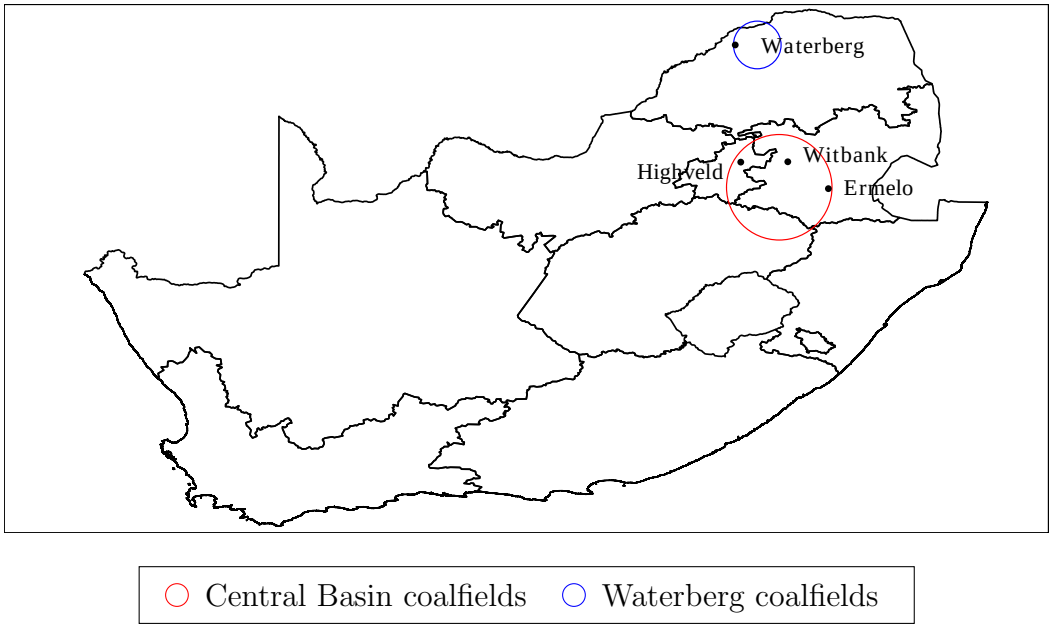

Figure 3.2: Major coalfields in South Africa.

Supply contracts with mines are mostly long term and can typically be up to 40 years. Eskom has two types of supply contracts, namely *cost-plus contracts* and *fixed-price contracts*. For cost-plus contracts, Eskom is the sole client of the mine and also pays for all mining operations. For fixed-price contracts, on the other hand, the mine has other clients besides Eskom. For these contracts, Eskom does not pay for mining operations.

The supply arrangements that Eskom has with the coal mines are increasingly under threat as mines divert higher-quality coal to the export market. This is a major concern in view of South Africa's continuous increase in electricity demand. Eskom has thus been forced into using low-grade coal with a high ash content. A high ash content in coal results in a lower thermal efficiency during combustion due to the reduced *calorific value* (CV). Calorific value refers to the amount of chemical energy released upon combustion. This problem has exposed Eskom to supplementary short-term contracts with the major coal producers and smaller mining companies (Eberhard, 2011).

The majority of Eskom's coal-fired power stations were built next to mines, which means that coal can be transported with large conveyor systems. Tutuka,

Hendrina, Grootvlei, Camden and Majuba, however, require road and/or rail transportation to move the coal from the mines. Deliveries to Tutuka, Hendrina and Grootvlei are by road while deliveries to Camden are by rail. Majuba's coal is delivered by both road (55%) and rail (45%) (Eskom Holdings SOC Ltd, 2014c). Contracts for road and rail transport are either with the mines themselves or with independent transportation companies.

3.2 An introduction to the energy flow simulator

The energy flow simulator (EFS) is a strategic decision support tool that enables various departments within Eskom to simulate and analyse the Eskom value chain from primary energy to end-use over a certain study horizon. The EFS was originally coded in the Java programming language, but after realising that it was too intricate and very complex to operate, it was converted to the statistical R programming language. The idea was that the new R version would enable members of Eskom to understand, update and modify the EFS without the need for a Java programmer.

Of the modelling trends and techniques discussed in Chapter 2, the EFS incorporates both a one-firm optimisation and a simulation component. One simulation output of the EFS is the coal stockpile levels at Eskom's coal-fired power stations. This allows for a logistics component to be added to the EFS through the formulation of a coal inventory model.

3.3 Architecture of the energy flow simulator

The EFS architecture described in this section is based on an internal Eskom report by van Harmelen *et al.* (2014).

The existing R version of the EFS consists of nine independently developed modules. The interaction between these modules and the primary information flows between them are shown in Figure 3.3. In the remainder of this section, the four primary modules, namely *load forecasting* (LF), *production planning* (PP),

fuel planning (FP) and *primary energy* (PE) are described. The inputs and outputs of the other five modules are also mentioned.

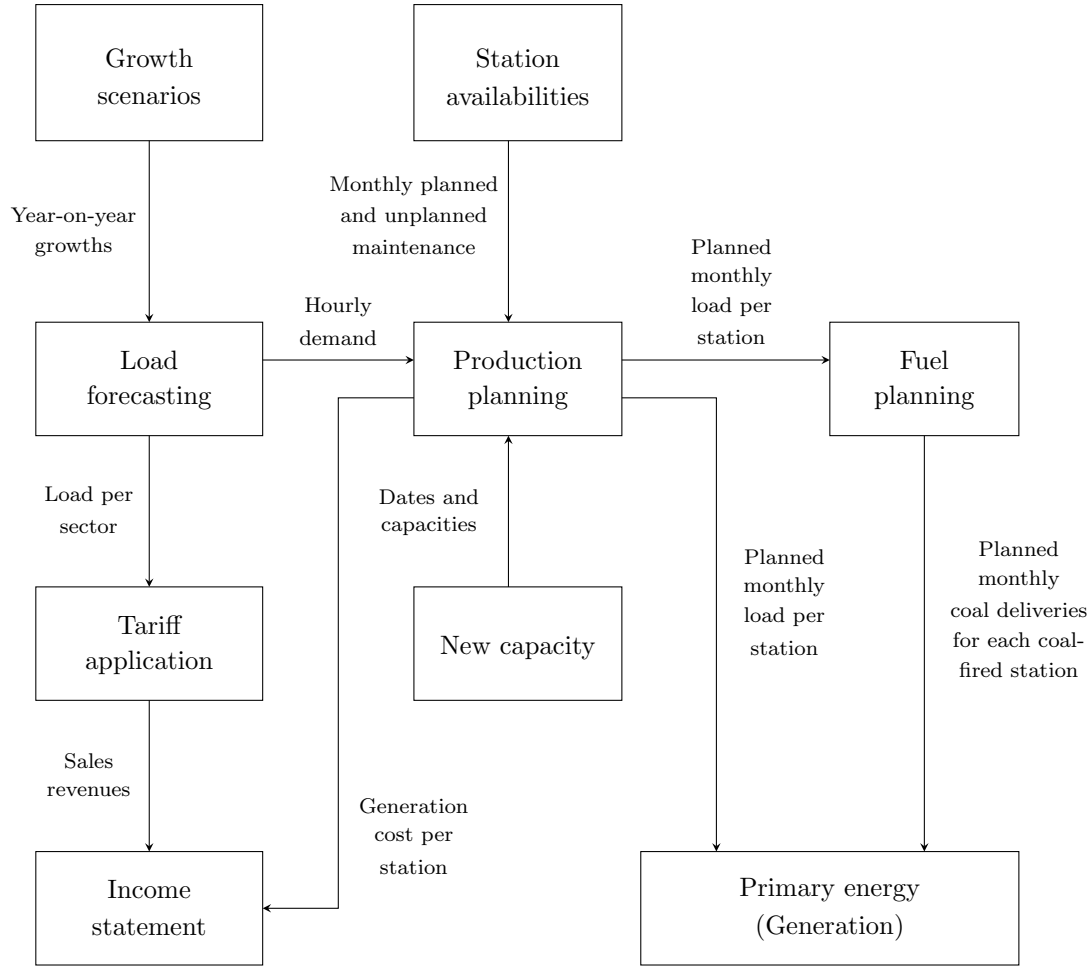

Figure 3.3: Existing EFS structure and primary information flows.

The architecture explanations that follow in Subsections 3.3.1 to 3.3.4 assume a study period of one year.

3.3.1 Load forecasting

The load forecasting (LF) module forecasts the electricity demand in South Africa for the study period. The forecast is based on a user-specified weather scenario

and a *gross domestic product* (GDP) scenario. With regard to the weather scenario (warm, normal and cold), the assumption was made that very cold and very warm weather both cause an increase in the consumption of electricity. For the GDP scenario (high, normal and low), the module assumes a correlation between electricity demand and economic growth, meaning that a high GDP results in a high electricity demand. Input data for the GDP scenarios are stored in the *growth scenarios* module.

The output of the module is the hourly electricity demand per sector for each of the three geographical zones in South Africa. There are four sectors, namely residential, manufacturing, mining and the rest. The three geographical zones are central, southern and eastern. The *tariff application* module uses the electricity tariffs for each sector to calculate revenue from electricity sales for each sector.

3.3.2 Production planning

The production planning (PP) module, which is essentially a very basic unit commitment model, is completely deterministic. It uses the country's hourly electricity demand forecast by the LF module, converts it to average weekly demand for each week, and then determines the planned weekly electricity generation at each power station for the entire study period. All base load and peak demand power stations discussed in Subsection 3.1.2 are included in the module. The user can select if and when any of the new power stations must be introduced. This is done through the *new capacity* module. The Cahora Bassa hydroelectric power station in Mozambique, from which Eskom imports electricity, is also included. In addition, a virtual power station, with a generation capacity equivalent to the total capacity of independent power producers (IPPs), is included. These two are both treated as base load power stations.

The problem of scheduling the planned electricity to be generated by each power station was formulated as a linear program (LP) with the objective of minimising the total weekly generation cost. In order to differentiate between peak and offpeak demand periods, the developers formulated the LP by sorting the hourly demand for each week in descending order. Each week is then divided

into 14 time periods of 12 hours each. The first seven are treated as peak demand periods while the second seven are treated as offpeak demand periods.

The LP's decision variable is defined as

$$G_{sq} = \text{planned electricity generation at power station } s \text{ during time period } q \tag{3.1}$$

where $s \in \mathcal{S} = \{1, \ldots, 32\}$ and $q \in \mathcal{Q} = \{1, \ldots, 14\}$.

The index values for the power stations are provided in Table 3.3. The reason for the 16 coal-fired stations in the LP formulation is because Kriel is treated as two stations in the EFS. A virtual power station named *Unmet* was created to represent the demand that cannot be met by the generation mix. A large penalty cost was assigned to it. Stations 30 to 32 are the pumps of the pumped storage schemes. Recall that the pumped storage schemes are only used for generation during peak demand periods. During the offpeak periods the water must be pumped back to the upper reservoirs. It was important to include the pumps in the LP formulation because, when they are in operation, they consume electricity, which means that the demand essentially increases.

Table 3.3: Index values for the power stations.

s	Power stations
1	Cahora Bassa
2	IPPs
3	Nuclear
4–19	Coal
20–23	OCGT
24	Unmet
25–26	Conventional hydroelectric
27–29	Pumped storage schemes
30–32	Pumped storage schemes (pumps)

Further definitions are the generation cost for power station s (C_s), the available generation capacity of power station s during time period q (A_{sq}), the forecast

electricity demand during time period q (F_q), the maximum weekly load for power station s ($l_s^{(\max_w)}$), the minimum weekly load for power station s ($l_s^{(\min_w)}$) and the weekly load requirement for power station s ($l_s^{(\text{req}_w)}$). C_s remains constant over the study period while A_{sq} differs for each month $m \in \mathcal{M} = \{1, \ldots, 12\}$. It is given by

$$A_{sq} = 12 \times I_s \times \text{EAF}_{sm} \tag{3.2}$$

where I_s is the installed generation capacity of power station s and EAF_{sm} is the energy availability factor for power station s during month m. A new EAF is thus used approximately every four weeks. EAF_{sm} is given by

$$\text{EAF}_{sm} = 100 - \text{PCLF}_{sm} - \text{UCLF}_{sm} - \text{OCLF}_{sm} \tag{3.3}$$

where

- PCLF_{sm} = planned capability loss factor (planned maintenance) for power station s during month m,
- UCLF_{sm} = unplanned capability loss factor (unplanned maintenance) for power station s during month m, and
- OCLF_{sm} = other capability loss factor (other unplanned outages) for power station s during month m.

Each of the above can be specified by the user to allow for *what-if* analysis. A default dataset for each is available for a period of five years. Negative EAFs are not allowed.

The maximum and minimum weekly loads for power station s are given by

$$l_s^{(\max_w)} = 14 \times A_{sq} \times \text{EUF}_s^{(\max)} \tag{3.4}$$

and

$$l_s^{(\min_w)} = 14 \times A_{sq} \times \text{EUF}_s^{(\min)} \tag{3.5}$$

respectively, where $\text{EUF}_s^{(\max)}$ is the maximum energy utilisation factor and $\text{EUF}_s^{(\min)}$ is the minimum energy utilisation factor. Both remain constant for each power station s throughout the course of a year.

The units of measurement for all the parameters in the module are provided in Table 3.4.

Table 3.4: Units of measurement for the parameters in the PP module.

Symbol	Unit of measurement
G_{sq}	MWh
C_s	ZAR/MWh
A_{sq}	MWh
F_q	MWh
$l_s^{(\max)}$	MWh
$l_s^{(\min)}$	MWh
$l_s^{(\text{req})}$	MWh
I_s	MW
EAF_{sm}	%
PCLF_{sm}	%
UCLF_{sm}	%
OCLF_{sm}	%
$\text{EUF}_s^{(\max)}$	%
$\text{EUF}_s^{(\min)}$	%

The LP is:

$$\text{Minimise} \sum_{q=1}^{14} \sum_{s=1}^{32} C_s G_{sq} \tag{3.6a}$$

subject to

$$G_{sq} \leq A_{sq} \qquad \forall s, q, \tag{3.6b}$$

$$\sum_{s=1}^{29} G_{sq} - \sum_{s=30}^{32} G_{sq} = F_q \qquad \forall q, \tag{3.6c}$$

$$\sum_{q=1}^{14} G_{sq} \leq l_s^{(\max_w)} \qquad \text{for} \quad s = 1, 2, ..., 19, \tag{3.6d}$$

$$\sum_{q=1}^{14} G_{sq} \geq l_s^{(\min_w)} \qquad \text{for} \quad s = 1, 2, ..., 14, \tag{3.6e}$$

$$\sum_{q=1}^{7} G_{sq} \geq \frac{1}{2} l_s^{(\min_w)} \qquad \text{for} \quad s = 15, 16, .., 19, \tag{3.6f}$$

$$\sum_{q=8}^{14} G_{sq} \geq \frac{1}{2} l_s^{(\min_w)} \qquad \text{for} \quad s = 15, 16, ..., 19, \tag{3.6g}$$

$$\sum_{q=1}^{14} G_{sq} = l_s^{(\text{req}_w)} \qquad \text{for} \quad s = 25, 26, \tag{3.6h}$$

$$\sum_{q=1}^{14} G_{27q} - 0.72 \sum_{q=1}^{14} G_{30q} = 0, \tag{3.6i}$$

$$\sum_{q=1}^{14} G_{28q} - 0.75 \sum_{q=1}^{14} G_{31q} = 0, \tag{3.6j}$$

$$\sum_{q=1}^{14} G_{29q} - 0.745 \sum_{q=1}^{14} G_{32q} = 0, \tag{3.6k}$$

$$\sum_{q=1}^{7} G_{sq} = 0 \qquad \text{for} \quad s = 30, 31, 32, \tag{3.6l}$$

$$G_{sq} \geq 0 \qquad \forall s, q. \tag{3.6m}$$

The objective function is defined in (3.6a). Constraint (3.6b) ensures that each power station's planned electricity generation during each time period does not exceed its available capacity during that time period. The constraint to balance the planned generation and the forecast demand during each time period is (3.6c). Referring to Table 3.3 for the numbering, the first 19 power stations are the base load stations. Each base load station has a maximum and a minimum weekly load requirement. The maximum weekly loads are ensured by (3.6d). The minimum weekly loads for stations 1 to 14 are ensured by (3.6e). Power stations 15 to 19 must produce at least half of the minimum load requirement

during peak time periods and at least half during offpeak time periods. This requirement, which is ensured by (3.6f) and (3.6g), was incorporated into the LP formulation in an attempt to keep these five power stations online during the night. The two conventional hydroelectric power stations each have an exact weekly load requirement. This is ensured by (3.6h). Constraints (3.6i) to (3.6k) are load balance constraints for the three pumped storage schemes. They ensure that the electricity used by the pumps during the offpeak periods are taken into account. Constraint (3.6l) ensures that the pumps are not used during peak demand periods while (3.6m) is a sign restriction constraint.

Every time the PP module is run, the LP is solved for each week to determine the planned weekly generation at each power station. After solving the LP for all weeks, the planned weekly generation at each power station is aggregated to determine the planned generation at each station during each month ($G_{sm}^{(\mathrm{p})}$). The same is done to obtain the monthly generation costs. The generation costs and the sales revenues are used by a module that draws up an income statement.

Because the hourly demand is averaged to a weekly demand, the total planned monthly generation output of the LP is not equal to the exact monthly demand. This means that either the monthly demand will not be met, or more electricity than required will be planned for. To obviate this, a load-pickup and a load-drop algorithm was incorporated into the module. Whenever the total planned monthly generation does not meet the monthly demand, the planned generation is picked up, starting at the power station with the lowest generation cost. A station's planned generation can only be picked up if the station has available capacity. On the other hand, when the total planned monthly generation is more than the monthly demand, the planned generation is dropped, starting at the power station with the highest generation cost. The planned generation can only be picked up and dropped at certain stations and all generation constraints must remain satisfied.

3.3.3 Fuel planning

Similarly to the PP module, the fuel planning (FP) module is completely deterministic. It uses the planned monthly electricity generation at the coal-fired

power stations to compute the expected amount of coal that each station will burn. This is subsequently used to estimate the planned monthly coal deliveries.

The planned coal to be burnt at power station s ($s = 4, 5, \ldots, 19$) during month m is given by

$$B_{sm}^{(\mathrm{p})} = G_{sm}^{(\mathrm{p})} \times \frac{H_s \times 10^{-6}}{\mathrm{CV}_s} \tag{3.7}$$

where H_s is the heat rate for power station s and CV_s the calorific value of the coal at power station s.

Each coal-fired power station is designed to operate at a specific heat rate and to burn coal within a specific CV range.

The planned coal delivery to power station s during month m is estimated by

$$D_{sm}^{(\mathrm{p})} = B_{sm}^{(\mathrm{p})} + S_{sm}^{(\mathrm{corr})} \tag{3.8}$$

where $S_{pm}^{(\mathrm{corr})}$ is the stockpile correction for power station s during month m.

A stockpile correction is added to the planned delivery in an attempt to have the coal stockpile level at each power station return to a user-specified target stockpile level by year-end. There are minimum and maximum constraints on the amount of coal that can be delivered to each power station in a month.

The units of measurement for all the parameters in the module are provided in Table 3.5.

Table 3.5: Units of measurement for the parameters in the FP module.

Symbol	Unit of measurement
$B_{sm}^{(\mathrm{p})}$	ktonnes
$G_{sm}^{(\mathrm{p})}$	MWh
H_s	MJ/MWh
CV_s	MJ/kg
$D_{sm}^{(\mathrm{p})}$	ktonnes
$S_{sm}^{(\mathrm{corr})}$	ktonnes

3.3.4 Primary energy

The primary energy (PE) module, which is a simplified version of the Coal Stockpile Simulator proposed by Micali & Heunis (2011), is a Monte Carlo simulation model. For each *replication* (or *sample path*), the model computes the following:

1. the actual electricity generation at each power station during each month
2. the coal stockpile level at each coal-fired power station at the end of each month.

Each of the above is computed by stochastically adding uncertainty (or *noise*) to the planned inputs that the model receives from the FP and PP modules. The following uncertainties are incorporated into the model:

1. A power station's actual UCLF during a given month may differ from the planned UCLF.
2. The actual CV of the coal at a coal-fired power station during a given month may differ from the planned CV.
3. A coal-fired power station's actual coal delivery during a given month may differ from the planned coal delivery.

Equations (3.9) to (3.12) show how the three uncertainties are incorporated for each power station during each month by sampling a random number from a standard normal probability density function. The notation and units of measurement from Subsections 3.3.2 and 3.3.3 also apply for the PE module.

For the base load power stations, constant energy utilisation factors (EUFs) are assumed and the actual electricity generation at power station s during month m is given by

$$G_{sm}^{(\mathrm{a})} = G_{sm}^{(\mathrm{p})} \times \left(\frac{100 - \mathrm{PCLF}_{sm} - \mathrm{OCLF}_{sm}}{\mathrm{EAF}_{sm}} - \frac{\mathrm{UCLF}_{sm} + N(0,1)\sigma_s^{(\mathrm{UCLF})}}{\mathrm{EAF}_{sm}} \right) \tag{3.9}$$

where $\sigma_s^{(\text{UCLF})}$ is a forecast standard deviation of the UCLF for power station s. It remains constant for all months.

For the peak demand power stations, the planned generation at power station s during month m is used as the actual generation unless it exceeds the actual maximum monthly generation at the station. This is mathematically expressed by

$$\begin{aligned} G_{sm}^{(\text{a})} = \min\{G_{sm}^{(\text{p})}; I_s \times 24 \times d_m \times (100 - \text{PCLF}_{sm} - \text{OCLF}_{sm} \\ - \quad (\text{UCLF}_{sm} + N(0,1)\sigma_s^{(\text{UCLF})})) \times \text{EUF}_s^{(\max)}\} \end{aligned} \tag{3.10}$$

where d_m is the number of days in month m.

For the coal-fired power stations, the actual coal burnt at power station s during month m is given by

$$B_{sm}^{(\text{a})} = G_{sm}^{(\text{a})} \times \frac{H_s \times 10^{-6}}{\text{CV}_s + N(0,1)\sigma_s^{(\text{CV})}} \tag{3.11}$$

where $\sigma_s^{(\text{CV})}$ is a forecast standard deviation for the CV of the coal at power station s. It remains constant for all months.

The actual coal delivery to coal-fired power station s during month m is given by

$$D_{sm}^{(\text{a})} = D_{sm}^{(\text{p})} + N(0,1)\sigma_s^{(\text{D})} \tag{3.12}$$

where $\sigma_s^{(\text{D})}$ is a forecast standard deviation of the coal delivery to power station s. It remains constant for all months.

After incorporating the uncertainties for power station s during month m, the coal stockpile level at the end of the month is calculated by

$$S_{s,m} = S_{s,m-1} + D_{sm}^{(\text{a})} - B_{sm}^{(\text{a})}. \tag{3.13}$$

Each coal-fired power station's stockpile level at the end of a given month can be expressed in kilotonnes (ktonnes) or in terms of stockpile days. To obtain

the number of stockpile days on hand at a given station, the amount of ktonnes must be divided by the station's standard daily burn (SDB). The SDB of a power station, measured in ktonnes per day, is the amount of coal that the station can burn if it was to operate for one full day without any outages (i.e. EAF = 100%).

Negative stockpile levels are not allowed. Thus, if $S_{s,m}$ is negative, the following happens:

$$S_{s,m} = 0. \tag{3.14}$$

Thereafter, the actual coal burnt and actual electricity generation is re-calculated by

$$B_{sm}^{(\mathrm{a})} = D_{sm}^{(\mathrm{a})} + S_{s,m-1} \tag{3.15}$$

and

$$G_{sm}^{(\mathrm{a})} = B_{sm}^{(\mathrm{a})} \times \frac{CV_s + N(0,1)\sigma_s^{(\mathrm{CV})}}{H_s \times 10^{-6}} \tag{3.16}$$

respectively, where $N(0,1)\sigma_s^{(\mathrm{CV})}$ is the same value as in (3.11).

For the first month, $S_{s,m-1} = S_s^{(\mathrm{i})}$ is substituted into (3.13) and (3.15) where $S_s^{(\mathrm{i})}$ is the user-specified initial stockpile level at power station s. Due to the uncertainties, the demand during a month and the actual generation during a month will not balance. This again calls for the load-pickup and load-drop algorithms to be run after each month's calculations.

The mean monthly generation and mean coal stockpile levels are computed by running the simulation model for a user-specified number of replications. Figure 3.4 is a conceptual diagram of the PE module that shows the controllable inputs, the uncontrollable inputs and the outputs.

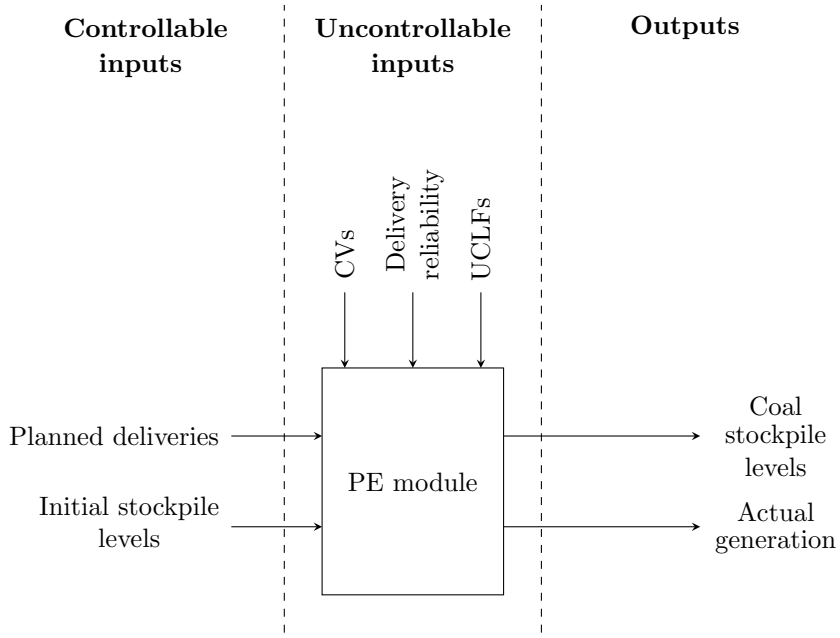

Figure 3.4: Conceptual diagram of the PE module.

3.4 Order of simulation

As described in Subsections 3.3.1 to 3.3.4, the main simulation component of the EFS is the PE module. The module simulates the actual electricity generation at each power station and the coal stockpile level at each coal-fired power station over the study period. Both outputs are expressed as mean monthly values.

To obtain the simulation outputs, the order of simulation for the EFS is as follows:

1. Run the LF module to forecast the hourly electricity demand for the study period.
2. Run the PP module over the same study period to determine the planned monthly electricity generation at each power station.
3. Run the FP module to estimate, for each coal-fired power station, the planned monthly coal delivery.

4. Run the PE module to simulate, for each power station, the actual monthly electricity generation and, for each coal-fired power station, the coal stockpile level at the end of each month.

3.5 Analysis capability of the energy flow simulator

The EFS is not just a model that is capable of simulating electricity generation and coal stockpile levels over a certain study period. The inputs that are subject to user specification make it possible for the simulation outputs to be analysed for a number of *what-if* scenarios.

Table 3.6: Analysis capability of the EFS.

User-specified input	Example *what-if* scenario
Weather scenario	Select a warm study period.
GDP scenario	Select a study period with low economic growth.
Initial stockpile level	Set a low initial stockpile level for all coal-fired power stations.
Target stockpile level	Set all year-end target stockpile levels equal to the initial stockpile levels.
New capacity	Specify that half of Medupi's generation capacity must be introduced during the first month of the study period.
PCLF	Set a specific maintenance plan.
UCLF	Set very high UCLFs for a specific power station during all months.
OCLF	Set zero OCLFs for all power stations during all months.

The parameters subject to user specification are the weather and gross domestic product (GDP) scenarios, the initial stockpile levels, the year-end target stockpile levels and the new generation capacity to be introduced. Furthermore,

the PCLF, UCLF and OCLF datasets can be modified by the user to create specific scenarios. By default, none of the three new stations (Kusile, Medupi and Ingula) are included in the analysis and the weather and GDP scenarios are set to *normal*. When running the EFS with the default inputs, it is referred to as the *baseline case*. The analysis capability of the EFS is summarised in Table 3.6.

3.6 Proposed modifications to the energy flow simulator

This section presents an overview of the proposed modifications to the architecture of the EFS. When reading this section, it is important to keep in mind the problem being addressed in this research, namely that of formulating and solving a multi-objective coal inventory model for the EFS. The coal stockpile levels are thus considered as the primary simulation output.

As noted throughout this chapter, the EFS currently operates on a monthly resolution (i.e. the simulation outputs are expressed as monthly values). The stochastic uncertainties within the PE module are thus also incorporated on a monthly basis. The danger in this is that the actual uncertainties that occur at the various power stations on a daily basis are covered up by average monthly simulation outputs. This is illustrated in Figure 3.5, which is a plot that shows an example of the simulated stockpile level at a specific power station for a monthly simulation resolution and a daily simulation resolution. By comparing the two, it can clearly be seen that the stockpile levels produced by the PE module do not truly reflect the variation in the stockpiles throughout the course of a month. For this reason, the main objective of the modification of the EFS is to change the resolution to daily.

In order to achieve this objective, the following must be considered:

1. The PP module must be modified in order for its output to be, for each day in the study period, the planned daily electricity generation at each power station. With regard to the inputs of the PP module, no changes to the LF module are required. However, the station availabilities module must be modified in order for its output to be daily EAFs.

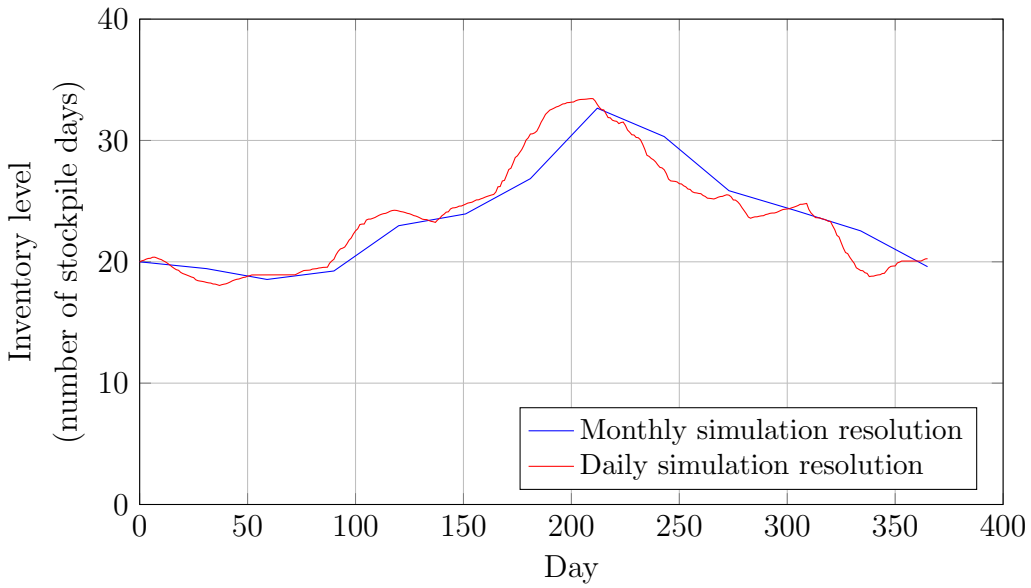

Figure 3.5: Monthly compared to daily simulation resolution.

2. The FP module must be modified in order for its output to be, for each day in the study period, the planned daily coal delivery to each coal-fired power station.

3. The PE module must be modified in order for the stochastic uncertainties to be incorporated on a daily basis. This will subsequently enable the module to produce daily simulation outputs.

3.7 Modifications to the architecture of the energy flow simulator

A detailed description of all modifications to the PP, FP and PE modules follows in this section. As mentioned, the main objective of the modification of the EFS is to change the resolution to daily.

The architecture explanations in this section again assume a study period of one year.

3.7.1 Production planning

In order to change the resolution of the PP module to daily, the LP that determines the planned electricity generation at each power station had to be reformulated. Before commencing with the modifications to the PP module, it must be mentioned that (3.6a) to (3.6m) were assumed to be correct and that, by slightly modifying them, they would remain correct.

The reader may recall from Subsection 3.3.2 that the LP in the existing PP module is solved for each week in the study period to obtain the planned weekly generation at each station. Thereafter, each station's planned weekly generation is aggregated to monthly values for all months. In the modified LP being proposed, the planned daily generation at each power station is determined by solving the LP for each day. The objective thus becomes to minimise the total daily generation cost. The LP was modified as follows:

The hourly demand for each day is sorted in descending order. Each day is then divided into two time periods of 12 hours each. The one with the highest demand is treated as the peak demand period while the other one is treated as the offpeak demand period. The LP's decision variable is defined as

$$G_{sq} = \text{planned electricity generation at power station } s \text{ during time period } q \tag{3.17}$$

where $s \in \mathcal{S} = \{1, \ldots, 32\}$ and $q \in \mathcal{Q} = \{1, 2\}$. Table 3.3 still applies.

Further definitions are the generation cost for power station s (C_s), the available generation capacity of power station s during time period q (A_{sq}), the forecast demand during time period q (F_q), the maximum daily load for power station s ($l_s^{(\max_d)}$), the minimum daily load for power station s ($l_s^{(\min_d)}$) and the daily load requirement for power station s ($l_s^{(\text{req}_d)}$). C_s remains the same as in the existing formulation. A_{sq} is now given by

$$A_{sq} = 12 \times I_s \times \text{EAF}_{sd} \tag{3.18}$$

where I_s is the installed generation capacity of power station s and EAF_{sd} is the energy availability factor for power station s on day $d \in \mathcal{D} = \{1, \ldots, 365\}$. EAF_{sd} is given by

$$\text{EAF}_{sd} = 100 - \text{PCLF}_{sd} - \text{UCLF}_{sd} - \text{OCLF}_{sd} \tag{3.19}$$

where

- PCLF_{pd} = planned capability loss factor (planned maintenance) for power station s on day d,
- UCLF_{sd} = unplanned capability loss factor (unplanned maintenance) for power station s on day d, and
- OCLF_{sd} = other capability loss factor (other unplanned shutdowns) for power station s on day d.

Unlike for the monthly planned and unplanned outages, no default daily datasets were made available by Eskom for this study. However, because PCLF, UCLF and OCLF can be specified by the user, a dataset for each could be created. This was done stochastically by sampling three random numbers from uniform probability density functions for each power station during each month. The first one determines the number of generating units to be off, the second one determines the day on which the outage should start and the third one determines the number of consecutive days for which the outage must continue. A constraint was added in order for

$$\sum_{d=1}^{d_m} (I_s \times 24 \times \text{PCLF}_{sd}) = I_s \times 24 \times d_m \times \text{PCLF}_{sm}, \tag{3.20}$$

$$\sum_{d=1}^{d_m} (I_s \times 24 \times \text{UCLF}_{sd}) = I_s \times 24 \times d_m \times \text{UCLF}_{sm}, \tag{3.21}$$

and

$$\sum_{d=1}^{d_m}(I_s \times 24 \times \text{OCLF}_{sd}) = I_s \times 24 \times d_m \times \text{OCLF}_{sm} \tag{3.22}$$

where d_m is the number of days in month m. Equations (3.20) to (3.22) ensure that the daily outages for all stations over the course of each month are similar to those of the existing default monthly datasets.

For F_q, the exact forecast demand during each time period is used. The maximum and minimum daily loads for power station s are given by

$$l_s^{(\text{max}_\text{d})} = 2 \times A_{sq} \times \text{EUF}_s^{(\text{max})} \tag{3.23}$$

and

$$l_s^{(\text{min}_\text{d})} = 2 \times A_{sq} \times \text{EUF}_s^{(\text{min})} \tag{3.24}$$

respectively, where $\text{EUF}_s^{(\text{max})}$ and $\text{EUF}_s^{(\text{min})}$ remain the same as in Subsection 3.3.2.

The daily load requirement for power station s is assumed to be

$$l_s^{(\text{req}_\text{d})} = \frac{l_s^{(\text{req}_\text{w})}}{7}. \tag{3.25}$$

Regardless of the slight changes in notation (EAF_{sm} to EAF_{sd}, etc.), the units of measurement remain the same as in the existing PP module. This also applies for the modified FP and PE modules.

The modified LP is:

$$\text{Minimise} \sum_{q=1}^{2}\sum_{s=1}^{32} C_s G_{sq} \tag{3.26a}$$

subject to

$$G_{sq} \leq A_{sq} \qquad \forall s, q, \tag{3.26b}$$

$$\sum_{s=1}^{29} G_{sq} - \sum_{s=30}^{32} G_{sq} = F_q \qquad \forall q, \tag{3.26c}$$

$$\sum_{q=1}^{2} G_{sq} \leq l_s^{(\max_d)} \qquad \text{for} \quad s = 1, 2, ..., 19, \tag{3.26d}$$

$$\sum_{q=1}^{2} G_{sq} \geq l_s^{(\min_d)} \qquad \text{for} \quad s = 1, 2, ..., 14, \tag{3.26e}$$

$$G_{s1} \geq \frac{1}{2} l_s^{(\min_d)} \qquad \text{for} \quad s = 15, 16, .., 19, \tag{3.26f}$$

$$G_{s2} \geq \frac{1}{2} l_s^{(\min_d)} \qquad \text{for} \quad s = 15, 16, ..., 19, \tag{3.26g}$$

$$\sum_{q=1}^{2} G_{sq} = l_s^{(\text{req}_d)} \qquad \text{for} \quad s = 25, 26, \tag{3.26h}$$

$$\sum_{q=1}^{2} G_{27q} - 0.72 \sum_{q=1}^{2} G_{30q} = 0, \tag{3.26i}$$

$$\sum_{q=1}^{2} G_{28q} - 0.75 \sum_{q=1}^{2} G_{31q} = 0, \tag{3.26j}$$

$$\sum_{q=1}^{2} G_{29q} - 0.745 \sum_{q=1}^{2} G_{32q} = 0, \tag{3.26k}$$

$$G_{s1} = 0 \qquad \text{for} \quad s = 30, 31, 32, \tag{3.26l}$$

$$G_{sq} \geq 0 \qquad \forall s, q. \tag{3.26m}$$

The objective function is defined in (3.26a). Constraint (3.26b) ensures that each power station's planned electricity generation during each time period does not exceed its available capacity during that time period. The constraint to balance the planned generation and forecast demand during each time period is (3.26c). Constraint (3.26d) ensures that, for each base load power station, the daily planned generation does not exceed the maximum daily load. The minimum daily load requirements for stations 1 to 14 are ensured by (3.26e). Constraints (3.26f) and (3.26g) ensure that stations 15 to 19 produce at least half of the minimum daily load requirement in each of the two time periods. Constraint (3.26h) ensures that each of the two conventional hydroelectric power stations (25 and 26) produce their exact daily load requirement. The load balance constraints for the three pumped storage schemes (27 to 29) are (3.26i) to (3.26k).

Constraint (3.26l) ensures that the pumps (30 to 32) are not used during peak demand periods while (3.26m) is a sign restriction constraint.

When the LP is solved for a given day, the planned generation at each power station during each of the two time periods is obtained. By summing the planned generation at station s over both time periods on day d, the station's planned daily generation ($G_{sd}^{(\mathrm{p})}$) is obtained.

The new LP was thoroughly tested by ensuring that all constraints are satisfied. Furthermore, because the exact forecast demand during each time period is used, and not the average demand as in the existing LP, the total planned daily generation always meets the demand exactly. The load-pickup and load-drop algorithms are thus not required.

3.7.2 Fuel planning

The proposed new FP module is a simplified version of the existing one. Recall from Subsection 3.3.3 that the planned coal deliveries for each coal-fired power station were estimated to be equal to the planned amount of coal to be burnt, plus a stockpile correction. This is not an accurate representation of the real-world system. The long-term nature of Eskom's coal supply contracts means that planned deliveries cannot be changed based on the coal requirements. Fixed planned deliveries are thus proposed for the entire duration of the study period.

Ideally, the planned deliveries should be set equal to the amounts specified in Eskom's supply contracts. However, this data was not made available for this study. An assumption was subsequently made that the planned daily coal delivery to power station s ($D_s^{(\mathrm{p})}$) is equal to the average planned daily coal required at station s over the entire study period. This is given by

$$D_s^{(\mathrm{p})} = \frac{\sum_{d=1}^{365} B_{sd}^{(\mathrm{p})}}{365} \tag{3.27}$$

where $B_{sd}^{(\mathrm{p})}$ is the planned coal to be burnt at power station s on day d. $B_{sd}^{(\mathrm{p})}$ is given by

$$B_{sd}^{(\mathrm{p})} = G_{sd}^{(\mathrm{p})} \times \frac{H_s \times 10^{-6}}{\mathrm{CV}_s}. \tag{3.28}$$

3.7.3 Primary energy

The proposed new PE module operates on the same principles as the existing one in that the same three uncertainties are incorporated (i.e. UCLF, CV and delivery reliability). However, the change in resolution meant that (3.9) to (3.12) had to be modified slightly.

The uncertainty of UCLF is incorporated by stochastically creating a daily UCLF dataset for each replication. This is done exactly as explained in Subsection 3.7.1. However, a constraint was added to ensure that

$$\sum_{d=1}^{d_m}\left(I_s \times 24 \times \mathrm{UCLF}_{sd}^{(\mathrm{s})}\right) = I_s \times 24 \times d_m \times \left(\mathrm{UCLF}_{sm} + N(0,1)\sigma_s^{(\mathrm{UCLF})}\right) \tag{3.29}$$

where $\mathrm{UCLF}_{sd}^{(\mathrm{s})}$ is the stochastically created unplanned capability loss factor for power station s on day d.

Equations (3.9) and (3.10) then become

$$G_{sd}^{(\mathrm{a})} = G_{sd}^{(\mathrm{p})} \times \left(\frac{100 - \mathrm{PCLF}_{sd} - \mathrm{OCLF}_{sd} - \mathrm{UCLF}_{sd}^{(\mathrm{s})}}{\mathrm{EAF}_{sd}}\right) \tag{3.30}$$

and

$$G_{sd}^{(\mathrm{a})} = \min\{G_{sd}^{(\mathrm{p})}; I_s \times 24 \times (100 - \mathrm{PCLF}_{sd} - \mathrm{OCLF}_{sd} - \mathrm{UCLF}_{sd}^{(\mathrm{s})}) \times \mathrm{EUF}_s^{(\max)}\} \tag{3.31}$$

respectively, where $G_{sd}^{(\mathrm{a})}$ is the actual electricity generation at power station s on day d.

For the coal-fired power stations, the actual coal burnt at station s on day d is given by

$$B_{sd}^{(\mathrm{a})} = G_{sd}^{(\mathrm{a})} \times \frac{H_s \times 10^{-6}}{\mathrm{CV}_s + N(0,1)\sigma_s^{(\mathrm{CV})}}. \tag{3.32}$$

3.7 Modifications to the architecture of the energy flow simulator

Due to the change in simulation resolution, the standard deviation of the coal deliveries cannot be used in the same way as in (3.12). A triangular distribution was assumed to be an appropriate alternative. A triangular distribution's probability density function, which is shaped like a triangle, is defined by three values, namely the minimum value, the most likely value and the maximum value. For the daily coal delivery to each coal-fired power station, the most likely value was set as $D_s^{(\mathrm{p})}$. The minimum and maximum values can be specified by the user. Default values of $0.9D_s^{(\mathrm{p})}$ and $1.1D_s^{(\mathrm{p})}$ were set for the baseline case. Thus, the actual coal delivery to power station s on day d is assumed to be

$$D_{sd}^{(\mathrm{a})} = Tri(0.9D_s^{(\mathrm{p})}, D_s^{(\mathrm{p})}, 1.1D_s^{(\mathrm{p})}). \tag{3.33}$$

After incorporating the uncertainties for power station s on day d, the calculations continue exactly as in Subsection 3.3.4. First, the coal stockpile level at the end of the day is calculated by

$$S_{s,d} = S_{s,d-1} + D_{sd}^{(\mathrm{a})} - B_{sd}^{(\mathrm{a})}. \tag{3.34}$$

Negative stockpile levels are again not allowed. Thus, if $S_{s,d}$ is negative, the following happens:

$$S_{s,d} = 0. \tag{3.35}$$

Thereafter, the actual coal burnt and actual electricity generation is recalculated by

$$B_{sd}^{(\mathrm{a})} = D_{sd}^{(\mathrm{a})} + S_{s,d-1} \tag{3.36}$$

and

$$G_{sd}^{(\mathrm{a})} = B_{sd}^{(\mathrm{a})} \times \frac{\mathrm{CV}_s + N(0,1)\sigma_s^{(\mathrm{CV})}}{H_s \times 10^{-6}} \tag{3.37}$$

respectively, where $N(0,1)\sigma_s^{(\mathrm{CV})}$ is the same value as in (3.32). For the first day $S_{s,d-1} = S_s^{(\mathrm{i})}$ is substituted into (3.34) and (3.36).

Due to the uncertainties, the demand and the actual generation for a day will again not balance. Thus, the load-pickup and load-drop algorithms must be run after each day's calculations.

3.8 Verification and validation of the modified primary energy module

As the simulation component of the EFS, the modified PE had to be verified and validated. Verification of a simulation model is software oriented and involves ensuring that the model was built right. Validation, on the other hand, is required to ensure that the model is a sufficient representation of the real-world system.

3.8.1 Verification

The PE module's R code was extensively debugged to ensure that it works correctly. Furthermore, the logic involved in the three stochastic uncertainties were tested by fixing the parameters that cause uncertainty. By doing this, the module's outputs became deterministic and could thus be computed and compared with the response produced from running the module. After obtaining complete confidence in the correctness of the module's logic, errors were further searched for by varying some of the input datasets in an attempt to crash the model. The model could not be crashed for any valid inputs.

3.8.2 Validation

Law & Kelton (2000) mention three considerations during validation of a simulation model:

1. **Conceptual validity:** Adequate representation of the real-world system.
2. **Operational validity:** Sufficient similarity between the model's generated data and the real-world system's behavioural data.

3. **Credibility:** End-user's confidence in the model's results.

The assumption was made that each of the above had been considered by the developers of the EFS. Also, for the strategic planning purposes of the EFS, the modifications made to the PE module in this study were deemed to be insignificant enough not to affect the validity or credibility of the module. However, it is recommended that the module be further tested for specific real-world scenarios and with updated input data.

The reasonableness exhibited by the PE module was investigated by measuring it against the following factors:

1. **Continuity:** Small changes to input parameters resulted in appropriate small changes to the module's output. For example, the actual daily generation decreased when higher UCLFs were specified. Also, lower CVs resulted in increased coal requirements which subsequently caused lower stockpile levels. The stockpile levels also decreased when lower planned coal deliveries were specified.

2. **Consistency:** Consistency was confirmed by similar simulation runs that consistently resulted in similar outputs.

3. **Absurd conditions:** Absurd conditions were introduced and the model did not produce equally absurd outputs. For example, very high UCLFs never resulted in negative EAFs while very low planned coal deliveries as well as low initial stockpile levels did not cause the stockpile levels to be negative. Zero electricity generation was also confirmed for all coal-fired stations during coal stockouts.

Figure 3.6 shows the coal stockpile levels for a one-year study period after running the PE module for 20 independent Monte Carlo replications. Initial stockpile levels were set to 20 stockpile days and only the 14 existing coal-fired stations (illustrated as A to N) were included. The variation that results from the stochastic uncertainties is clearly visible. Power stations C and F exhibit greater variation, mainly due to their larger $\sigma_s^{(\text{UCLF})}$ values. On the other hand, the variation is much less for stations A, H and I. Also note that the stockpile level

at power stations C, F and G reached zero stockpile days for some replications, but never became negative.

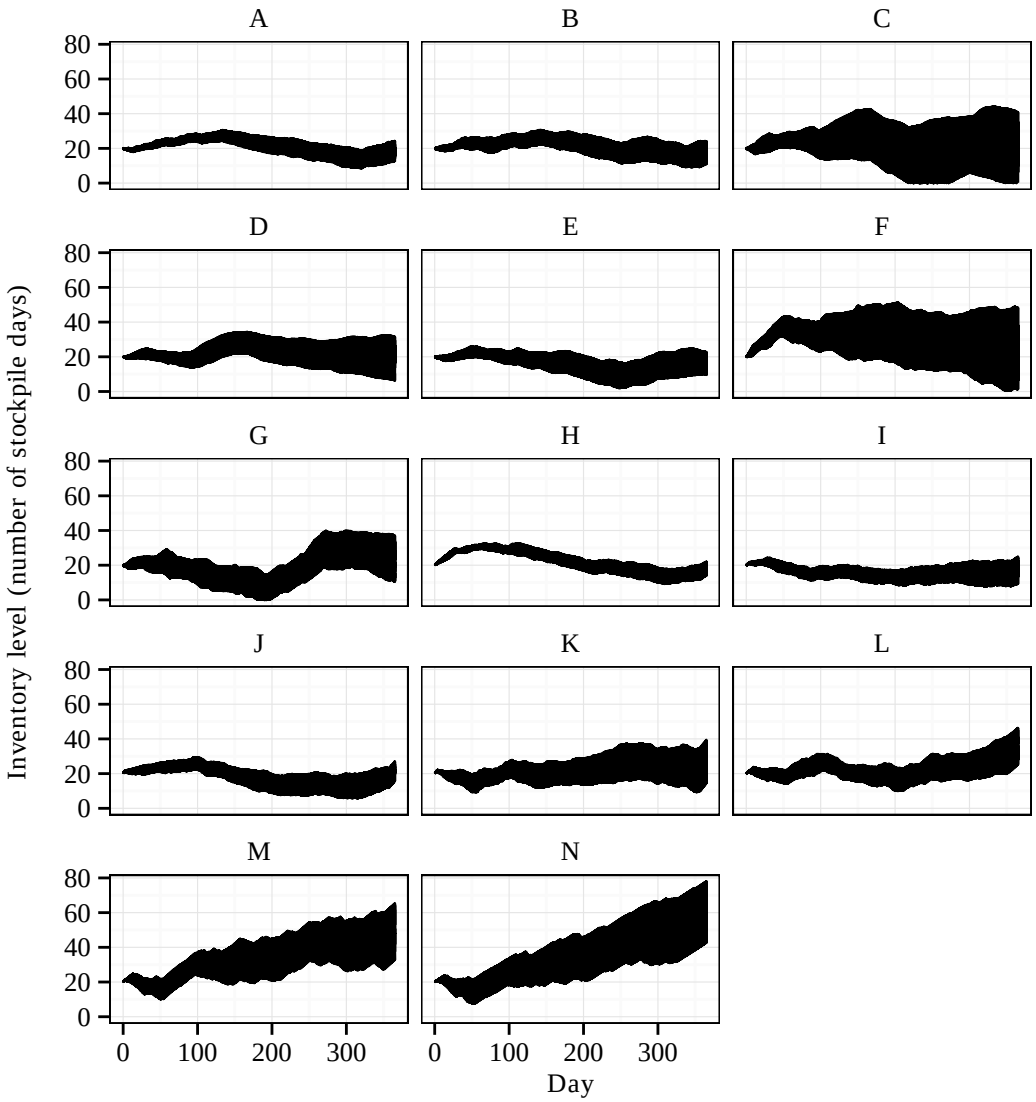

Figure 3.6: Variation exhibited by the modified PE module.

3.9 Summary: Chapter 3

This chapter provided background to the South African electricity sector and Eskom's generation mix and coal supply chain. This was followed by an introduction

to the EFS. Thereafter, the current architecture of the EFS was described. The focus was on the four primary modules. The PE module is the main simulation component while the LF, PP and FP modules compute inputs that are either directly or indirectly fed to the PE module. The monthly electricity generation at each power station and the monthly coal stockpile level at each coal-fired power station are the two simulation outputs produced when running the PE module.

After summarising the order of simulation and the analysis capability of the EFS, modifications to the EFS architecture were proposed. By keeping the main research objective in mind, all modifications to the EFS were directed towards changing the simulation resolution to daily instead of monthly. All modifications to the PP, FP and PE modules were described. Verification and validation of the modified PE module instilled sufficient confidence in the simulation model for the study to proceed to the formulation of the multi-objective inventory model.

Chapter 4 is a literature study on simulation optimisation.

Chapter 4

Literature: Simulation optimisation

Chapter 3 presented the current architecture of the energy flow simulator (EFS) as well as the proposed modifications to it. This chapter is a literature study on simulation optimisation (SO). The knowledge gained from this study will be used to achieve the main research objective, namely to formulate and solve a multi-objective coal inventory model for the EFS.

According to Fu *et al.* (2014) simulation and optimisation are arguably the two most powerful techniques in operations research. Stochastic computer simulation is a useful tool for evaluating the performance of real-world systems that are too complex to be modelled analytically. However, it is often insufficient to simply evaluate the performance of the system. Some projects may require a more exploratory evaluation, hence the need to merge simulation and optimisation technologies (Ólafsson & Kim, 2002). Most commercial Monte Carlo or discrete-event simulation software packages on the market today have an optimisation module.

This chapter starts off by introducing the basic principles of SO. This is followed by an overview of SO techniques, specifically for the single-objective case. Thereafter the focus shifts to multi-objective SO and multi-objective optimisation (MOO) techniques.

4.1 An introduction to simulation optimisation

Ólafsson & Kim (2002) defines SO as "*the process of finding the best values of some decision variables for a system where the performance of the system is evaluated based on the output of a simulation model of the system*". Considering this definition, the traditional single-objective SO model is defined as

$$\text{Minimise } f(\theta) \tag{4.1}$$

$$\text{subject to } \theta \in \Theta, \tag{4.2}$$

where $f(\theta)$, which cannot be expressed analytically, is estimated by $\hat{f}(\theta)$ from samples (or replications) of a simulation model using instances of feasible input parameters θ.

Input parameters can be discrete or continuous, and are constrained within some feasible set $\Theta \in \mathbb{R}^D$ for D decision variables. The most common form for $f(\theta)$ is the expected value of the system performance measure, i.e.

$$f(\theta) = \mathbb{E}[\psi(\theta, \omega)] \tag{4.3}$$

where ψ represent the sample performance and ω the stochastic effects of the simulation model (Bekker, 2012; Rosen *et al.*, 2007).

In order to obtain optimal values for a simulation model's input parameters, an optimisation technique must be integrated with the model. This is illustrated in Figure 4.1. Each simulation run, which refers to a certain number of replications, produces a response value. The optimisation technique guides the process by evaluating the response value and adjusting the values for the input parameters based on the response. The process terminates when no more improvement of the response value is shown.

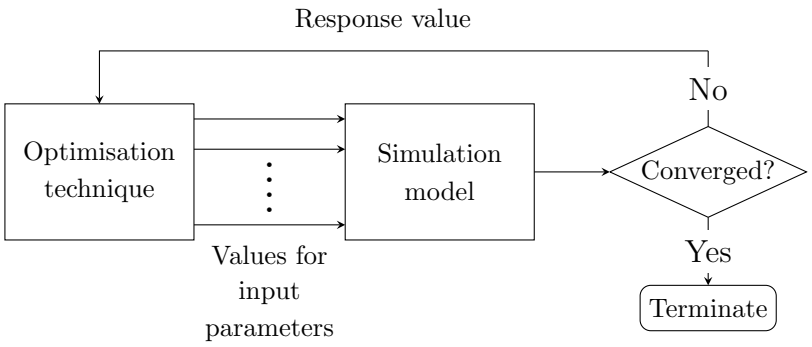

Figure 4.1: Integration of a simulation model and optimisation technique.

Azadivar (1999) mentions a few specific challenges of SO. Because no analytical expression for the objective function exists, differentiation or the exact calculation of local gradients is not an option. The stochastic nature of the objective function also presents a problem when having to estimate approximate gradients. Furthermore, running a computer simulation program is much more expensive compared to evaluating analytical functions. Integration of an optimisation technique and some kind of simulation language can also present a potential obstacle, especially when the optimisation technique is coded in a different programming language.

4.2 Simulation optimisation techniques

The majority of "classical" approaches that account for most of the early literature in SO assume a uni-modal response surface. This is a major drawback that often causes these techniques to perform poorly when the response surface is high-dimensional, discontinuous and non-differentiable. Optimisation techniques capable of overcoming the trap of local optimality are thus preferred. Most such techniques are *metaheuristics* (Tekin & Sabuncuoglu, 2004).

A broad overview of "classical" SO approaches and metaheuristics is presented in this section.

4.2.1 Classical approaches

Several researchers, including Ólafsson & Kim (2002) and Swisher *et al.* (2000), classify SO techniques based on the nature of the decision space. This arrangement is also used here.

In a discrete decision space, the feasible region consists of discrete input parameters (e.g. the number of machines in a factory) whereas in a continuous decision space, the input parameters take a set of continuous values (e.g. the reorder quantity in an inventory problem) (Ammeri *et al.*, 2010).

4.2.1.1 Discrete input parameters

For discrete input parameters, SO techniques can further be differentiated based on the size of the decision space. In the case of a finite and small decision space, *statistical selection* methods are well suited because every solution can be evaluated. The two most popular examples are *ranking and selection* and *multiple comparison procedures* (Ammeri *et al.*, 2010).

Generally, real-world systems have very large and infinite decision spaces, which makes it impossible to evaluate every solution. This calls for different methods such as *ordinal optimisation* where, instead of trying to find the very best solution, the focus is on finding "good" solutions (Ammeri *et al.*, 2010; Tekin & Sabuncuoglu, 2004). Another option for an infinitely large decision space is *random search* algorithms. These algorithms typically involve an iterative process in which input parameters are randomly selected from the search area (Tekin & Sabuncuoglu, 2004).

4.2.1.2 Continuous input parameters

SO techniques for continuous input parameters can be arranged into three categories: *metamodel methods*, *gradient-based approaches* and *non-gradient based approaches* (Ammeri *et al.*, 2010).

Metamodel methods attempt to develop a mathematical relationship between the input parameters and the response value. One such procedure is *response surface methodology* in which a series of regression models are fitted to the simulation response (Ammeri *et al.*, 2010; Carson & Maria, 1997).

Gradient-based methods usually take the form of *stochastic approximation* algorithms. These procedures are iterative and the search direction is based on an estimate of the response gradient (Fu *et al.*, 2005; Ólafsson & Kim, 2002). Gradient estimation techniques include *perturbation analysis*, *finite difference estimation*, *likelihood ratio estimation* and *frequency domain analysis* (Ammeri *et al.*, 2010).

Non-gradient based approaches provide an alternative to procedures that require an estimation of the response gradient. These techniques, which include the *sample path method*, the *Nelder-Mead method* and the *Hooke and Jeeves method*, attempt to turn the stochastic problem into a deterministic problem by taking a large enough set of samples. This subsequently allows for the tools of nonlinear programming to be applied (Ammeri *et al.*, 2010).

4.2.2 Metaheuristics

The SO techniques mentioned in Subsection 4.2.1 often fail to find the optimal solution when the response surface is multi-modal. A different approach is thus required.

Metaheuristics are efficient global search algorithms that are widely recognised for their ability to obtain near-optimal solutions within reasonable time periods (Gendreau & Potvin, 2005). These algorithms are "higher-level" heuristics, as indicated by the Greek prefix "meta". A major advantage of metaheuristics lies in their ability to approximately solve problems for which no satisfactory problem-specific algorithm is available. Metaheuristics are generally designed for combinatorial optimisation problems in the deterministic context, but have in recent years been applied to SO with success (Boussaïd *et al.*, 2013).

Two contradictory criteria should be considered when designing a metaheuristic, namely *exploration* of the decision space and *exploitation* of the best solutions found (Talbi, 2009). Metaheuristics can be classified as either single-solution based or population-based. Single-solution based metaheuristics improve a *single* solution by iteratively "walking" through the decision space of the problem. These algorithms, which include *simulated annealing* and *tabu search*, are exploitation

oriented in that the search can intensify in local regions. Population-based metaheuristics, on the other hand, iteratively improve a *population* of solutions. Most metaheuristics of this class are related to *evolutionary computation*. Collectively they are known as *evolutionary algorithms* (EAs) (Boussaïd *et al.*, 2013; Talbi, 2009).

EAs, which are inspired by Darwin's evolutionary theory, allow for better exploration of the entire search space (Talbi, 2009). The idea behind EAs is to improve the average quality within the population from one *generation* to the next. The solution candidates in the population are called *individuals*. New generations are created through both a *selection* process and *evolutionary operators*, usually *mutation* and *recombination*, that operate on the current generation's population. High-quality individuals are selected to be part of the next generation based on their so-called *fitness functions*. The fitness value of a particular individual provides a measure of how well the optimality condition is satisfied (Coello *et al.*, 2007; Zitzler, 1999). Arguably the most popular EA is the *Genetic Algorithm*. Other EAs include *differential evolution*, *evolution strategy*, *evolutionary programming* and *genetic programming*. For more on this, see the book by Simon (2013) in which a wide range of EAs are discussed.

A number of population-based metaheuristics are inspired by other natural processes. A few examples are *particle swarm optimisation*, *ant systems optimisation* and algorithms based on *artificial immune systems* (Boussaïd *et al.*, 2013).

4.3 Multi-objective simulation optimisation

The SO model defined in Section 4.1 can be extended to the multi-objective case. The basic principles of SO remain the same for multi-objective optimisation (MOO) and metaheuristics are also the preferred solution approach. However, because MOO problems have at least two conflicting objective functions that must be optimised simultaneously, many acceptable solutions exist for a given problem (Bekker, 2012). This subsequently means that the algorithms required for solving MOO problems differ from the ones used for single-objective problems.

In this section, the MOO problem is defined (Subsection 4.3.1). This is followed by an overview of approaches to MOO (Subsection 4.3.2), Pareto termi-

nology in MOO (Subsection 4.3.3) and some well-known metaheuristics for MOO (Subsection 4.3.4).

4.3.1 The multi-objective optimisation problem

The MOO problem for K objectives, D decision variables and $M+Q$ constraints is defined by

$$\begin{aligned} \text{Minimise } \mathbf{f(x)} &= [f_1(\mathbf{x}), f_2(\mathbf{x}), \ldots, f_K(\mathbf{x})]^T && (4.4)\\ \text{subject to } \mathbf{x} &\in \Omega && (4.5)\\ \Omega &= \{\mathbf{x} \mid g_i(\mathbf{x}) \leq 0, i = 1, 2, \ldots, M; && (4.6)\\ h_j(\mathbf{x}) &= 0,\ j = 1, 2, \ldots, Q\} && (4.7) \end{aligned}$$

where $\mathbf{x} = [x_1, x_2, \ldots, x_D]^T$ is a D dimensional vector of decision variables.

Each x_i $(i = 1, 2, \ldots, D)$ can be real-valued, integer-valued or boolean-valued and is constrained within some feasible set Ω, which consists of M equality constraints g_i and Q inequality constraints h_j. The degrees of freedom is given by $M - Q$ and, to avoid an overconstrained problem, it is required that $Q < M$ (Bekker, 2012).

Solutions in the objective space (domain $\mathbb{R}^K$) are formed by many combinations of decision variables in the decision space (domain $\mathbb{R}^D$). This is illustrated in Figure 4.2, for an MOO problem with two objectives and two decision variables (Bekker, 2012; Scholtz, 2014).

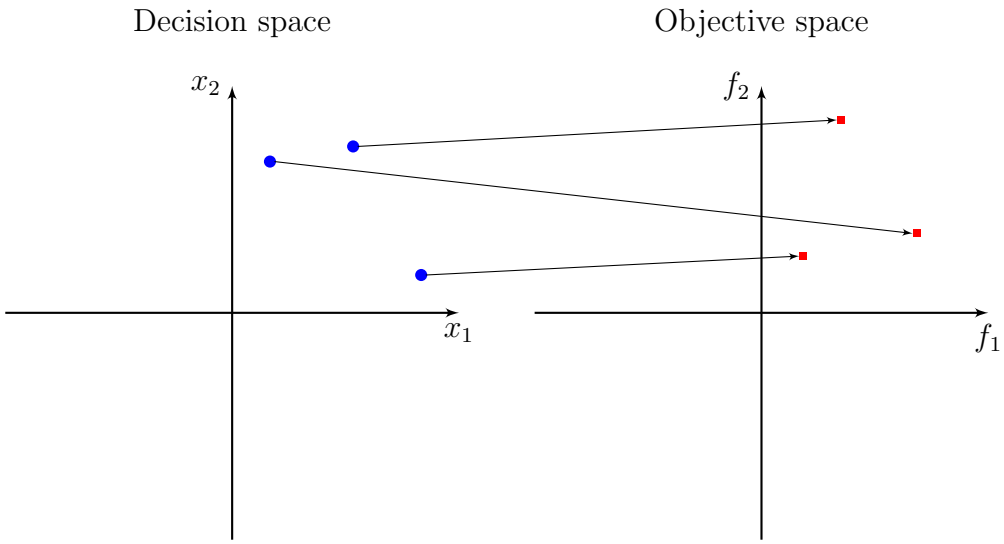

Figure 4.2: MOO mapping.

4.3.2 Approaches to multi-objective optimisation

Approaches for solving MOO problems can be broadly organised into two categories: *scalarisation approaches* and *Pareto approaches* (De Weck, 2004).

In scalarisation approaches, the MOO problem is solved by translating it back to a single-objective problem (or a series of single-objective problems). The preferences of the decision maker must thus be incorporated into the optimisation model *before* solutions are found. These approaches are therefore often called *priori* (De Weck, 2004; Scholtz, 2014). A few examples are the *weighted sum approach*, *lexicographic ordering* and *goal programming*. The weighted sum approach involves assigning weights to the various objective functions after which they are summed together to form a single objective function. In lexicographic ordering, the objective functions are optimised one at a time starting with the one considered to be most important. This is done without lowering the quality of the previously found objective values. In goal programming, each objective function is associated with a target value. Deviations from the target values are minimised using the weighted sum approach or lexicographic ordering (Scholtz, 2014).

Pareto approaches differ from scalarisation approaches in that they do not admit a unique solution but a set of solutions based on the concept of *Pareto-optimality* (see Subsection 4.3.3). Pareto-based MOO techniques are referred to as *posteriori* methods because the decision-maker's preferences are incorporated *after* the optimisation model is solved (De Weck, 2004; Scholtz, 2014). The MOO metaheuristics discussed in Subsection 4.3.4 belong to this category.

De Weck (2004) also mentions a third category of MOO approaches in which the preferences of the decision maker are taken into account during optimisation. However, these approaches are not as well developed.

4.3.3 Pareto terminology

Since MOO problems have at least two conflicting objective functions, the notion of "optimum" changes. Many acceptable solutions exist for a given problem and the aim is to find good "trade-offs" between the various objective functions (Bekker, 2012; Coello *et al.*, 2007).

To solve an MOO problem, a set of decision variable vectors, known as the *Pareto optimal set*, must be found. Given this, the following definitions from Coello *et al.* (2007) are necessary (minimisation is assumed):

Definition 1 (Pareto dominance): For two vectors $\mathbf{u}$ and $\mathbf{v}$, both in domain $\mathbb{R}^K$, $\mathbf{u}$ is said to *dominate* $\mathbf{v}$ ($\mathbf{u} \prec \mathbf{v}$) if $\mathbf{u} < \mathbf{v}$.

Definition 2 (Pareto optimality): For a given MOO problem, solution $\mathbf{x}^* \in \Omega$ is said to be *Pareto optimal* if and only if no $\mathbf{x} \in \Omega$ exist for which $\mathbf{f(x)}$ *dominates* $\mathbf{f(x^*)}$.

Definition 3 (Pareto optimal set): The *Pareto optimal set* is defined as $\mathcal{P}^* = \{\mathbf{x} \in \Omega \mid \mathbf{x} = \mathbf{x}^*\}$.

Definition 4 (Pareto front): The *Pareto front* is defined as $\mathcal{PF}^* = \{\mathbf{f(x)} \in \mathbb{R}^K \mid \mathbf{x} \in \mathcal{P}^*\}$.

Figure 4.3 shows a Pareto front for an MOO problem in which two objectives are minimised. All members of the Pareto front (blue dots) are *non-dominated*.

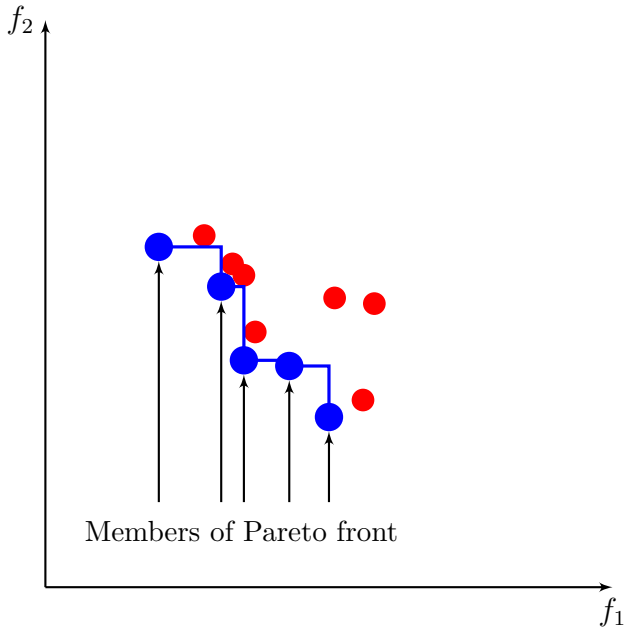

Figure 4.3: Pareto front explained for two minimised objectives.

4.3.4 Metaheuristics for multi-objective optimisation

Similar to the single-objective case, metaheuristics are the preferred approach for SO when multiple objectives are involved. Several single-solution based and population-based metaheuristics have successfully been adapted to approximately solve MOO problems. Evolutionary algorithms (EAs) have been found to be particularly suitable for MOO problems since they simultaneously deal with a population of possible solutions. Several members of the Pareto optimal set can thus be obtained with a single run of the algorithm (Coello *et al.*, 2007).

For many complex problems it is often not possible to generate the entire Pareto optimal set. Therefore, Zitzler (1999) mentions that the optimisation goal for MOO problems may be reformulated based on the following three objectives:

1. The distance between the Pareto front and the non-dominated front obtained by the metaheuristic should be minimised.

2. A good distribution of solutions is desired.

3. The non-dominated solutions should cover a wide range of values for each objective function.

Given this, two main problems must be addressed when applying a metaheuristic to an MOO problem (Zitzler, 1999). First, in order to guide the search towards the non-dominated set, the fitness assignment and selection must allow for multiple objectives. *Pareto ranking*, which is based on the work of Goldberg (1989), is the best-known ranking method. This algorithm is described in Subsection 5.3.1. The second problem involves maintaining a diverse population to prevent premature convergence. The metaheuristic must thus perform a multi-modal search, which will allow for a widely distributed and well-spread Pareto optimal set to be found. A few frequently-used methods for maintaining population diversity are discussed in Zitzler (1999).

The following are some of the best-known EAs for MOO:

- *multi-objective genetic algorithm* (Fonseca & Fleming, 1993)
- *niched-Pareto genetic algorithm* (Erickson *et al.*, 1999)
- *strength Pareto evolutionary algorithm* (Zitzler & Thiele, 1999)
- *Pareto archived evolution strategy* (Knowles & Corne, 2000)
- *multi-objective messy genetic algorithm* (Van Veldhuizen & Lamont, 2000)
- *Pareto envelope-based selection algorithm* (Corne *et al.*, 2000)
- *non-dominated sorting genetic algorithm* (Deb *et al.*, 2002).

Each of the above algorithms and some of their variants are discussed in chapter 2 of Coello *et al.* (2007).

4.4 Summary: Chapter 4

This chapter presented literature on SO, with the main focus on MOO. Since several in-depth literature studies have been done on both SO and MOO, this chapter only included some basic principles and important concepts while also providing references for a few well-known solution techniques.

The aim of this chapter was to gain sufficient knowledge of SO and MOO in order to first, formulate a multi-objective coal inventory model for the energy flow simulator (EFS) and secondly, to be able to integrate an appropriate MOO algorithm with the EFS to solve the proposed model.

The model formulation and solution approach follows in Chapter 5.

Chapter 5

Multi-objective model formulation and solution approach

Chapter 3 described the existing energy flow simulator (EFS) and the proposed modifications to it while Chapter 4 presented literature on simulation optimisation (SO). In this chapter, the multi-objective coal inventory model is formulated using the outputs of the EFS, and the solution approach for the inventory model is discussed.

Some general concepts related to inventory models are presented as background to the chapter. The importance of managing coal stockpiles as well as Eskom's inventory management policy at its coal-fired power stations are also discussed. Thereafter, the proposed model formulation and solution approach are presented. This includes a detailed description of the multi-objective optimisation (MOO) algorithm that was selected for solving the model and a brief discussion on how the algorithm is applied to this study.

5.1 Background to Chapter 5

The introductory literature study in Chapter 2 presented a broad overview of power station logistics systems (see Section 2.3). A clear conclusion from the

study was that the management of coal inventory levels are crucial throughout the supply chain of coal-fired power stations.

In this section, which serves as background to the chapter, some general concepts related to inventory models are briefly discussed. This is followed by a discussion on the importance of managing coal stockpiles and an overview of Eskom's inventory management policy.

5.1.1 Inventory models

Inventory management generally refers to the making of optimal decisions to keep inventory costs as low as possible while also satisfying customer needs. According to Mercado (2007) inventory problems can be simplified by asking the following three questions:

1. What and how much inventory is currently on hand?
2. What and how much is required?
3. When and how much of each inventory item should be ordered?

A major reason for carrying *inventory* within an organisation is related to *safety stock*. Safety stock provides a way of protecting organisations against fluctuations in *demand* and unreliability of *supply* (Toomey, 2000).

The costs associated with inventory systems typically include *ordering cost*, *purchasing cost*, *holding cost* and *shortage cost*. The ordering cost includes all the costs associated with placing an order. It is independent of the *order quantity*. Purchasing cost and holding cost are both variable costs. The first is associated with purchasing a single unit while the latter is the cost of carrying a single unit for one time period. A shortage cost is incurred when a product is demanded and the demand cannot be met. In some situations, customers will accept the purchased items at a later date. When this is the case, it is said that demand may be *back-ordered* (Winston, 2004).

The inventory strategies employed by firms are almost always based on some form of model (Muckstadt & Sapra, 2010). The *economic order quantity* (EOQ) method is a common approach for modelling deterministic inventory systems.

The EOQ formula was developed in 1915 by FW Harris to help stockkeepers determine the number of products that should be purchased (Muller, 2003). The model is based on the following assumptions (Winston, 2004):

- **Repetitive ordering:** Orders are placed repetitively based on the depletion of inventory. Also, orders arrive in a single batch and both stockouts and back orders are not allowed.
- **Constant demand:** Demand is known and occurs at a constant rate.
- **Constant lead time:** The lead time, which is the length of time between an order placement and the arrival of the order, is a known constant.
- **Continuous ordering:** Orders may be placed at any time, which means that the on-hand inventory is reviewed continuously. Models that allow for this are known as *continuous review models*. In contrast, *periodic review models* can be used when orders may only be placed periodically.

Since these assumptions do not reflect the real world, several variations of the EOQ model have been developed. Each allows for the optimal order quantity, reorder level, total cost, average inventory level and maximum inventory level to be determined (Muller, 2003). Variations of the EOQ model that allow for quantity discounts, continuous arrivals, back orders and multiple products are discussed in chapter 15 of Winston (2004).

The EOQ model has also been adapted for the case where demand is uncertain, in the form of the (r, q) and (s, S) inventory models. The aim is to determine the reorder level (or reorder point) and reorder quantity, such that the average holding cost is kept at a minimum. For an (r, q) inventory policy, a certain quantity is ordered at the exact moment when the inventory level reaches the reorder point. An (s, S) policy, on the other hand, allows for the inventory level to "undershoot" the reorder point. Thus, an order may be triggered when the inventory level is less than the reorder point. For situations where the number of items on demand may be greater than one, (s, S) policies have proven to be optimal and (r, q) policies not (Winston, 2004). The characteristics of the (s, S) inventory process are shown in Figure 5.1.

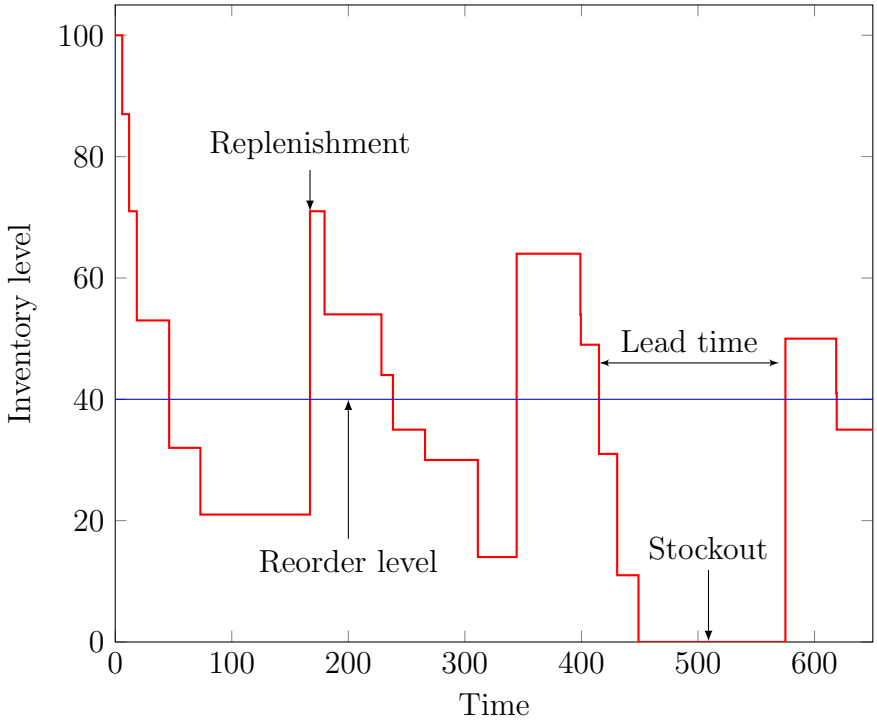

Figure 5.1: Characteristics of the (s, S) inventory process.

5.1.2 Why manage coal stockpiles?

As discussed in Subsection 5.1.1, organisations carry inventory to accommodate uncertainties in supply and demand. This also applies for coal-fired power stations and, similar to any other inventory system, a minimum holding cost is desired. However, the cost associated with storing coal is not the only reason for keeping inventory levels as low as possible. Coal stockpiles that are exposed to certain weather conditions for a period of time can have very damaging consequences.

When a coal stockpile is exposed to oxygen, the percolation of air through the stockpile will result in a measurable rise in temperature. If the heat generated from the hot air is greater than the heat dissipated from the stockpile, the temperature of the coal itself will rise (Pone *et al.*, 2007). This occurrence is commonly known as *self-heating* (Taraba *et al.*, 2014). Coal stockpiles that continue to self-heat are at risk of *spontaneous combustion*. This not only holds safety risks but, according to Ozdeniz *et al.* (2008) combustion within a stockpile

significantly decreases the quality of the coal. Banerjee *et al.* (2000) mention that, regardless of whether a fire occurs or not, an increase in temperature is enough to cause *weathering* of the coal. This means that certain properties of the coal, most notably the calorific value (CV), will gradually be impaired. Under windy conditions, the air that enters a stockpile plays a more complex role. On the one hand the oxidation process becomes more intense while on the other hand, the stockpile cools down (Taraba *et al.*, 2014).

Coal stockpiles are also affected by exposure to water. According to Banerjee *et al.* (2000) an economic way to stop weathering is to keep coal at its saturated moisture level. This can be done by frequent watering of the stockpiles. Improper watering as well as heavy rain can, however, promote the oxidation process. The reason for this is that, as water is first absorbed and then desorbed, the coal matrix swells and shrinks. This causes the coal structure to disintegrate, leading to a higher rate of oxidation (Pone *et al.*, 2007). Another effect of excessive rainfall on stockpiled coal is the significant quantities of sediments and pollutants that are delivered to receiving water bodies through water run-off. Curran *et al.* (2002) conducted a study on this.

5.1.3 Inventory management at Eskom's coal-fired power stations

Eskom's coal-fired power stations represent continuous systems in that a certain load is constantly produced and fed into the transmission network. Also, coal arrives every day at different times and in quantities that vary from one delivery to the next. After arriving from the mines via conveyor, road or rail transportation systems, the coal is stored on large stockpiles at the power stations. The coal requirements for each station are stipulated in the supply contracts, which means that no further processing of the coal is necessary after it is delivered. Coal properties (CV, ash content, etc.) are tested every day to ensure that all requirements are met. Also specified in the supply contracts is the quantity to be delivered to each station over a certain period of time.

Eskom's primary client is essentially the South African economy and since the system is heavily constrained at present, coal stockouts have serious consequences.

To obviate the unreliability of coal deliveries, the effects of using lower-quality coal and the fluctuations in electricity demand, Eskom employs an inventory management policy by which it attempts to maintain a certain inventory level at each coal-fired power station. This is referred to as the *target stockpile level*. When a given station's inventory level drops below the target, it indicates that the station is burning coal at a faster rate than the suppliers are delivering. The ideal is to keep all stockpiles above their target levels. The long-term nature of the coal supply contracts presents a challenge in managing inventory at the power stations in that emergency deliveries and order cancellations are not an option. In times of inventory shortages, Eskom is thus forced to redirect deliveries or move inventory between the stations. There are, however, certain constraints involved since each power station is designed to burn coal with specific properties.

In 2008, South Africa started experiencing electricity shortages which forced Eskom to introduce load shedding. Several factors contributed to this, including depleted stockpile levels at some of the coal-fired power stations (Hatton, 2015). At the time, a target stockpile level of 20 stockpile days was the norm for each station. Senior management took action by increasing this number to 42 stockpile days. Figure 5.2 from Hatton (2015) shows the total value of coal reserves (in ZAR) at Eskom's coal-fired power stations since 2002. The constant increase since 2008 is reason to believe that the change was too drastic at certain stations. Also, since each coal-fired power station has a different standard daily burn, a stockpile day is equivalent to a different amount of coal for each station. It is thus most likely that an optimal inventory management policy would involve a different target stockpile level for each coal-fired power station. The question that needs to be asked is: *what is the optimal target stockpile level for each of Eskom's coal-fired power stations?* The multi-objective inventory model described in Section 5.2 is aimed at answering this question.

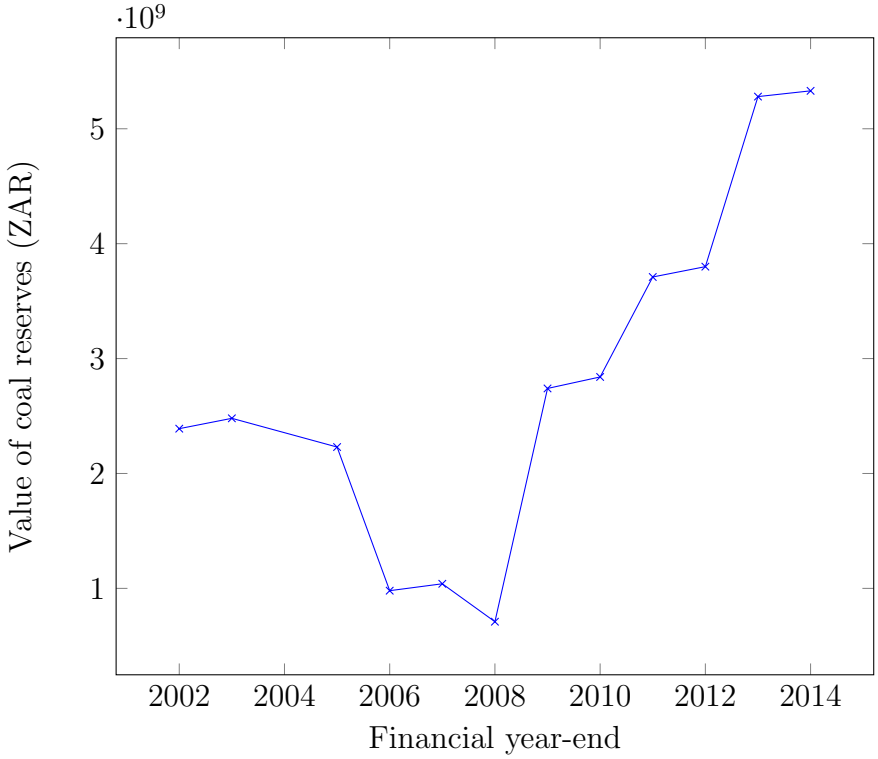

Figure 5.2: The monetary value of coal inventory on hand.

5.2 Model formulation

In this section, the proposed multi-objective inventory model for the EFS is described and the reasoning behind the modelling approach is explained. The decision variables and objectives are discussed next.

5.2.1 Decision variables

The complexity of Eskom's coal inventory system requires a different modelling approach to the inventory models discussed in Subsection 5.1.1. First consider a "classical" inventory system: stock is depleted based on the demand, which is generally stochastic for real-world systems. Upon reaching a specific reorder point, an order is placed to replenish inventory to a certain level. The order arrives after a certain lead time, during which the on-hand inventory continues

to be depleted. This process repeats itself. Now consider Eskom's situation: there are 14 coal-fired power stations that make up the inventory system, with two more to be introduced in the near future. Coal demand at a given station is not only based on the station's electricity production requirements but also on the quality of the coal. Inventory is replenished every day regardless of the current stockpile level. There is thus no reorder point. Also, the amount of coal that arrives vary from one day to the next and, as discussed in Subsection 5.1.3, emergency deliveries and order cancellations are not an option. However, coal can be moved between certain stations in emergency situations.

For this study, the stockpile at each coal-fired power station s ($s = 4, 5, \ldots, 19$) is simulated by the modified primary energy (PE) module described in Subsection 3.7.3. Recall that the PE module is a Monte Carlo simulation model that adds *noise* to the planned electricity generation and planned coal deliveries, which are produced by the production planning (PP) and fuel planning (FP) modules respectively. The noise is added in the form of uncertainty with regard to *unplanned maintenance*, *coal quality* and *delivery reliability*. The unplanned maintenance and coal quality at a particular power station affect the amount of coal being burnt by the station. Ideally, coal delivery and burn should balance each other out so that the target stockpile level (T_s) can be maintained. However, this is almost never the case in the real world.

Two hypothetical simulation scenarios for extreme variation between coal delivery and burn at a power station are shown in Figure 5.3. *Scenario 1* on the left may illustrate low delivery reliability. The effective decrease in stockpile level may also be as a result of poor coal quality or less unplanned maintenance than was expected. *Scenario 2* illustrates the opposite, where the amount of coal delivered is significantly more than the coal burnt. A typical case would involve a combination of the two scenarios throughout the course of a year, as shown in Figure 5.4, where the inventory level fluctuates around the target stockpile level.

The idea for the proposed inventory model is to allow coal transfers between the various coal-fired power stations when inventory levels become very high or dangerously low. To achieve this, two *transfer levels*, called the *lower warning limit* (L_s) and the *upper warning limit* (U_s), are required for each coal-fired station s to trigger the movement of coal.

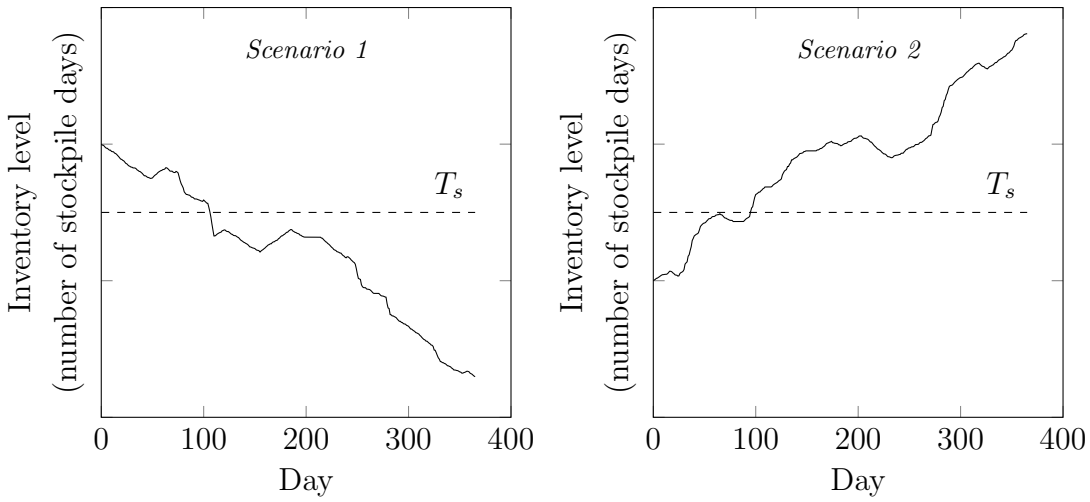

Figure 5.3: Two hypothetical scenarios for extreme variation between coal delivery and burn.

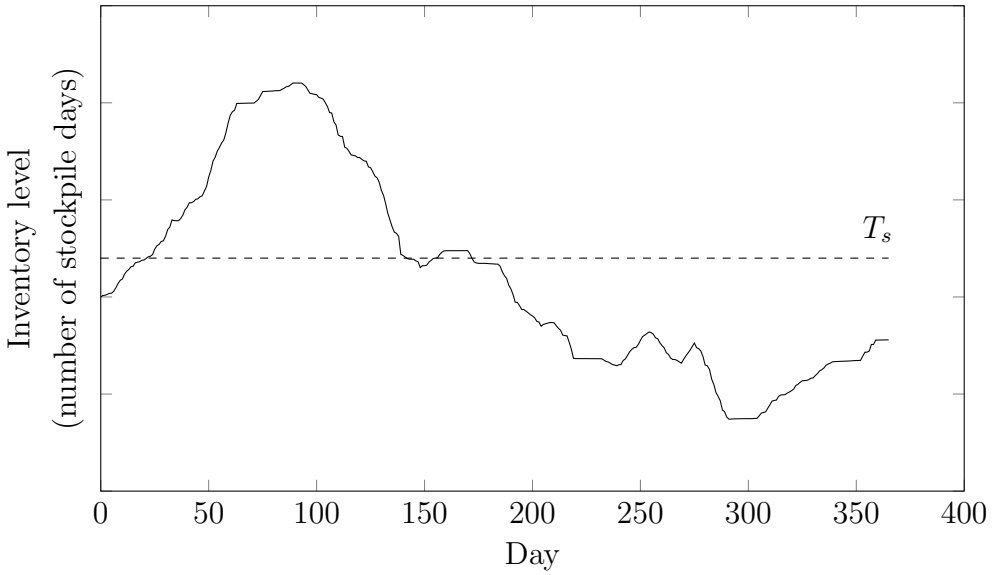

Figure 5.4: Hypothetical scenario for typical variation between coal delivery and burn.

After every day d, each coal-fired power station's stockpile level at the end of the day ($S_{s,d}$) is evaluated to determine whether transfers are required. When a given station's stockpile is depleted below L_s, inventory is replenished by transferring coal from one or more of the other stations. Similarly, when a given station's stockpile becomes more than U_s, coal is transferred to some of the other stations in order to reduce the inventory level. Both L_s and U_s are decision variables for the inventory model, and since the main goal is to determine each T_s, it also has to be included as a decision variable. The best way to trigger T_s is to **only** allow a transfer when, for at least one of the stations involved in the *transaction*, the stockpile level can be forced towards T_s. Furthermore, coal can **only** be moved between power stations capable of burning similar coal. All transfers are expressed in terms of the station from which the coal is moved. The coal transferred from power station s on day d is denoted by $Y_{s,d}$. The basic constraints on the decision variables are

$$L_s < T_s < U_s \qquad \forall s, \tag{5.1}$$

$$L_s > 0 \qquad \forall s, \tag{5.2}$$

$$L_s, T_s, U_s \in \mathbb{Z}^+ \qquad \forall s. \tag{5.3}$$

To simplify Eskom's complex inventory system, the following assumptions are made:

1. L_s, T_s and U_s must be positive integers when expressed in terms of stockpile days.

2. There is no limit on the maximum stockpile level at any of the power stations.

3. No constraints are placed on the amount of coal that can be moved during a transfer transaction.

4. Transfers are allowed on any day throughout the course of the study period and there is no limit on the number of transfers that may be made.

5. All lead times are one day. Thus, if a coal transfer is triggered on a given day d, the changes to the stockpiles are visible on day $d+1$.

One of the experiments presented in Chapter 6 involves adding additional constraints to the model in order for assumptions 3 and 4 to be discarded.

For a better description of the coal transfer functions, consider the following: two coal-fired power stations, $s = A$ and $s = B$, are capable of burning coal of similar quality. One stockpile day is equivalent to the same amount of coal for both stations. If $S_{A,d} < L_A$ becomes true on a given day d, a transfer is sought from station B. However, coal may only be moved if $S_{B,d} > T_B$. If this condition is true, the amount of coal transferred from B to A on day $d+1$ is calculated by

$$Y_{B,d+1} = \min\{S_{B,d} - T_B; T_A - S_{A,d}\}. \tag{5.4}$$

After incorporating both the actual delivery and burn on day $d+1$, $S_{B,d+1}$ and $S_{A,d+1}$ are adjusted according to

$$S_{B,d+1} \leftarrow S_{B,d+1} - Y_{B,d+1} \tag{5.5}$$

and

$$S_{A,d+1} \leftarrow S_{A,d+1} + Y_{B,d+1} \tag{5.6}$$

respectively.

Figure 5.5 illustrates the characteristics of coal transfers between power stations A and B with another example. Two transactions occur on the plot, one on day $d = 111$ and one on day $d = 248$. At $d = 110$, the stockpile at station A reached L_A. This resulted in a transfer $Y_{B,111}$ to station A, which forced the inventory at station A to T_A. At $d = 247$, the stockpile at station B reached L_B. A transfer $Y_{A,248}$ was made from station A, which forced the inventory at station B to T_B.

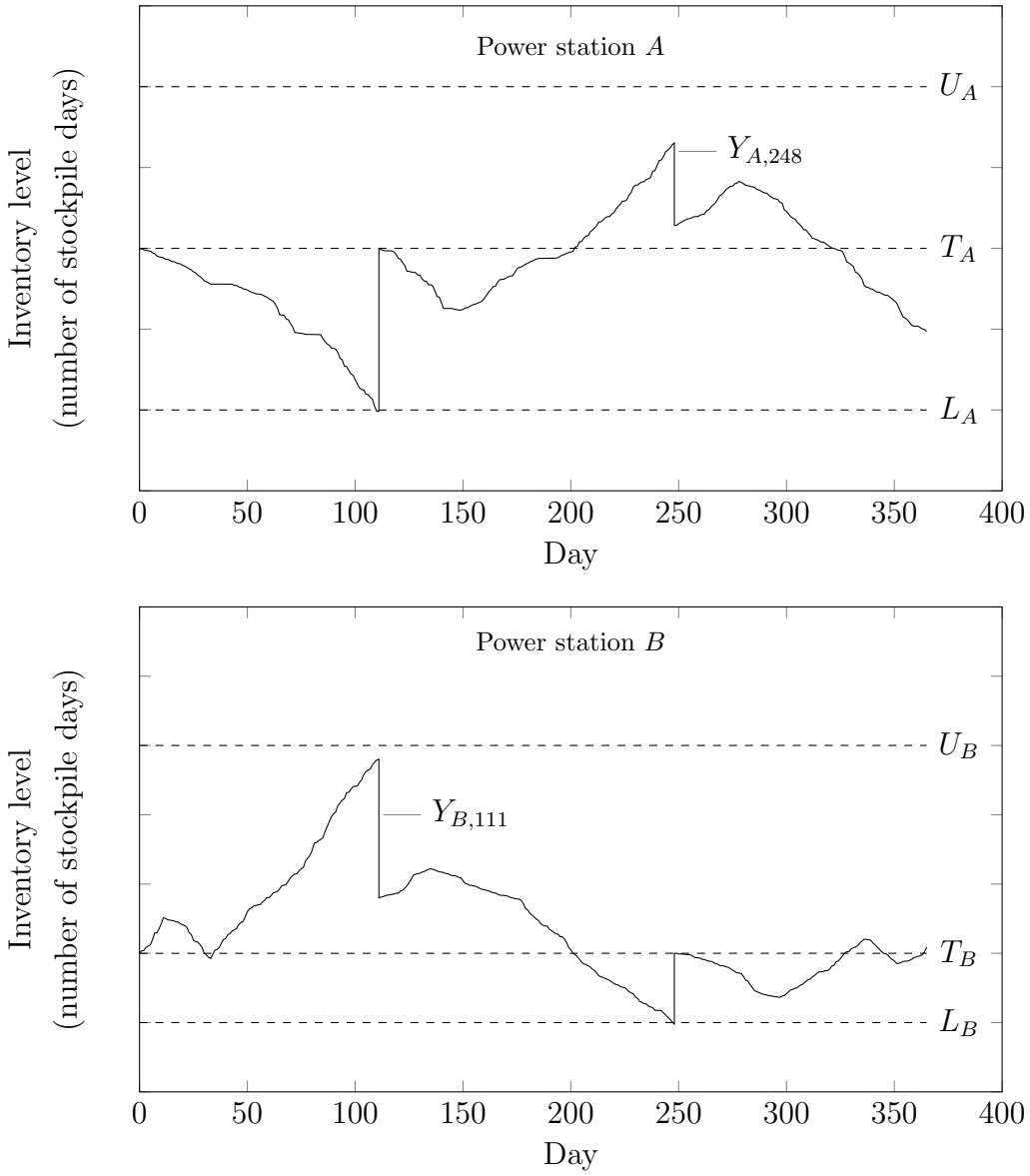

Figure 5.5: Characteristics of the coal transfer functions.

The power stations at which $S_{s,d} < L_s$ receive priority (i.e. coal transfers for them are sought first) and the stations are *served* in descending order based on the difference between $S_{s,d}$ and L_s. Two policies are proposed for selecting the power stations involved in a transfer transaction:

1. **Closest first:** If a given power station requires coal ($S_{s,d} < L_s$), the stations from which the transfer will be made are selected by considering the closest one first. Similarly, if a given power station has too much coal ($S_{s,d} > U_s$), the stations to which the transfer is made are selected by considering the closest one first.

2. **Most urgent:** If a given power station requires coal, the stations from which the transfer is made are selected by first considering the one at which $S_{s,d}$ is furthest above T_s. Similarly, if a given station has too much coal, the stations to which the transfer is made are selected by first considering the one at which $S_{s,d}$ is furthest below T_s.

Both policies are experimented with in Chapter 6.

5.2.2 Objective functions

The first objective proposed for the model is to minimise the *total average coal stockpile level* ($\bar{S}$), measured in ktonnes. This is a relatively standard objective for inventory management models. Assuming a study period of $d = 365$ days, $\bar{S}$ is given by

$$\bar{S} = \sum_{s=4}^{19} \left(\frac{\sum_{d=1}^{365} S_{s,d}}{365} \right). \tag{5.7}$$

As a second objective, it is proposed that the *total coal transfers* (Z) throughout the course of the study period be minimised. This is given by

$$Z = \sum_{s=4}^{19} \sum_{d=1}^{365} Y_{s,d} X_{sd} \tag{5.8}$$

where X_{sd} is the total distance (in km) of coal transfers from power station s on day d. The unit of measurement for Z is thus ktonnes·km.

Equation (5.7) is aimed at obtaining low values for all T_s. Equation (5.8), on the other hand, is aimed at spacing L_s, T_s and U_s so that coal is transferred

optimally, since there is a trade-off between large coal transfers that occur occasionally and frequent smaller transfers. The two objectives are conflicting and the combinatorial nature of the problem makes it impossible to predict "good" solutions without an optimisation algorithm.

The main problem with the manner in which the coal transfers are triggered in this model is that some power stations may, throughout the course of the study period, seek to increase or decrease their inventory levels without a transfer ever becoming available. The stockpiles at these stations would thus only change based on the stochastic variation of the simulation model. This opens the door for possible coal stockouts as well as periods during which inventory levels rise very high.

In an attempt to deal with this problem, another objective is proposed, namely that of minimising the *total average coal inventory outside the warning limits* ($\bar{R}$). Also measured in ktonnes, $\bar{R}$ is given by

$$\bar{R} = \sum_{s=4}^{19} \left(\frac{\sum_{d=1}^{365}(S_{s,d} - U_s) + \sum_{d=1}^{365}(L_s - S_{s,d})}{365} \right). \tag{5.9}$$

Equation (5.9) is aimed at obtaining solutions for which the coal stockpiles are maintained between L_s and U_s as far as possible.

Since this study is primarily an investigation of whether MOO capability can successfully be added to the EFS, it was decided to only incorporate two of the three objectives at a time. This simplifies the analysis of experimental results.

The following is subsequently proposed: two model formulations, each with two conflicting objectives (f_1 and f_2), where f_1 is (5.7) for both models and f_2 is (5.8) for *model 1* and (5.9) for *model 2*.

The solution approach to solving the inventory model is discussed next.

5.3 Solution approach

Multi-objective optimisation using the cross-entropy method (MOO CEM) was selected as a suitable approach for solving the inventory model described in Subsection 5.2. The MOO CEM algorithm is a population-based metaheuristic. It is

not inspired by evolutionary theory or any other natural process, but by statistical principles.

The *cross-entropy method* (CEM) for optimisation is a versatile Monte Carlo method, developed by Rubinstein & Kroese (2004). The approach was motivated by the work of Rubinstein (1997) on variance minimisation methods for rare-event probability estimation and modified in Rubinstein (1999) to solve continuous and combinatorial optimisation problems (Kroese *et al.*, 2006, 2013). In contrast to a random search algorithm that searches for an optimal solution by sampling decision variable values from the same probability density function (pdf), the CEM assigns a pdf to each decision variable. The search works on the principle that the parameters of each of these pdfs are iteratively adjusted in order to increase the probability of drawing decision variables that result in good objective function values. The aim of the CEM is to estimate the parameters of each decision variable's ideal pdf in order for them to converge to an optimal (or near optimal) solution. The algorithm does this by using the *cross-entropy* (or *Kullback-Leibler distance*). As a measure of the distance between two pdfs, a minimum cross-entropy is desired between the sampling distribution associated with each decision variable and the optimal pdf from which to sample (Rubinstein & Kroese, 2004; Scholtz, 2014).

The CEM has been proven to converge quickly when applied to optimisation problems with one objective. It is thus an ideal approach for the computationally expensive time-dependent problems often encountered in simulation optimisation (SO). This was the motivational factor for expanding the CEM to solve multi-objective problems. The MOO CEM was introduced by Bekker & Aldrich (2010) and Bekker (2012), and has since been the topic of multiple research studies.

In the remainder of this section, a detailed description of the MOO CEM is presented. This is followed by a survey of some existing research and applications of the MOO CEM. The section is concluded with a discussion on how the algorithm is applied to this study.

5.3.1 The cross-entropy method for multi-objective optimisation

The MOO CEM algorithm described here is based on the main CEM algorithm of Rubinstein & Kroese (2004), also outlined in Bekker & Aldrich (2010) and Bekker (2012).

Since the Pareto optimal set of an MOO problem very often contains multiple solutions, Bekker & Aldrich (2010) suggested expanding the CEM in order to find the set of parameter vectors for the non-dominated set of solutions. To do this, the algorithm requires a working matrix $\mathbf{W}$ consisting of $D+K+1$ columns and N rows, where D is the number of decision variables, K is the number of objectives and N is the number of solutions in the population. Columns 1 to D of the matrix are populated by sampling a vector of size N for each decision variable from a truncated normal distribution, where the sample $\mathbf{X}_i$ $(1 \leq i \leq D)$ is formed from the density $h_i(\cdot; \hat{\mathbf{v}}_{t-1})$. The truncated normal distribution ϕ_i, with mean μ_i and standard deviation σ_i, is given by

$$\phi_i(x) = \begin{cases} 0, & x < a_i \\ \frac{h_n(x)}{\int_{b_i}^{a_i} h_n(x)dx}, & a_i \leq x \leq b_i \\ 0, & x > b_i \end{cases} \tag{5.10}$$

where a_i and b_i are the limits of the range on which decision variable x_i is defined and the function $h_n(x)$ is the normal pdf defined on $-\infty < x < \infty$. An arbitrary large initial value for σ_i is required, using $\sigma_i = 10 \cdot (b_i - a_i)$ (Bekker, 2012).

Forming sample vectors like this makes it easy to contain the search (Bekker, 2012).

After populating the first D columns of the working matrix, the objective functions are evaluated for each of the N row vectors. The performance measures $f_j(\mathbf{X})$ with $1 \leq j \leq K$ for each row vector are stored in columns $D+1$ to $D+K$ of the matrix (Bekker & Aldrich, 2010).

To find the best combinations of objective functions, the Pareto ranking method of Goldberg (1989) is used. Presented in pseudo-code as Algorithm 1 (Bekker, 2012), the Pareto ranking method works as follows: in the working matrix, the columns numbered $D+i-1$ $(1 < i \leq K)$ are sorted consecutively. After

column $i = D + K - 1$ is sorted, the $(i+1)$-th column is ranked. The ranking value of a given solution indicates the number of other solutions in the population by which it is dominated. These values are stored in column $D + K + 1$ of the working matrix. A rank of $\rho = 0$ indicates that the solution is non-dominated. Each solution for which ρ is less or equal to a specified threshold value ρ_E is appended to the current (weakly) non-dominated set or the elite vector called *Elite* (Bekker & Aldrich, 2010).

Algorithm 1 Pareto ranking algorithm (Minimisation)

1: Input: working matrix $\mathbf{W}$ with N rows and $D + K + 1$ columns, and user-selected threshold ρ_E.
2: $j \leftarrow D + 1$.
3: Sort the working matrix $\mathbf{W}$ with the values in column j in *descending* order.
4: $r_p \leftarrow 1$.
5: $r_q \leftarrow r_p$.
6: If $\mathbf{W}(r_p, j+1) \geq \mathbf{W}(r_q + 1, j + 1)$, increment the rank value ρ_{r_p} in $\mathbf{W}(r_p, D + K + 1)$.
7: $r_q \leftarrow r_q + 1$.
8: If $\mathbf{W}(r_p, D + K + 1) < \rho_E$ and $r_q < N$, return to Step 6.
9: $r_p \leftarrow r_p + 1$.
10: If $r_p < N$, return to Step 5.
11: $j \leftarrow j + 1$.
12: If $j < D + K - 1$, return to Step 3, otherwise return the rows in $\mathbf{W}$ with rank value not exceeding ρ_E as the weakly or non-dominated vector *Elite*.

The values in the elite vector are used to construct a histogram for each decision variable x_i, $1 \leq i \leq D$. Each histogram contains $r + 2$ classes, where r is determined by the outer loop of the algorithm. The histogram for a decision variable x_i defined on the range $[a_i, b_i]$ is constructed as follows: for the first class, the lower boundary is set equal to a_i and the upper boundary is set equal to the minimum value of x_i in the elite vector, namely $\min(Elite(\cdot, i))$. For the last class, the upper boundary is set equal to b_i and the lower boundary is set equal to the maximum value of x_i in the elite vector, i.e. $\max(Elite(\cdot, i))$.

The remaining classes are of equal size and are formed using $(\max(Elite(\cdot, i)) - \min(Elite(\cdot, i)))/r$. The class boundaries for the histogram of x_i are recorded in a vector $\mathbf{C}_i = \{c_{i1}, c_{i2}, \ldots, c_{i(r+2)}, c_{i(r+2)+1}\}$, i.e. $[c_{i1}, c_{i2}]$ is the width of the first class, $[c_{i2}, c_{i3}]$ is the width of the second class, and so on. The frequency values for each class are recorded in a vector $\mathbf{R}_i = \{\tau_{i1}, \tau_{i2}, \ldots, \tau_{i(r+1)}, \tau_{i(r+2)}\}$, where $\tau_{i\kappa}$ is the frequency count of x_i in the range $[c_{i\kappa}, c_{i(\kappa+1)})$ (Bekker, 2012). An example of a histogram is shown in Figure 5.6.

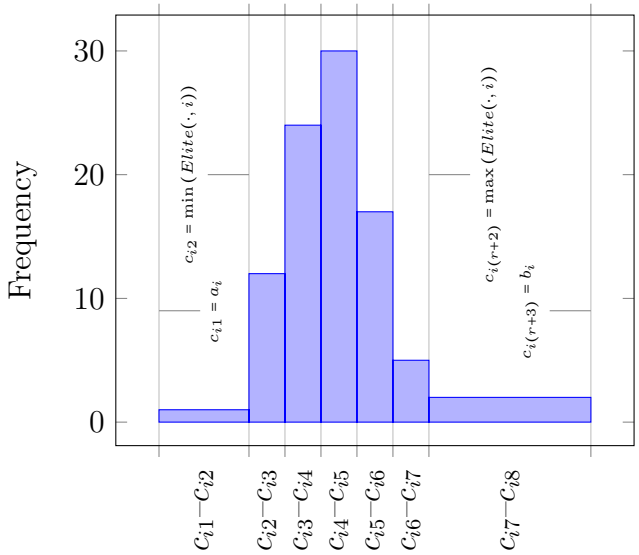

Figure 5.6: Example of a histogram for the decision variable x_i.

The histograms are used to generate a new population of size N for the next iteration of the algorithm. First, however, each histogram is inverted with a pre-set probability p_h in order to prevent premature convergence. An example of a histogram before and after inversion is shown in Figure 5.7. Refer to Bekker & Aldrich (2010) for more on this very simple procedure.

The new population is created as follows: suppose the current elite vector contains E_r rows, then the decision variable vector $\mathbf{X}_i$ is formed by sampling $\lfloor N\tau_{i\kappa}/E_r \rfloor$ values from each class range $[c_{i\kappa}, c_{i(\kappa+1)})$, $1 \geq \kappa \geq r + 2$. Temporary parameters $\mu'_{i\kappa} = c_{i\kappa} + U(c_{i(\kappa+1)} - c_{i\kappa})$ and $\sigma'_{i\kappa} = (c_{i(\kappa+1)} - c_{i\kappa})$ are used for each class, where U is a uniformly distributed random number. The candidate solutions in the new population are thus proportional to the class frequencies of

the histograms that were created from the current elite vector. This guides the MOO CEM towards non-dominated solutions by allowing for the accommodation of continuous search spaces (Bekker & Aldrich, 2010).

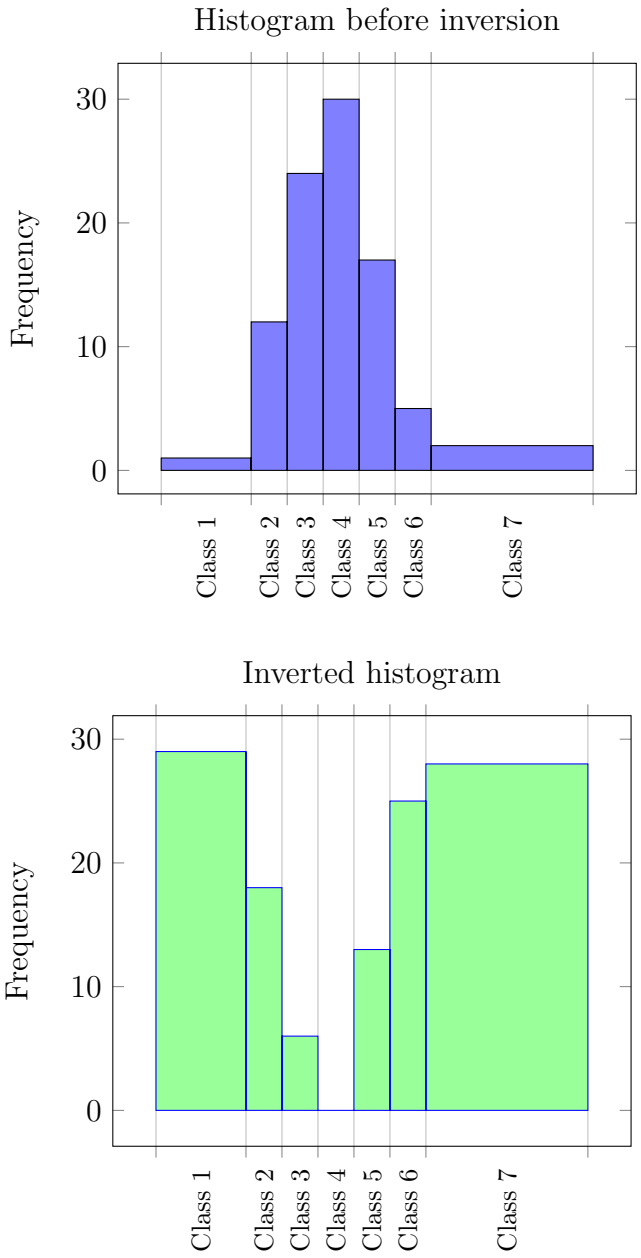

Figure 5.7: Example of an inverted histogram.

Before the algorithm proceeds to the next iteration, the values in the elite vector are used to compute $\tilde{\mathbf{v}}_{it}$, which is a parameter vector containing the mean and standard deviation of the values in $Elite(, i)$. This is used to update the current parameters μ_i and σ_i for all i, $1 \leq i \leq D$. Each vector $\hat{\mathbf{v}}_t$ is updated as follows:

$$\hat{\mathbf{v}}_t = \alpha\tilde{\mathbf{v}}_t + (1-\alpha)\hat{\mathbf{v}}_{t-1} \tag{5.11}$$

where α is the smoothing parameter (Bekker & Aldrich, 2010). This process iteratively continues until each σ_i becomes less than a specified threshold ϵ.

Refer to Rubinstein (1999) and Rubinstein & Kroese (2004) for the theoretical foundations of the CEM.

Similar to the CEM, the MOO CEM assumes independent decision variables. One would, however, expect the decision variables to be correlated for combinatorial problems. Bekker & Aldrich (2010) mention that the algorithm can maintain good combinations of decision variable values when the number of classes in each histogram is incremented as the search progresses.

In order to better exploit the decision space, the entire process is repeated for a specified number of loops (the outer loop of the algorithm). Exploration and exploitation are further supported by initially ranking the objective function values with a relaxed threshold of $\rho_E = 2$. This means that the first three non-dominated fronts are included in the initial elite vector. The solutions that remain in the elite vector for the next outer loop are ranked with a threshold of $\rho_E = 1$. Upon termination of the search, the elite vector is trimmed for a final time with a threshold of $\rho_E = 0$ in order for the final set of solutions to be completely non-dominated (Bekker & Aldrich, 2010). The MOO CEM algorithm, as presented in Bekker (2012), is given in pseudo-code as Algorithm 2.

Algorithm 2 MOO CEM Algorithm

1: Set *Elite*= $\varnothing$, $t = 1$, $k = 1$.
2: Initialise variable vectors $\mathbf{X}_i = \varnothing$, $1 \leq i \leq D$, and compute initial objective values.
3: For each decision variable x_i, $1 \leq i \leq D$, initialise a histogram class vector $\mathbf{C}_i = \{c_{i1}, c_{i2}, \ldots, c_{i(r+2)}, c_{i((r+2)+1)}\}$ and histogram frequency vector $\mathbf{R}_i = \{\tau_{i1}, \tau_{i2}, \ldots, \tau_{i(r+1)}, \tau_{i(r+2)}\}$.
4: Set $i = 1$.
5: Set $\kappa = 0$.
6: Increment κ.
7: **for** each frequency element $\tau_{i\kappa}$ in $\mathbf{R}_i$ **do**
8: Generate a class-based $\tilde{\mathbf{v}}'$ in the range $[c_{i\kappa}, c_{i(\kappa+1)})$, $1 \leq \kappa \leq r+2$.
9: Generate a subsample $\mathbf{Y}$ according to the pdf $\phi_i(\mathbf{x}_i, \tilde{\mathbf{v}}')$
10: with $\mathbf{x}_i \in [c_{i\kappa}, c_{i(\kappa+1)})$ and $|\mathbf{Y}| = \tau_{i\kappa}$, $1 \leq \kappa \leq r+2$.
11: Append $\mathbf{Y}$ to $\mathbf{X}_i$.
12: **end for**
13: If $\kappa < r+2$ return to Step 6.
14: Invert the histogram counts with probability p_h.
15: Increment i.
16: If $i \leq D$, return to Step 5.
17: Compute the NK objective function values using $\mathbf{X}_i$, $1 \leq i \leq D$.
18: Rank the objective function values using Algorithm 1 with $\rho_E = 2$ to obtain an updated elite vector *Elite*.
19: Form new histogram class vectors $\mathbf{C}_i$ and histogram frequency vectors $\mathbf{R}_i$ based on *Elite*, $1 \leq i \leq D$.
20: Use the values in *Elite* to compute $\tilde{\mathbf{v}}_{it}$ for all i, $1 \leq i \leq D$.
21: Smooth the vectors $\tilde{\mathbf{v}}_{it}$ for all i, $1 \leq i \leq D$, using (5.11).
22: If all $\sigma_{it} > \epsilon$ or less than the allowable number of evaluations has been done, increment t and reiterate from Step 4.
23: Rank *Elite* using Algorithm 1 with $\rho_E = 1$.
24: Increment k.
25: If k is smaller than the allowable number of loops, return to Step 2.
26: Rank *Elite* using Algorithm 1 with $\rho_E = 0$ to obtain the final elite set.

5.3.2 Existing research and applications of the cross-entropy method for multi-objective optimisation

Since it was first introduced, the MOO CEM algorithm described in Subsection 5.3.1 has been applied in multiple studies and to a number of different problems. Existing research and applications of the MOO CEM algorithm include the following:

1. In his PhD thesis, Bekker (2012) assessed the MOO CEM by using nine different continuous, deterministic benchmark problems. Four quality indicators were used to evaluate the algorithm's performance and the Pareto fronts achieved compared very well with the true fronts. Next, he used a discrete, deterministic problem in the form of the *vehicle routing problem* (VRP). The assessment involved optimising different combinations of the five objectives identified by Castro-Gutierrez *et al.* (2011) for VRP analysis.

2. Bekker (2012) also applied the MOO CEM to dynamic, stochastic problems, most notably, a modified version of the classical (s, S) inventory model. Solutions of such problems can only be evaluated using computer simulation. The Pareto front that was achieved compared well with a reference front obtained from a near-exhaustive enumeration. However, the MOO CEM required far fewer objective function evaluations than the near-exhaustive search.

3. The MOO CEM was evaluated in Bekker (2012) and Bekker (2013) using the *buffer allocation problem*. Once again, computer simulation was used and the conclusion was made that the algorithm is capable of estimating Pareto fronts for MOO problems with large solution spaces using fairly few objective function evaluations.

4. Stadler (2012) applied the MOO CEM in a practical research project where the aim was to optimise the utilisation of carbon monoxide gas at an ilmenite smelter in South Africa. The MOO CEM was evaluated by comparing its performance to that of another metaheuristic, the MOO genetic algorithm of Matlab®, which is a commercial version of the non-dominated

sorting genetic algorithm. The results of the comparison between the two algorithms were in favour of the MOO CEM (Bekker, 2012; Stadler, 2012).

5. Hauman (2012) successfully applied the MOO CEM to a practical inventory problem in the context of a blood supply chain in South Africa.

6. Scholtz (2014) conducted a study to determine under which circumstances the MOO CEM would be outperformed by an algorithm that accounts for relationships between decision variables (recall that the MOO CEM assumes independent decision variables). The algorithms included in the study were the multi-objective covariance matrix adaptation evolution strategy, Pareto differential evolution and two hybrid algorithms based on the MOO CEM. The results varied for different problems. It was found that the MOO CEM performed particularly well for larger problems, typically with more that a hundred decision variables.

5.3.3 The cross-entropy method for multi-objective optimisation applied to this study

In order to successfully apply the MOO CEM to this study, the algorithm had to be integrated with the primary energy (PE) module of the EFS. This, as well as the parameter settings used for the algorithm, are discussed in this subsection.

5.3.3.1 Integration with the primary energy module

The basic principles of simulation optimisation were discussed in Section 4.1. Keeping in mind the decision variables and objectives of the proposed inventory model, integration of the PE module and the MOO CEM algorithm is illustrated in Figure 5.8. During each iteration of the algorithm, N values are sampled for each decision variable using the histograms created from the current elite vector. The PE module evaluates each solution candidate in the population by running for a specified number of replications. The values returned to the algorithm depend on the output statistic (e.g. expected value). The algorithm proceeds as described in Subsection 5.3.1 by ranking the objective function values in the working matrix and appending the best solutions to the elite vector.

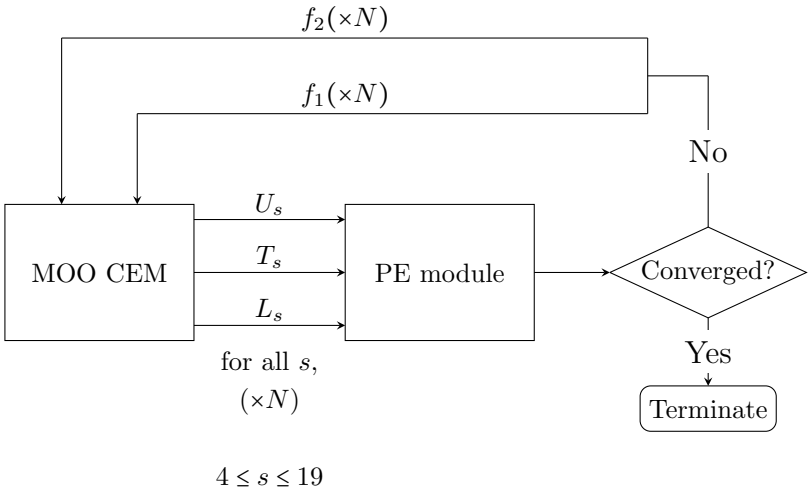

Figure 5.8: Integration of the PE module and the MOO CEM algorithm.

Since the MOO CEM assumes independent decision variables, both T_s and U_s cannot be sampled directly. For the reader to better understand what is meant by this, consider the working matrix of the MOO CEM algorithm shown in Table 5.1. For each member of the population, the three decision variables associated with the first coal-fired power station are stored in columns 1 to 3, the three decision variables associated with the second station are stored in columns 4 to 6, and so on. Say $L_4 = x_1$, $T_4 = x_2$ and $U_4 = x_3$. If L_4 is sampled on the range $[a_1, b_1]$, then T_4 cannot be sampled on a fixed range $[a_2, b_2]$ because $L_4 < T_4$, i.e. the value of a_2 depends on L_4. The same applies for U_4, because the value of a_3 is dependent on T_4.

Table 5.1: Working matrix of the MOO CEM algorithm.

Decision variables					Objectives		Rank
x_1	x_2	x_3	x_4	$\ldots$	f_1	f_2	ρ
$\vdots$	$\vdots$	$\vdots$	$\vdots$		$\vdots$	$\vdots$	$\vdots$
(for N rows)							

To deal with the problem described above, the relative "distances" between L_s, T_s and U_s are sampled and stored in the working matrix. Thus, the values to

be stored in the first three columns, x_i, $1 \leq i \leq 3$, are sampled on the range $[a_i, b_i]$ such that

$$x_1 = L_4,$$
$$x_2 = T_4 - L_4,$$
$$x_3 = U_4 - T_4.$$

This allows for each vector $\mathbf{X}_i$, $1 \leq i \leq D$, to be sampled from a fixed, independent range $[a_i, b_i]$.

5.3.3.2 Parameter settings

The parameter settings for the MOO CEM algorithm used in this study are given in Table 5.2. All parameters are set according to the recommendations provided in Bekker (2012).

Table 5.2: Parameter settings for the MOO CEM algorithm.

Description	Symbol	Value
Smoothing parameter	α	0.7
Population size	N	100
Histogram inversion probability	p_h	0.3
Common termination threshold	ϵ	0.1
Maximum evaluations	-	10 000

5.4 Summary: Chapter 5

This chapter presented the multi-objective coal inventory model formulated for the EFS as well as the solution approach for solving the model. As background to the chapter, some general principles related to inventory models were provided, the importance of managing coal stockpiles was discussed and an overview of Eskom's inventory management policy was presented.

5.4 Summary: Chapter 5

For the proposed inventory model, coal transfer functions were developed in order to allow for coal to be moved between the various coal-fired power stations when stockpile levels decrease below a lower warning limit or rise above an upper warning limit. Three objective functions were identified. However, the decision was made to only include two of these at a time and to experiment with two different formulations (*model 1* and *model 2*). The aim of the model is to determine the upper warning limit, the lower warning limit and the target stockpile level for each station by simultaneously minimising both objectives included in the model.

Multi-objective optimisation using the cross-entropy method (MOO CEM) was selected as a suitable metaheuristic for solving the inventory model approximately. A detailed description of the MOO CEM algorithm was presented, existing research and applications of the MOO CEM were surveyed and a brief discussion was included on how the algorithm is applied in this study.

The experiments and experimental results follow in Chapter 6.

Chapter 6

Experiments and results

Chapter 5 presented the proposed multi-objective coal inventory model for the energy flow simulator (EFS) as well as the multi-objective optimisation using the cross-entropy method (MOO CEM) algorithm that was selected as a suitable metaheuristic for solving the model approximately. The experiments and results are documented in this chapter.

The *baseline* inputs to the EFS and the simulation settings for the primary energy (PE) module are briefly discussed. This is followed by an overview of the experiments. Four experiments are presented. The experimental design and analysis of the experimental results are provided for each. The chapter is concluded with a summary of the findings made from the experimental results.

The experiments in this chapter serve as validation for the multi-objective simulation optimisation (SO) model while also testing the effectiveness of the MOO CEM algorithm in finding approximate solutions for the model.

6.1 Baseline inputs to the energy flow simulator

Before commencing with the experiments, it is important to first discuss the baseline inputs to the EFS.

By default, none of the new power stations are included in any of the calculations. The *normal* weather and growth domestic product scenarios are used to forecast the electricity demand in the load forecasting module and the default

datasets for the planned and unplanned outages are used to compute the energy availability factor in the production planning module.

With regard to the modified PE module, the reader may recall that the baseline variation for coal deliveries are incorporated by sampling a random number from a triangular probability density function (pdf). The most likely value was set equal to the planned coal deliveries $D_s^{(\mathrm{p})}$ while the minimum and maximum values were set equal to $0.9D_s^{(\mathrm{p})}$ and $1.1D_s^{(\mathrm{p})}$ respectively. The variation for both the calorific value (CV) and the unplanned capability loss factor (UCLF) are incorporated by sampling a random number from a standard normal pdf and then multiplying it with a certain standard deviation. The baseline CV for each coal-fired power station as well as the CV standard deviation $\sigma_s^{(\mathrm{CV})}$ and UCLF standard deviation $\sigma_s^{(\mathrm{UCLF})}$ for each is given in Table 6.1. The 14 existing coal-fired power stations are again illustrated as A to N throughout this chapter.

Table 6.1: Baseline variation for the PE module.

Power station	**CV (MJ/kg)**	$\sigma_{\mathbf{s}}^{(\mathrm{CV})}$	$\sigma_{\mathbf{s}}^{(\mathrm{UCLF})}$
A	19.65	1.5	1.4
B	15.50	1.5	3.1
C	22.85	1.5	10.0
D	22.85	1.5	5.3
E	19.65	1.5	3.9
F	22.85	1.5	8.5
G	22.85	1.5	8.5
H	19.65	1.5	1.8
I	19.65	1.5	3.3
J	22.85	1.5	3.9
K	22.85	1.5	8.5
L	22.85	1.5	4.4
M	22.85	1.5	3.9
N	22.85	1.5	14.0

The baseline coal transfer matrix in Table 6.2 shows the transfers that are allowed between the various coal-fired power stations. A zero indicates that a transfer may not take place between two stations while a one indicates that a transfer is allowed. Note that no coal transfers involving power station B are allowed for the baseline case. This scenario is hypothetical. The matrix is generic and can be modified by the user. The distances (in km) between the power stations are given in Table 6.3. The distances are approximate and not based on specific routes.

Table 6.2: Baseline coal transfer matrix.

	A	B	C	D	E	F	G	H	I	J	K	L	M	N
A	-	0	0	0	1	0	0	1	1	0	0	0	0	0
B	-	-	0	0	0	0	0	0	0	0	0	0	0	0
C	-	-	-	1	0	1	1	0	0	1	1	1	1	1
D	-	-	-	-	0	1	1	0	0	1	1	1	1	1
E	-	-	-	-	-	0	0	1	1	0	0	0	0	0
F	-	-	-	-	-	-	1	0	0	1	1	1	1	1
G	-	-	-	-	-	-	-	0	0	1	1	1	1	1
H	-	-	-	-	-	-	-	-	1	0	0	0	0	0
I	-	-	-	-	-	-	-	-	-	0	0	0	0	0
J	-	-	-	-	-	-	-	-	-	-	1	1	1	1
K	-	-	-	-	-	-	-	-	-	-	-	1	1	1
L	-	-	-	-	-	-	-	-	-	-	-	-	1	1
M	-	-	-	-	-	-	-	-	-	-	-	-	-	1
N	-	-	-	-	-	-	-	-	-	-	-	-	-	-

Table 6.3: Distance matrix for the coal-fired power stations (km).

	A	B	C	D	E	F	G	H	I	J	K	L	M	N
A	-	343.2	308	328.8	329.6	328.6	328.7	302	439	387.7	411.8	336	328.3	356
B	-	-	160.6	180	126.5	131.2	131.3	122.6	182.3	127.5	210.2	201.2	165	51.9
C	-	-	-	26.9	40.7	35.8	35.9	39.5	134	90.9	105.1	45.7	18.9	122.3
D	-	-	-	-	53.8	49	49.1	62.6	121.5	87.8	83.1	21.6	14.6	137.5
E	-	-	-	-	-	5	4.9	28.1	100.9	57.9	101.7	75.5	38.9	83.1
F	-	-	-	-	-	-	0.1	26.9	111.1	60.6	99.7	70.2	34.2	88.9
G	-	-	-	-	-	-	-	27	111.2	60.7	99.6	70.1	34.1	89
H	-	-	-	-	-	-	-	-	138	85.5	125.5	83.1	50.7	89.5
I	-	-	-	-	-	-	-	-	-	55.6	62.1	127.6	115.3	131.7
J	-	-	-	-	-	-	-	-	-	-	76.9	103.3	77.2	83.9
K	-	-	-	-	-	-	-	-	-	-	-	80.9	84.9	159.6
L	-	-	-	-	-	-	-	-	-	-	-	-	37.6	158.3
M	-	-	-	-	-	-	-	-	-	-	-	-	-	122.9
N	-	-	-	-	-	-	-	-	-	-	-	-	-	-

6.2 Simulation settings for the primary energy module

Since the experimental results depend on the simulation settings of the PE module, they must also be discussed. The simulation settings include the following:

- study period (start date and end date)
- number of replications
- output statistic
- seed.

The EFS is a strategic decision support tool, which means that the study horizon should typically be long. However, all experiments were conducted for a period of only one year to avoid very long simulation runs. Data for the year 2015 (1 January to 31 December) was used.

The relatively slow R programming language in which the EFS was coded makes the PE module computationally expensive. This means that the number of replications could not be set too high. All experiments presented in this chapter were conducted with the number of replications set as 10.

It was specified in the modified PE module that the objective function values of the inventory model can be returned as the expected value, the 20-th percentile value or the 80-th percentile value.

Since this study is not a comparison of two or more algorithms, it was not required to specify the seed for the random number generator.

6.3 Overview of experiments

The four experiments that are presented in this chapter are arranged as follows:

- **Experiment 1:** Testing the two model formulations with both coal transfer policies (Section 6.4)
- **Experiment 2:** Adding additional constraints to the model (Section 6.5)

- **Experiment 3:** Varying the coal transfer matrix (Section 6.6)
- **Experiment 4:** Varying input parameters of the PE module (Section 6.7)

Experiment 1 involves testing the two model formulations with both coal transfer policies (i.e. *closest first* and *most urgent*) as discussed in Section 5.2. The aims of this experiment are to 1) determine whether the MOO CEM algorithm can effectively be applied to this problem by finding a logical set of non-dominated solutions and 2) determine what the effect of the two coal transfer policies are on each model formulation. The results of this experiment are also used to determine which of *model 1* or *model 2* to use for the other three experiments.

Since unlimited coal transfers are assumed in the inventory model, some of the solutions achieved in Experiment 1 may be unrealistic due to the requirement for very large coal transfers on certain days. Limited transportation resources might also mean that it is unrealistic to allow transfers on several consecutive days. Experiment 2 is aimed at overcoming these problems with two additional constraints. The first one places a cap on the amount of coal that may be moved between any two power stations on a given day while the second one specifies that the coal stockpiles may only be evaluated on certain days.

For Experiment 3, the baseline coal transfer matrix is modified to illustrate that different scenarios can be examined with regard to the allowable coal transfers. The two constraints of Experiment 2 are also included.

Experiment 4 involves varying two input parameters that add uncertainty in PE module, namely the delivery reliability and the calorific values. The aims of this experiment are to 1) show the effect that these two inputs have on the non-dominated set of solutions found by the algorithm and 2) illustrate that different scenarios can be examined with regard to the parameters that cause variation in the coal stockpiles.

The experimental design and results for the experiments are presented next. The results should not be considered as ready for implementation since most of the inputs that were used do not reflect a current and accurate real-world scenario. The results merely serve as validation for the model while also giving the reader an indication of the outputs that the model can produce.

6.4 Testing the two model formulations with both coal transfer policies

The experimental design and the results for Experiment 1 are presented in this section.

6.4.1 Experimental design

This experiment involves testing the two model formulations with both coal transfer policies. The reader may recall that the first objective f_1 for both models is the total average coal stockpile level (in ktonnes) while the second objective f_2 is the total coal transfers (in ktonnes·km) for model 1 and the total average coal inventory outside the warning limits (in ktonnes) for model 2. Both objective functions are minimised in each model.

The baseline inputs to the EFS are used for this experiment. Since only the 14 existing coal-fired power stations are included in the model, $D = 42$. Each vector $\mathbf{X}_i$, $1 \leq i \leq D$, is sampled from the range $[a_i, b_i]$ and stored in the MOO CEM algorithm's working matrix as described in Subsection 5.3.3. Because most of the input data to the model do not reflect a current real-world scenario, the author expects the near-optimal target stockpile levels found by the algorithm to be significantly lower than Eskom's existing policy of 42 stockpile days. For this reason, the range limits are set to $a_i = 1$ and $b_i = 20$ for all $\mathbf{X}_i$. This means that the maximum values allowed for L_s, T_s and U_s are 20 stockpile days, 40 stockpile days and 60 stockpile days respectively. The three decision variables associated with each coal-fired power station s are thus constrained by

$$1 \leq L_s \leq 20 \qquad \forall s, \tag{6.1}$$

$$L_s + 1 \leq T_s \leq L_s + 20 \qquad \forall s, \tag{6.2}$$

$$T_s + 1 \leq U_s \leq T_s + 20 \qquad \forall s. \tag{6.3}$$

Also recall that the decision variables must be positive integers when expressed in terms of stockpile days. No maximum stockpile levels are specified and each station's initial stockpile level is set to T_s.

6.4.2 Results for the first model formulation

The Pareto fronts achieved for model 1 with the two coal transfer policies are given Figure 6.1. The output statistic is the expected value. A good distribution of solutions was obtained with both transfer policies and the non-dominated solutions cover a wide range of values for each objective function. One can see that there is not much difference between the two transfer policies when only the non-dominated sets are considered. Figure 6.2 is a comparison of the Pareto fronts achieved for model 1 when different output statistics are used. The difference between the fronts achieved for the three output statistics is clearly visible.

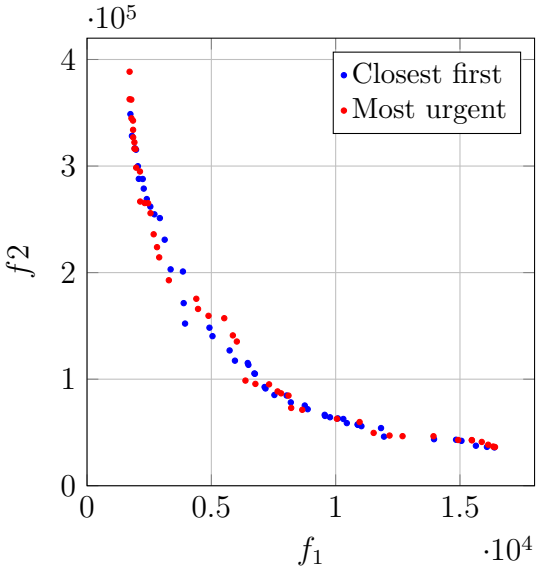

Figure 6.1: Pareto fronts achieved for model 1 with the two transfer policies, expected value as output statistic.

To confirm that the decision variables converged, plots that show the progression of the parameter vectors of the decision variables for model 1 with the closest first transfer policy and the expected value as output statistic are provided in Appendix A. The progression plots for the most urgent transfer policy show similar patterns and are not included in this document.

When solving a multi-objective optimisation problem, the process does not stop when the Pareto front is achieved. A single best solution must still be selected

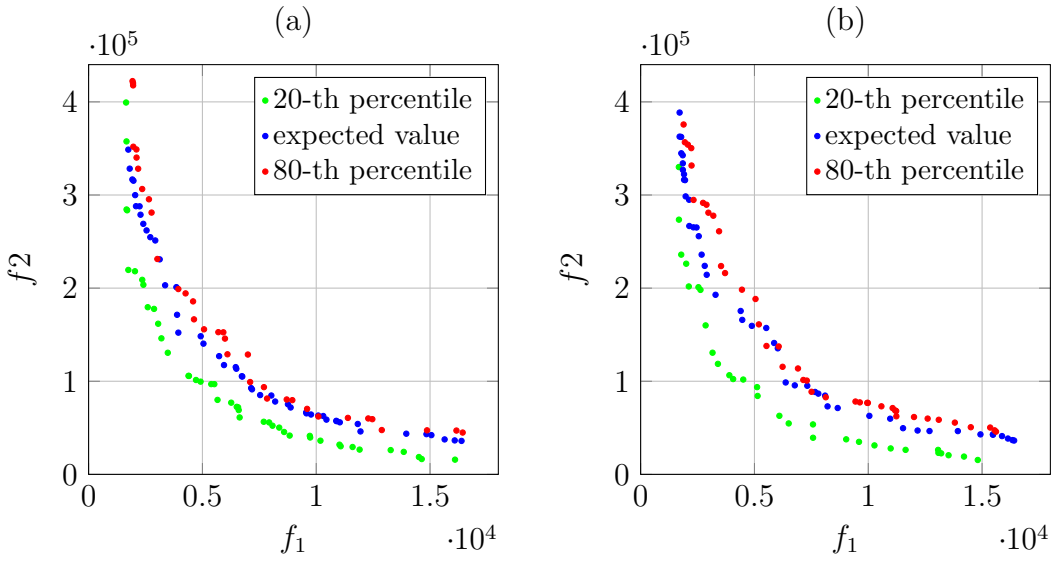

Figure 6.2: A comparison of the Pareto fronts achieved for model 1 with (a) the closest first transfer policy and (b) the most urgent transfer policy when different output statistics are used.

by the decision maker. This process is not trivial. In fact, several methodologies for multi-criteria decision making have been developed over the years (Coello *et al.*, 2007). One such method is the *technique for order preference by similarity to ideal solution* (TOPSIS) of Hwang & Yoon (1981). TOPSIS is a simple ranking method that attempts to choose alternatives such that the distance to the positive ideal solution is at a minimum while the distance to the negative ideal solution is at a maximum. A stepwise framework for performing the TOPSIS methodology is provided in Behzadian *et al.* (2012). Another approach is to construct a multi-attribute utility function that will yield a solution consistent with the decision maker's preferences (Winston, 2004). Refer to chapter 9 of Coello *et al.* (2007) for more on multi-criteria decision making.

Figure 6.3 gives the reader an indication of the target stockpile level ranges achieved for model 1 with the two transfer policies. The output statistic for both is again the expected value. The red dots represent each station's target stockpile level for an extreme solution with respect to f_1 while the green dots represent the target stockpile levels for an extreme solution with respect to f_2. The blue dots represent each station's target stockpile level for a solution that the author

considers a good trade-off between f_1 and f_2. No particular method was used for selecting the good solutions.

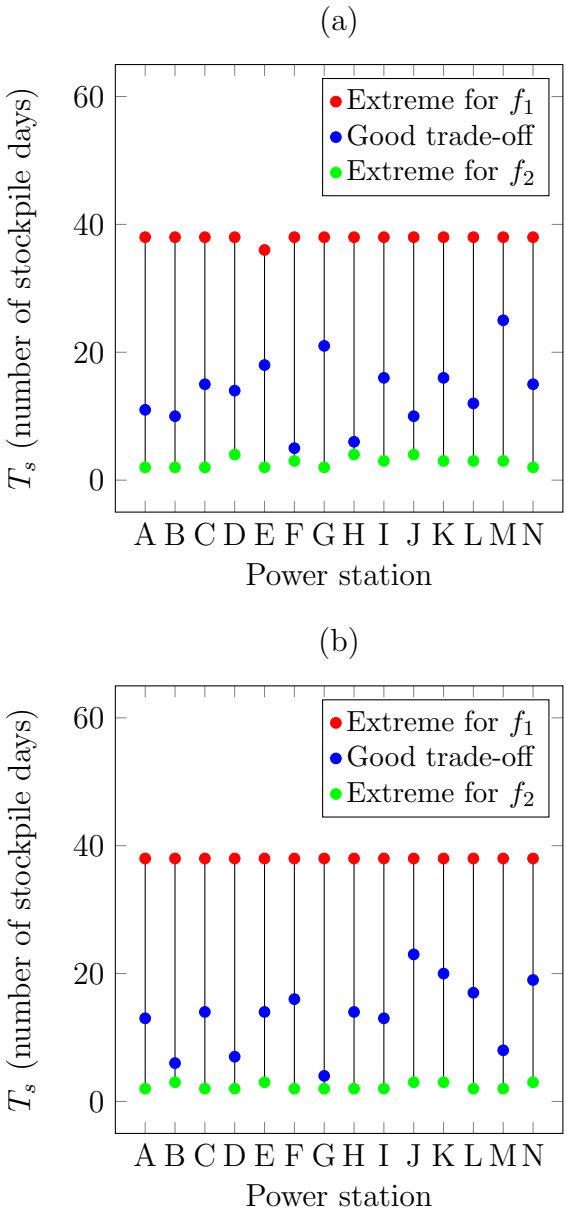

Figure 6.3: Ranges of the T_s values achieved for model 1 with (a) the closest first transfer policy and (b) the most urgent transfer policy, expected value as output statistic.

6.4 Testing the two model formulations with both coal transfer policies

The objective function values for the same good solutions shown in Figure 6.3 are given in Table 6.4. The decision variable values for these solutions are given in Table 6.5. To give the reader an indication of the inventory levels and the movement of coal between the power stations, the PE module was run for each of these solutions over the same one year study period that was used to evaluate the objective functions during the optimisation.

Table 6.4: Approximation of the objective function values for a good solution of model 1 with both transfer policies, expected value as output statistic.

	Closest first	**Most urgent**
f_1 (ktonnes)	5 734	6 025
f_2 (ktonnes·km)	126 965	135 343

For the closest first transfer policy, coal was transferred on 113 days. The majority of transfers were relatively small. Less than 15 ktonnes of coal was moved on 101 days and less than 10 ktonnes of coal was moved on 97 days. The largest transfer occurred when 69 ktonnes of coal was moved between power stations D and G. The most coal that was moved between all the stations on a given day was 165 ktonnes. The stockpile level at power station B was less than the station's standard daily burn (SDB) for a total of 43 days. However, this could not be controlled since station B cannot burn coal from any of the other stations. Power station H experienced a coal shortage on 34 days. Low inventory levels were not a problem at any of the other stations.

For the most urgent transfer policy, coal was transferred on 158 days. In general, the transfers were slightly larger compared to the closest first policy. Less than 25 ktonnes of coal was moved on 141 days. The largest transfer occurred when 121 ktonnes of coal was moved between power stations D and N while the most coal that was moved between all the stations on a given day was 292 ktonnes. Power station G was without sufficient coal for one day.

Matrices that show the total amount of coal moved between the power stations throughout the study period for these two solutions are provided in Appendix A.

Table 6.5: Approximation of the decision variable values for a good solution of model 1 with both transfer policies, expected value as output statistic.

	Closest first						**Most urgent**					
	Stockpile days			ktonnes			Stockpile days			ktonnes		
Power station	L_s	T_s	U_s	L_s	T_s	U_s	L_s	T_s	U_s	L_s	T_s	U_s
A	7	11	21	324.1	509.3	972.2	5	13	23	231.5	601.9	1 064.8
B	5	10	23	272.7	545.4	1 254.5	5	6	17	272.7	327.3	927.2
C	8	15	25	287.4	538.8	898.0	3	14	15	107.8	502.9	538.8
D	4	14	29	78.4	274.5	568.6	1	7	8	19.6	137.2	156.9
E	7	18	30	292.4	751.9	1 253.1	3	14	18	125.3	584.8	751.9
F	4	5	17	59.9	74.8	254.4	12	16	22	179.6	239.5	329.3
G	9	21	28	134.7	314.3	419.1	1	4	16	15.0	59.9	239.5
H	1	6	18	47.8	286.5	859.6	4	14	25	191.0	668.6	1 194.0
I	3	16	26	143.1	763.0	1 239.9	5	13	20	238.4	620.0	953.8
J	1	10	23	36.5	364.6	838.6	12	23	34	437.5	838.6	1 239.6
K	4	16	24	60.3	241.1	361.6	9	20	25	135.6	301.3	376.7
L	9	12	20	211.2	281.6	469.4	12	17	26	281.6	399.0	610.2
M	12	25	31	112.6	234.5	290.8	1	8	11	9.4	75.0	103.2
N	6	15	17	71.8	179.6	203.6	7	19	29	83.8	227.5	347.2

6.4.3 Results for the second model formulation

The Pareto fronts achieved for model 2 with the two coal transfer policies are given in Figure 6.4. The output statistic is the expected value. The distribution of solutions found by the algorithm is not as good as for model 1, i.e. there are a few open spaces in both fronts where possible solutions might be. However, because the true Pareto fronts for the model are not known, one can still conclude that two relatively good sets of solutions were obtained. The two fronts have very similar shapes. Slightly better solutions were achieved with the most urgent transfer policy while the non-dominated solutions cover a wider range of f_2 values for the closest first policy. At first glance, it might seem as if both fronts contain several dominated solutions at $f_2 = 0$. However, the f_2 values for these solutions are just very small and all of them are non-dominated.

Figure 6.5 is a comparison of the Pareto fronts achieved for model 2 when different output statistics are used. One can again see that the fronts for model 2 are not very well distributed.

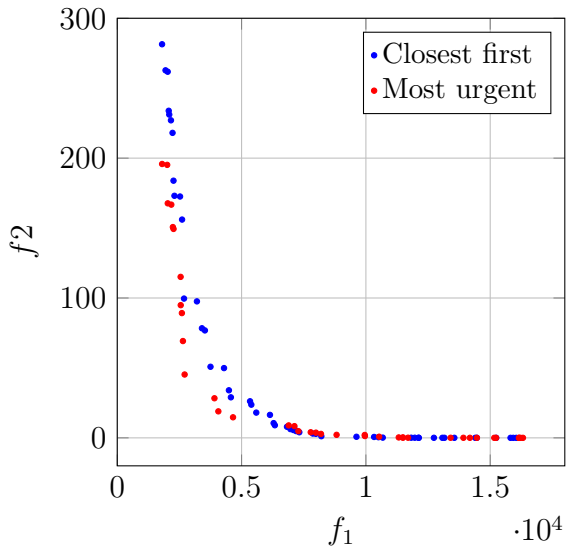

Figure 6.4: Pareto fronts achieved for model 2 with the two transfer policies, expected value as output statistic

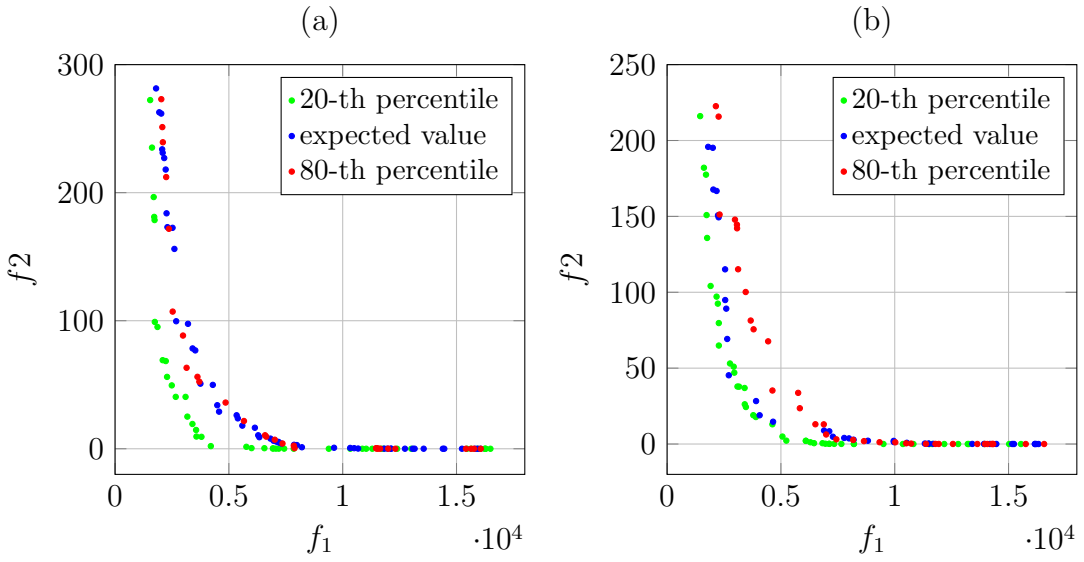

Figure 6.5: A comparison of the Pareto fronts achieved for model 2 with (a) the closest first transfer policy and (b) the most urgent transfer policy when different output statistics are used.

To confirm that the decision variables converged, plots that show the progression of the parameter vectors of the decision variables for model 2 with the closest first transfer policy and the expected value as output statistic are provided in Appendix A. As for model 1, the progression plots for the most urgent transfer policy show similar patterns and are not included in this document.

Figure 6.6 gives the reader an indication of the target stockpile level ranges achieved for model 2 with the two transfer policies, again with the expected value as output statistic. The red, green and blue dots represent the same as previously discussed. The combinatorial nature of the problem means that two completely different solutions can have similar values for one or more of the decision variables. This can be seen in Figure 6.6(a) where $T_{\mathrm{J}} = 2$ for two different solutions. Furthermore, the two extreme solutions does not necessarily have extreme decision variable values for all the power stations. This can be seen in Figure 6.6(b) where T_{E} and T_{M} are smaller for the good solution than for the extreme solution with respect to f_2.

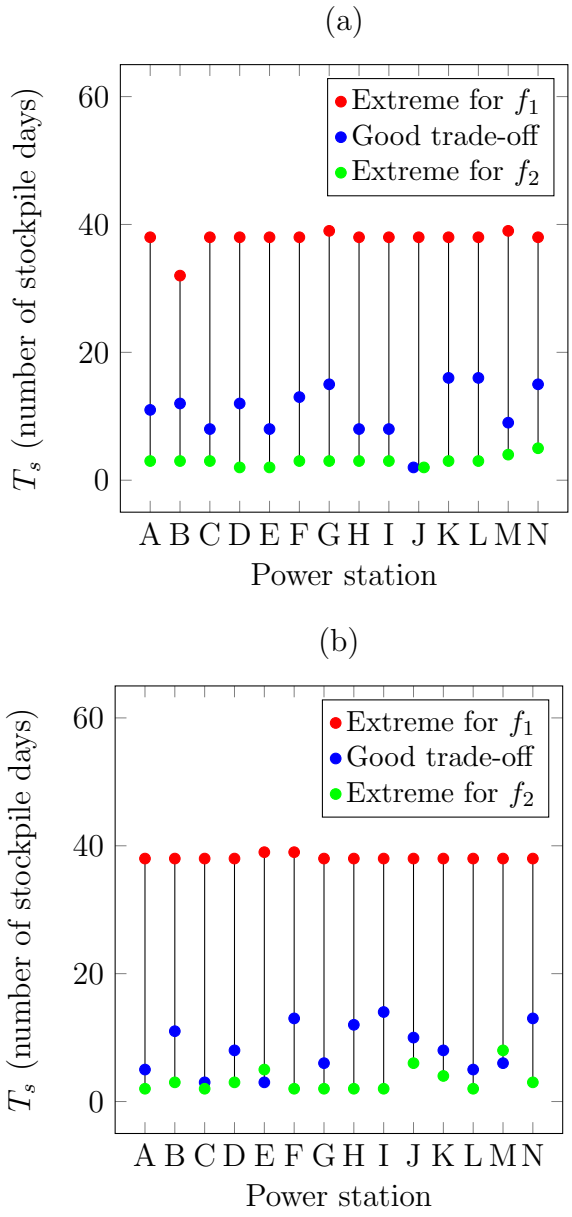

Figure 6.6: Ranges of the T_s values achieved for model 2 with (a) the closest first transfer policy and (b) the most urgent transfer policy, expected value as output statistic.

The objective function values for the same good solutions shown in Figure 6.6 are given in Table 6.6. The decision variable values for these solutions are given in Table 6.7. To examine the inventory levels and the movement of coal between

the power stations, the PE module was again run for each of these solutions over the same one year study period that was used to evaluate the objective functions during the optimisation.

Table 6.6: Approximation of the objective function values for a good solution of model 2 with both transfer policies, expected value as output statistic.

	Closest first	**Most urgent**
f_1 (ktonnes)	4 569	4 066
f_2 (ktonnes)	29	19

For the closest first transfer policy, coal was transferred on 132 days. The majority of transfers were again relatively small. Less than 15 ktonnes of coal was moved on 114 days. The largest transfer occurred when 130 ktonnes of coal was moved between power stations A and E while the most coal that was moved between all the stations on a given day was 157 ktonnes. The stockpile level at power station F was less than the station's SDB for a total of 44 days. Power station J experienced a coal shortage on 28 days while power station L was without sufficient coal on three days. Low inventory levels were not a problem at any of the other stations.

For the most urgent transfer policy, coal was transferred on 144 days. Less than 20 ktonnes of coal was moved on 127 days. The largest transfer occurred when 282 ktonnes of coal was moved between power stations C and J. This is extremely high and may be unrealistic. The most coal that was moved between all the stations on a given day was 331 ktonnes. The stockpile level at power station A was less than the station's SDB for a total of 57 days while power station E experienced a coal shortage on 78 days. Power stations J and L were each without sufficient coal on one day. Coal stockouts were not a problem at any of the other stations.

Matrices that show the total amount of coal moved between the power stations throughout the study period for these two solutions are provided in Appendix A.

Table 6.7: Approximation of the decision variable values for a good solution of model 2 with both transfer policies, expected value as output statistic.

	Closest first						**Most urgent**					
	Stockpile days			ktonnes			Stockpile days			ktonnes		
Power station	L_s	T_s	U_s	L_s	T_s	U_s	L_s	T_s	U_s	L_s	T_s	U_s
A	4	11	20	185.2	509.3	925.9	1	5	9	46.3	231.5	416.7
B	3	12	21	163.6	654.5	1 145.4	1	11	19	54.5	600.0	1 036.3
C	7	8	17	251.4	287.4	601.7	2	3	14	71.8	107.8	502.9
D	6	12	18	117.6	235.3	352.9	1	8	16	19.6	156.9	313.7
E	1	8	15	41.8	334.2	626.6	1	3	6	41.8	125.3	250.6
F	7	13	19	104.8	194.6	284.4	12	13	22	179.6	194.6	329.3
G	9	25	22	134.7	224.5	329.3	2	6	20	29.9	89.8	299.3
H	1	8	17	47.8	382.1	811.9	4	12	17	191.0	573.1	811.9
I	1	8	10	47.7	381.5	476.9	8	14	17	381.5	667.6	810.7
J	1	2	8	36.5	72.9	291.7	1	10	11	36.5	364.6	401.1
K	9	16	25	135.6	241.1	376.7	7	8	25	105.5	120.5	376.7
L	9	16	27	211.2	375.5	633.7	1	5	15	23.5	117.3	352.0
M	1	9	20	9.4	84.4	187.6	5	6	13	46.9	56.3	121.9
N	9	15	22	107.8	179.6	263.4	6	13	31	71.8	155.7	371.2

6.5 Adding additional constraints to the model

The experimental design and the results for Experiment 2 are presented in this section.

6.5.1 Experimental design

This experiment involves adding two additional coal transfer constraints to the inventory model. The first one places a cap on the amount of coal that may be moved between any two power stations on a given day while the second one specifies that the coal stockpiles may only be evaluated on certain days.

The reader may recall that the motivation behind the formulation of model 2 was the concern that the author had about the manner in which the coal transfers are triggered (see Subsection 5.2.2). The inventory model was formulated with the condition that coal can only be transferred between two power stations if the stockpile level at one of them can be forced towards the target level. The concern was that some of the stations may, throughout the course of the study period, seek to increase or decrease their inventory levels without a transfer ever becoming available. However, the results of Experiment 1 showed that this is not a problem because very few coal stockouts were recorded for model 1. In fact, more coal stockouts were recorded for model 2. There was also a concern about unrealistically large coal transfers. However, it was found that the majority of transfers were relatively small for model 1. This means that a large enough transfer cap would still allow for the target stockpile levels to be triggered during most transfers. Furthermore, the distribution of solutions found for model 1 was significantly better than for model 2. For these reasons, model 1 with the closest first coal transfer policy is selected for this experiment.

The experimental design for Experiment 2 is given in Table 6.8. Six scenarios (Experiments 2.1 to 2.6) are examined. For Experiments 2.1 and 2.2, the amount of coal that may be moved between any two stations on a given day is capped at 10 and 15 ktonnes respectively. The stockpiles may be evaluated every day. For Experiment 2.3, the stockpiles may only be evaluated every second day while for Experiment 2.4, the stockpiles may only be evaluated every fifth day. No transfer caps are specified for these two. For Experiment 2.5, a transfer cap of

20 ktonnes is specified while the stockpiles may only be evaluated every fifth day. For Experiment 2.6, the transfer cap is 25 ktonnes and the stockpiles may only be evaluated every tenth day. The scenarios in Table 6.8 are not strategies that the author recommends for Eskom. The idea is only to examine the effects that the two additional constraints have on the solutions found by the algorithm and to demonstrate to the reader that these constraints can be added to the model.

Table 6.8: Experimental design for Experiment 2.

Experiment	**Coal transfer cap**	**Evaluation of the stockpiles**
2.1	10 ktonnes	Every day
2.2	15 ktonnes	Every day
2.3	Unlimited	Every 2nd day
2.4	Unlimited	Every 5-th day
2.5	20 ktonnes	Every 5-th day
2.6	25 ktonnes	Every 10-th day

To deal with the problem of coal stockouts, the sampling range for the decision variables $\mathbf{X}_i = L_s$ is changed to [5,20], i.e. each L_s must be at least five stockpile days. The sampling ranges for the variables $\mathbf{X}_i = T_s - L_s$ and $\mathbf{X}_i = U_s - T_s$ remain [1,20] as in Experiment 1. The three decision variables associated with each coal-fired power station s are thus constrained by

$$5 \leq L_s \leq 20 \qquad \forall s, \tag{6.4}$$

$$L_s + 1 \leq T_s \leq L_s + 20 \qquad \forall s, \tag{6.5}$$

$$T_s + 1 \leq U_s \leq T_s + 20 \qquad \forall s. \tag{6.6}$$

The decision variables must once again be positive integers when expressed in terms of stockpile days. No maximum stockpile levels are specified and each station's initial stockpile level is set to T_s. Only the expected value is examined and the baseline inputs to the EFS are once again used.

6.5.2 Results

The Pareto fronts achieved for Experiments 2.1 to 2.6 are given in Figures 6.7 to 6.9. To illustrate the effect of the additional constraints, each Pareto front is compared with a reference front that was achieved without the constraints.

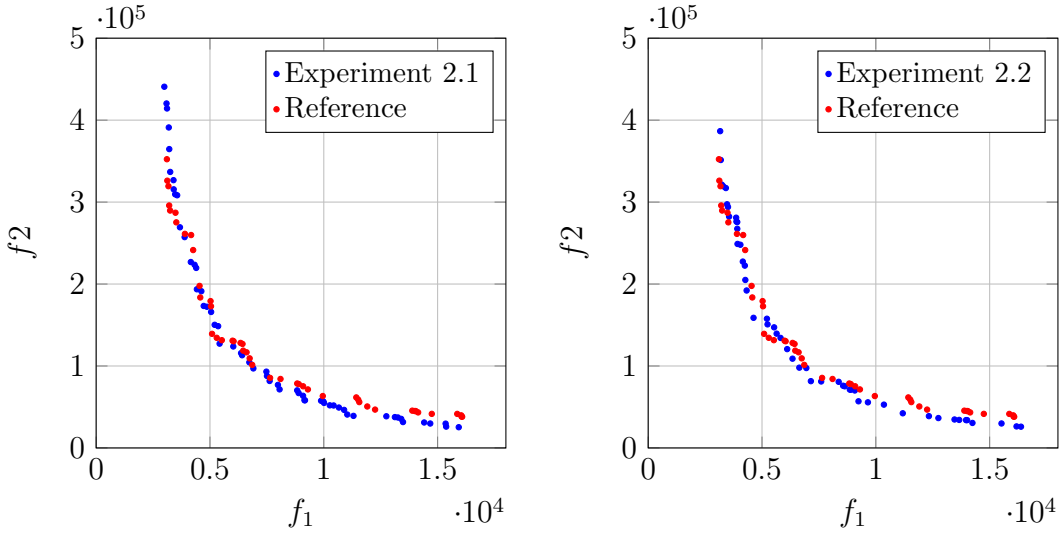

Figure 6.7: Pareto fronts achieved for Experiment 2.1 and Experiment 2.2.

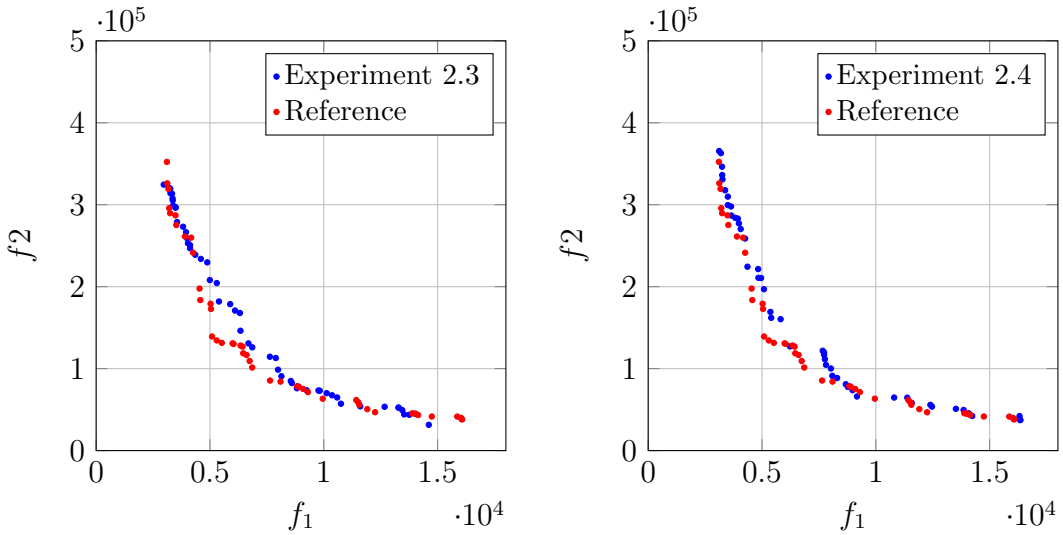

Figure 6.8: Pareto fronts achieved for Experiment 2.3 and Experiment 2.4.

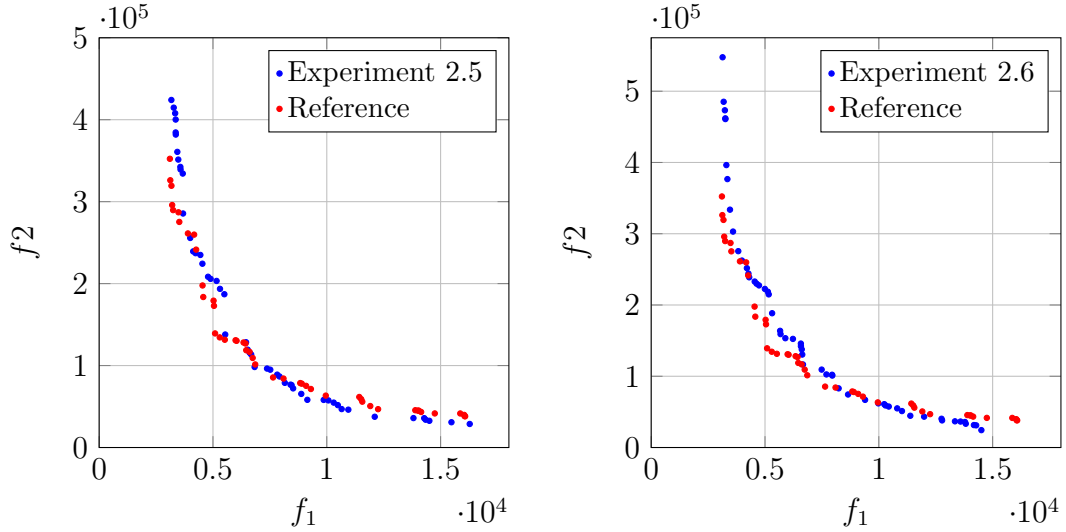

Figure 6.9: Pareto fronts achieved for Experiment 2.5 and Experiment 2.6.

By comparing the reference Pareto front with the fronts achieved for Experiments 2.1 and 2.2, one can see that there is not much difference between them. However, slightly smaller f_2 values were obtained when transfers caps were specified. Also, the non-dominated solutions cover a wider range of f_2 values with the transfer caps, especially for Experiment 2.1. The Pareto fronts achieved for Experiments 2.3 and 2.4 indicate that slightly better solutions were obtained when the stockpiles could be evaluated every day. The Pareto fronts achieved for Experiments 2.5 and 2.6 have very similar shapes to those achieved for Experiments 2.3 and 2.4. The main difference is that the non-dominated solutions cover a significantly smaller range of f_2 values for the latter. Decision makers thus have a wider range of solutions to select from when both the constraints are included.

Since the true Pareto fronts for these six scenarios are not known, the quality of the solutions cannot measured. However, the shapes of the various fronts can be considered as relatively good given the two minimisation objectives. The solutions in each front are also relatively well distributed despite a few open spaces.

To give the reader an indication of inventory levels and the movement coal of between the power stations for these six scenarios, the PE module was run for

solutions that the author considers a good trade-off between f_1 and f_2. No particular method was used for selecting the good solutions. The objective function values and the decision variable values for these good solutions are provided in Appendix A.

For Experiment 2.1, coal was transferred on 115 days. The transfer cap ensured that no transaction between two stations exceeded 10 ktonnes while the most coal that was moved between all the stations on a given day was 60 ktonnes. The stockpile level at power station H was less than the station's SDB for a total of 23 days. Low inventory levels were not a problem at any of the other stations. For Experiment 2.2, coal was transferred on 169 days. The transfer cap ensured that no transaction between two stations exceeded 15 ktonnes while the most coal that was moved between all the stations on a given day was 84 ktonnes. The stockpile level at power station H was less than the station's SDB for a total of 42 days. None of the other stations experienced a coal shortage.

By placing a cap on the movement of coal, it was found that transfers occur on more days throughout the study period. This is a logical response by the model.

For Experiment 2.3, coal was transferred on 83 days. The constraint on the evaluation of the stockpiles ensured that transfers were never made on two consecutive days. The largest transfer occurred when 177 ktonnes of coal was moved between power stations H and I. This was also the most coal that was moved between all the power stations on a given day. Power station H was again the only station that experienced a coal shortage. It was without sufficient coal on 20 days. For Experiment 2.4, coal was transferred on only 30 days. The constraint on the evaluation of the stockpiles ensured that there were always at least five days between transfers. The largest transfer occurred when 129 ktonnes of coal was moved between power stations C and L while the most coal that was moved between all the stations on a given day was 158 ktonnes. The stockpile level at power station B was less than the station's SDB for a total of 20 days. None of the other stations experienced a coal shortage.

By only allowing the stockpiles to be evaluated on certain days, it was found that coal is moved on fewer days. However, the amount of coal moved on a day is generally more. This response is again logical.

For Experiment 2.5, coal was transferred on 30 days. The transfer cap ensured that no transaction between two stations exceeded 20 ktonnes while the constraint on the evaluation of the stockpiles ensured that there were always at least five days between transfers. The most coal that was moved between all the stations on a given day was 152 ktonnes. The stockpile level at power station A was less than the station's SDB for a total of 20 days while power station B experienced a coal shortage for 34 days. For Experiment 2.6, coal was transferred on 32 days. The transfer cap ensured that no transaction between two stations exceeded 25 ktonnes while the constraint on the evaluation of the stockpiles ensured that there were always at least 10 days between transfers. The most coal that was moved between all the stations on a given day was 213 ktonnes. Low inventory levels were not a problem at any of the stations.

By placing a cap on the movement of coal and only allowing the stockpiles to be evaluated on certain days, it was found that coal is moved on significantly fewer days. Also, the amount of coal moved on a day is generally a lot more. Similar to the aforementioned cases, this again seems to be a logical response by the model.

Matrices that show the total amount of coal moved between the power stations throughout the study period for the six solutions described above are provided in Appendix A.

6.6 Varying the coal transfer matrix

The experimental design and the results for Experiment 3 are presented in this section.

6.6.1 Experimental design

This experiment involves varying the baseline coal transfer matrix to illustrate that different scenarios can be specified with regard to the allowable coal transfers. The two constraints that were introduced in Experiment 2 are also included, i.e. a cap is placed on the amount of coal that may be moved between two power stations on a given day and the coal stockpiles may only be evaluated on certain

days. The modified coal transfer matrix for Experiment 3 is given in Table 6.9. Apart from the modified matrix, all baseline inputs are used as discussed in Section 6.1.

Table 6.9: Modified coal transfer matrix for Experiment 3.

	A	B	C	D	E	F	G	H	I	J	K	L	M	N
A	-	0	0	0	0	0	0	1	0	0	0	0	0	0
B	-	-	0	0	0	0	0	0	0	0	0	0	0	0
C	-	-	-	1	0	0	0	0	0	0	0	0	1	0
D	-	-	-	-	0	0	0	0	0	0	0	0	1	0
E	-	-	-	-	-	0	0	0	1	0	0	0	0	0
F	-	-	-	-	-	-	1	0	0	0	0	0	0	0
G	-	-	-	-	-	-	-	0	0	0	0	0	0	0
H	-	-	-	-	-	-	-	-	0	0	0	0	0	0
I	-	-	-	-	-	-	-	-	-	0	0	0	0	0
J	-	-	-	-	-	-	-	-	-	-	1	0	0	0
K	-	-	-	-	-	-	-	-	-	-	-	0	0	0
L	-	-	-	-	-	-	-	-	-	-	-	-	0	1
M	-	-	-	-	-	-	-	-	-	-	-	-	-	0
N	-	-	-	-	-	-	-	-	-	-	-	-	-	-

The experimental design for Experiment 3 is given in Table 6.10. Two scenarios are experimented with. The coal transfers are capped at 10 and 15 ktonnes respectively while the stockpiles may only be evaluated every fifth day. As previously discussed, these scenarios are not strategies that the author recommends for Eskom. The aim is just to illustrate the model's capability.

For the same reasons provided in Subsection 6.5.1, model 1 is again selected for this experiment. The closest coal transfer policy is used and only the expected value is examined. The decision variable values are sampled from the same ranges as in Experiment 2. No maximum stockpile levels are specified and each station's initial stockpile level is again set to T_s.

Table 6.10: Experimental design for Experiment 3.

Experiment	Coal transfer cap	Evaluation of the stockpiles
3.1	10 ktonnes	Every 5-th day
3.2	15 ktonnes	Every 5-th day

6.6.2 Results

The Pareto frons achieved for Experiment 3.1 and Experiment 3.2 are given in Figure 6.10. Both fronts are relatively well distributed and the non-dominated solutions cover a wide range of values for each objective function. One can clearly see that the total coal transfers (f_2) are significantly less with the modified transfer matrix. This is because there are fewer transfer options for the various power stations.

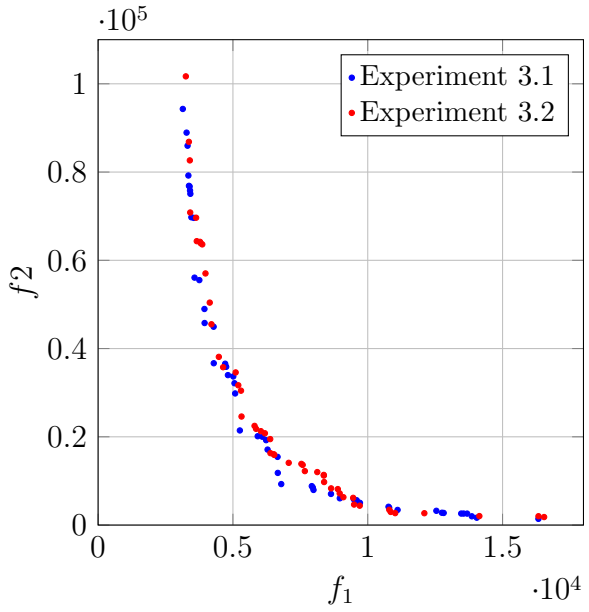

Figure 6.10: Pareto fronts achieved for Experiment 3.1 and Experiment 3.2.

To give the reader an indication of the inventory levels and the movement of coal between the various stations, the PE module was again run with two

solutions that the author considers a good trade-off between f_1 and f_2. No particular method was used for selecting these good solutions. The objective function values and decision variable values are provided in Appendix A.

For Experiment 3.1, coal was transferred on 49 days. The transfer cap ensured that no transaction between two power stations exceeded 10 ktonnes while the constraint on the evaluation of the stockpiles ensured that there were always at least five days between transfers. The most coal that was moved between all the stations on a day was 30 ktonnes. Only one power station experienced a coal shortage. It was station F and the duration was three days.

For Experiment 3.2, coal was transferred on 27 days. The two constraints ensured that no transaction exceeded 15 ktonnes and that there were always at least five days between transfers. The most coal that was moved between all the stations on a day was again 30 ktonnes. The stockpile level at power station B was less than the station's SDB for a total of 17 days. Coal shortages were not a problem at any of the other stations.

Matrices that show the total amount of coal moved between the power stations throughout the study period for these two solutions are provided in Appendix A.

6.7 Varying input parameters of the primary energy module

The experimental design and the results for Experiment 4 are presented in this section.

6.7.1 Experimental design

This experiment involves varying the uncertainty of coal deliveries and calorific values. This is done by adjusting the ranges of the sampling distributions from which each is sampled in the PE module. The aims of this experiment are to 1) show the effect that these two inputs have on the non-dominated set of solutions found by the algorithm and 2) illustrate that different scenarios can be examined with regard to the parameters that cause variation in the coal stockpiles.

The adjusted ranges of the triangular distribution used for the delivery reliability and standard normal distribution used for the CVs are given in Table 6.11. For the triangular distribution, a "–" indicates that the minimum value is decreased by 0.15 while the most likely and maximum values remain as in the baseline case. A "+" indicates the opposite where the maximum value is increased by 0.15 while the minimum and most likely values remain as in the baseline case. The standard normal distribution truncated on the positive side is indicated by a "–" because lower values can be sampled on the negative side. Similarly, a "+" indicates that the standard normal distribution is truncated on the negative side because higher values can be sampled on the positive side. A range limit of 1.5 is set for both the negative and positive sides.

Table 6.11: Sampling distribution ranges for Experiment 4.

	Triangular	**Standard normal**
Baseline	$[0.9D_s^{(\mathrm{p})}, D_s^{(\mathrm{p})}, 1.1D_s^{(\mathrm{p})}]$	$[-\infty, \infty]$
–	$[0.75D_s^{(\mathrm{p})}, D_s^{(\mathrm{p})}, 1.1D_s^{(\mathrm{p})}]$	$[-\infty, 1.5]$
+	$[0.9D_s^{(\mathrm{p})}, D_s^{(\mathrm{p})}, 1.25D_s^{(\mathrm{p})}]$	$[-1.5, \infty]$

The experimental design for Experiment 4 is given in Table 6.12. Four scenarios (Experiments 4.1 to 4.4) are examined. Experiments 4.1 and 4.2 are scenarios that would typically be considered as "bad", i.e. reduced coal deliveries and CVs. Experiments 4.3 and 4.4 are scenarios that would typically be considered as "good", i.e. increased coal deliveries and CVs.

Table 6.12: Experimental design for Experiment 4.

Experiment	**Delivery Reliability**	**CV**
4.1	–	
4.2		–
4.3	+	
4.4		+

To illustrate the effects on the entire system, the scenarios given in Table 6.12 are applicable to each of the existing coal-fired power stations. Apart from the

varied ranges of the sampling distributions, all baseline inputs are used as discussed in Section 6.1. Each vector $\mathbf{X}_i$, $1 \leq i \leq D$, is again sampled from the range [1,20] as in Experiment 1. No maximum stockpile levels are specified and each station's initial stockpile level is set to T_s. Model 1 with the most urgent coal transfer policy is used for this experiment and only the expected value is examined.

6.7.2 Results

The Pareto fronts achieved for Experiments 4.1 to 4.4 are given in Figures 6.11 and 6.12. To illustrate the effect of the varied input parameters, each Pareto front is compared with a reference front from Experiment 1, i.e. the Pareto front achieved for model 1 with the most urgent coal transfer policy and with the baseline sampling distribution ranges.

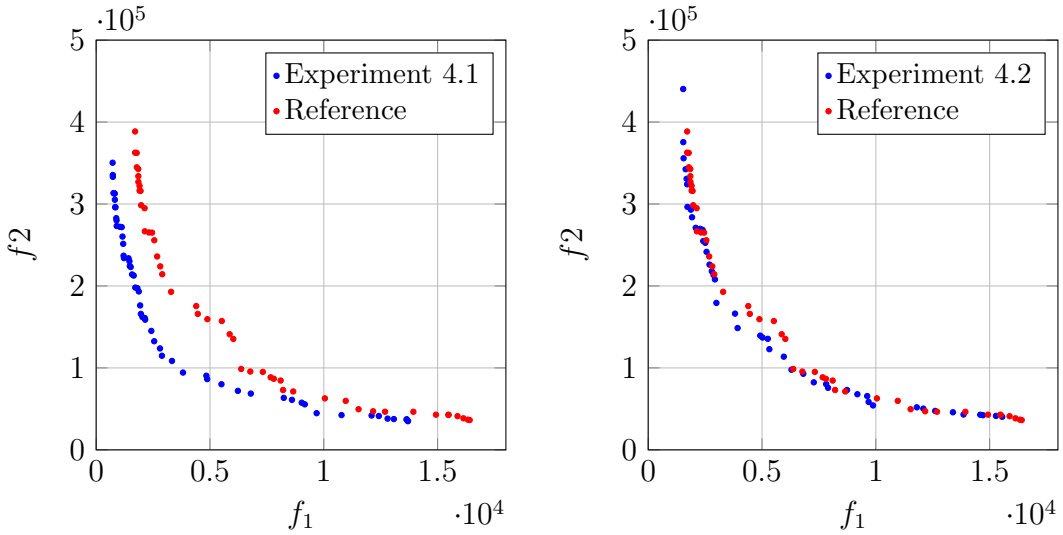

Figure 6.11: Pareto fronts achieved for Experiment 4.1 and Experiment 4.2.

From the Pareto front achieved for Experiment 4.1, one can clearly see the effect of reduced coal deliveries. Significantly lower f_1 values were obtained. This seems correct since the trends on the stockpiles should theoretically be downward for this scenario. The Pareto front achieved for Experiment 4.2 shows that the effect of reduced CVs is not nearly as much as the effect of reduced coal deliveries.

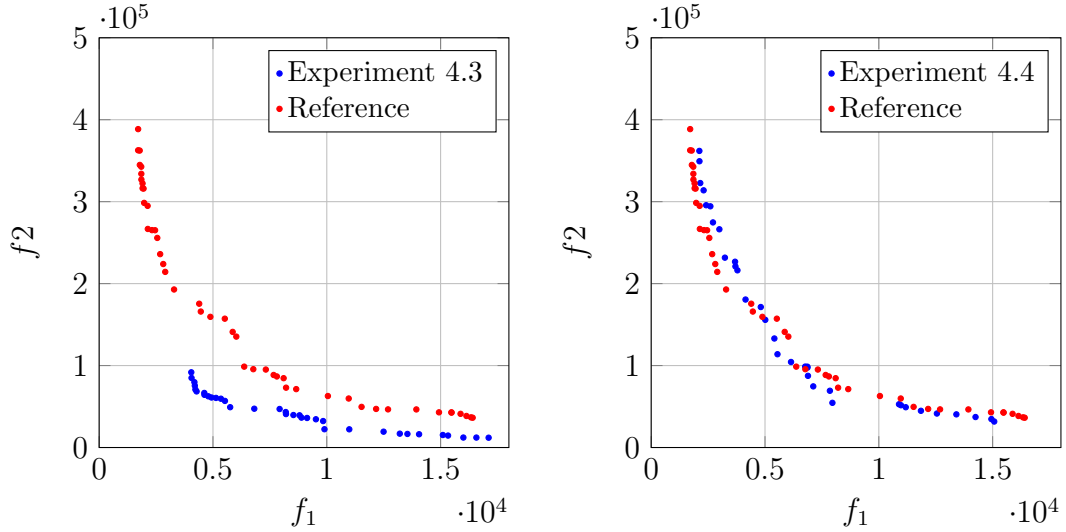

Figure 6.12: Pareto fronts achieved for Experiment 4.3 and Experiment 4.4.

From the Pareto front achieved for Experiment 4.3, one can see that the non-dominated set contains significantly fewer solutions as a result of the increased coal deliveries. Also, the non-dominated solutions cover a very small range of f_2 values. Because the trend on all the stockpiles should theoretically be upward for this scenario, inventory levels very rarely dropped below L_s during the simulation runs. Furthermore, the power stations at which the stockpiles grew very large might not have been able to reduce their inventory levels because none of the other stations were fit to receive coal. As reflected in the Pareto front, very few transfers were subsequently made and inventory levels were generally higher.

The Pareto front achieved for Experiment 4.4 again shows that the CVs do not have a major effect on the solutions found by the algorithm. This conclusion will most probably differ if the sampling distribution was to be adjusted to favour one side significantly more. Another option could be to specify different $\sigma_s^{(\text{CV})}$ values than the ones given in Table 6.1.

This concludes the experiments. A summary of the findings made from the experimental results are presented next.

6.8 Findings made from the experimental results

As a conclusion to the experiments, the findings made from the experimental results are summarised in this section. The findings are as follows:

1. A logical set of non-dominated solutions was obtained for each of the two model formulations with both coal transfer policies. It can thus be said that the multi-objective optimisation using the cross-entropy method (MOO CEM) algorithm was successfully applied in this study.

2. For both model 1 and model 2, it was found that the different coal transfer policies do not have a significant effect on the Pareto fonts achieved by the algorithm. However, the different policies do have an effect on the amount of coal moved between the various power stations. Refer to the coal transfer matrices in Appendix A (Tables A.1 to A.4).

3. The motivation behind the formulation of model 2 was the concern that the author had about the manner in which the coal transfers are triggered. The concern was that some of the power stations may, throughout the course of the study period, seek to increase or decrease their inventory levels without a transfer ever becoming available. However, the results of model 1 in Experiment 1 showed that this is not a major problem because very few coal stockouts were recorded. It was found that most of the coal shortages were as a result of low initial stockpile levels.

4. Another concern was that some of the solutions found by the algorithm would be unrealistic due to the assumptions made in the model formulation, especially with regard to unlimited coal transfers. However, it was found that unrealistically large coal transfers were not a major problem.

5. By limiting the amount of coal that may be moved between two power stations during a transfer transaction and specifying that the stockpiles may only be evaluated on certain days, it was shown that these two additional constraints can successfully be incorporated into the model. By modifying

the baseline coal transfer matrix, it was illustrated that the inventory model is generic with regard to the allowable coal transfers. Furthermore, by varying the uncertainty of coal deliveries and CVs, it was shown that the model can be used to examine a number of different scenarios with regard to the parameters that cause variation in the stockpiles. Logical solutions were obtained for all the scenarios that were examined in Experiments 2, 3 and 4.

6. The author acknowledges that it is not ideal to move large amounts of coal over long distances. In practice, the preferred approach may be to rather redirect coal deliveries directly from the mines. The inventory model indirectly allows for this. When the amount of coal that may be moved between two power stations on a given day is capped at a number less or equal to the planned coal deliveries, the effect on the stockpiles is exactly the same as that of a delivery redirection.

7. As is, the multi-objective simulation optimisation model is capable of providing decision makers with a wide range of near-optimal solutions to assist with inventory management at Eskom's coal-fired power stations. That said, the author acknowledges that several factors must be considered before making decisions. The limited modelling capability of the R programming language makes it very difficult to include variables such as human resources, transportation availability, and coal loading and handling equipment. This is a major drawback of the model.

6.9 Summary: Chapter 6

The experiments and the analysis of the experimental results were presented in this chapter.

Four experiments were conducted. The first one involved testing the two model formulations with both coal transfer policies. For the second experiment, two additional constraints were added to the model. The first one places a cap on the amount of coal that may be moved between two power stations on a day and the second one specifies that the stockpiles may only be evaluated on certain days.

For the third experiment, the baseline coal transfer matrix was modified while for the fourth experiment, the uncertainty of coal deliveries and CVs were varied. The aim of the experiments was to provide validation for the multi-objective SO model while also testing the effectiveness of the MOO CEM algorithm in finding approximate solutions for the model. The chapter concluded with a summary of the findings made from the experimental results.

The summary and conclusions of the thesis follows in Chapter 7.

Chapter 7

Summary and conclusions

The research conducted in this thesis was presented in the previous chapters. This chapter serves as a summary of the project. The value of the study is presented, along with suggestions for future research. The chapter is concluded on a personal note with a summary of the value gained by the researcher.

7.1 Project summary

The aim of the research project was to determine whether multi-objective optimisation (MOO) capability can successfully be added to Eskom's energy flow simulator (EFS). To achieve this, the primary research objective was defined as to formulate and solve a multi-objective coal inventory model using the outputs of the EFS. Since this study forms part of the bigger EFS project, which is currently still a work-in-progress, a secondary objective was to propose modifications to the existing EFS architecture to improve its potential as an optimisation tool. A number of research tasks was identified and successfully completed.

Introductory literature on electricity markets and power station logistics systems were presented in **Chapter 2**. This, as well as research on Eskom's generation mix and coal supply chain, served as a foundation before studying the architecture of the EFS. The EFS is a strategic decision support tool that enables its users the simulate and analyse the Eskom value chain from primary energy to end-use. The EFS is not an optimisation tool. This lack of optimisation capability was the foundation of the research. The main simulation component of

the EFS was identified as the primary energy (PE) module. The module's two simulation outputs are the electricity generation at all of Eskom's power stations and the coal stockpile levels at its coal-fired power stations. The existing EFS operates on a monthly simulation resolution, i.e. the outputs are expressed as monthly values. After studying the architecture of the EFS and considering recommendations from a previous research project, it was proposed that the EFS be modified in order for the simulation resolution to be daily. To achieve this, three of the nine EFS modules required changes, namely the production planning (PP) module, the fuel planning (FP) module and the PE module. The scope of the study was limited to these three modules, even though inputs from some of the other modules were used. A detailed description of the existing EFS architecture as well as the modifications to it were presented in **Chapter 3**.

In order to gain sufficient knowledge of simulation optimisation (SO) and MOO, relevant literature was studied and documented in **Chapter 4**. Further research on inventory models, the importance of managing coal stockpiles and Eskom's inventory management policy were presented in **Chapter 5**. This was followed by the formulation of the proposed coal inventory model. The model is based on the movement of coal between the various coal-fired power stations in an attempt to maintain an optimal target stockpile level at each station as far as possible. Three objectives were identified and two policies were proposed for transferring coal between the power stations. To find approximate solutions for the inventory model, the algorithm for multi-objective optimisation using the cross-entropy method (MOO CEM) was selected as a suitable metaheuristic. From previous research, the MOO CEM has proved to be an ideal approach for the computationally expensive time-dependent problems often encountered in SO.

After successfully integrating the MOO CEM algorithm with the PE module, four experiments were conducted. The experimental design and analysis of the experimental results were documented in **Chapter 6**. The experiments served as validation for the inventory model while also testing the effectiveness of the MOO CEM algorithm in finding approximate solutions for the model. As conclusion to the experiments, a summary of all the findings made was presented. With regard to the main objective of the study, the experimental results illustrated that the

researcher could successfully formulate and solve a multi-objective coal inventory model for the EFS.

7.2 Value of the study

The problem that was addressed in this thesis mainly adds value to Eskom's greater EFS project. The modified PP module is being used by Lindner *et al.* (2015) in another research project. The study involves estimating an optimal generator maintenance schedule for the generating units at all of Eskom's power stations using multi-objective simulated annealing. The three modules that were modified in this study can be integrated with the EFS framework to be used for strategic planning purposes in the original context of the EFS. When the coal transfer functions and the MOO CEM algorithm are added to the equation, the EFS can be used for decision support with regard to inventory management at the coal-fired power stations. As is, the author does not regard the inventory model as the finished product. However, it does serve as a reasonable decision support tool with potential for future improvements.

By successfully applying the MOO CEM algorithm to this problem, further evidence was made available of the algorithm's capability to approximately solve problems with large solution spaces using fairly few objective function evaluations.

7.3 Suggestions for future research

During the progression of the project, a few areas were identified for future work. These are briefly summarised below.

1. The introductory literature study in **Chapter 1** included a broad overview of one-firm optimisation models as a modelling tool to solve unit commitment (UC), economic load dispatch and short-term hydrothermal coordination problems. Since the PP module of the EFS is essentially a very basic UC model, the module can possibly be improved through further research on such problems.

2. As mentioned throughout **Chapters 5** and **6**, a few assumptions were made with regard to Eskom's complex coal inventory system. Furthermore, most of the input data that was used are outdated and not based on current and accurate real-world scenarios. To further validate the multi-objective inventory model and improve the PE module, the following items can be considered for inclusion in future research projects:

   (a) With the model as-is, it is necessary that the optimisation solutions be analysed when updated and accurate inputs are specified. These include the gross domestic product and weather scenarios, the generation capacities and costs, the coal transfer matrix, the distance matrix and the planned coal deliveries. Other inputs are the initial stockpile levels, the energy utilisation factors (EUFs), the heat rates and the calorific values (CVs). Also, an actual daily planned maintenance schedule must be used and a realistic scenario must be specified for daily unplanned outages.

   (b) Rather than to add uncertainty in the PE module by sampling from a triangular and a standard normal probability density function, historical data for coal deliveries, CVs and UCLFs should be used to estimate a more accurate sampling distribution for each. This was initially the plan for this study, but the data was not made available.

   (c) The EFS is coded in the open source R programming language. If this remains the desired platform in the future, a study that involves adding simulation detail to the PE module is a possibility. This can include the incorporation of constraints related to transportation availability, human resources, coal handling and loading equipment, and lead times for coal transfers. However, the limited modelling capability of R will make this very difficult.

   (d) The author believes that it would ultimately be best if the PE module was to be modelled in a discrete-event simulation software package such as Simio®. This would allow for the simulation detail mentioned in (c) to be incorporated with relative ease. Simio® has its own optimisation

module, but can also be integrated with other programming languages to experiment with different MOO algorithms. A number of alternative simulation packages are also available.

7.4 Value gained by the researcher

MOO was, before the study, a relatively new field for the researcher. In this field of finding a set of near-optimal solutions, the researcher learned that there is not one absolute correct answer. Certain solutions may be better than others, but the final "correct" answers are those that satisfy the preferences of the stakeholders.

In order to achieve the research objectives of the study, it was required to choose a suitable MOO algorithm and master it. Subsequently, the MOO CEM and its single-objective counterpart were learned. Furthermore, it was required for the researcher to learn and understand how to integrate an optimisation algorithm with a simulation model.

The electricity generation industry was a completely new field to work in for the researcher. A large amount of research was required in order to gain sufficient background of the field. By studying the manner in which Eskom operates, good insight was gained into the South African electricity generation sector and electricity suppliers in general.

To reverse engineer the existing EFS modules and then modify them, the open source R programming language had to be mastered. The MOO CEM algorithm was also coded in R. In addition, the document preparation system LaTeX had to be learned in order to prepare this document.

References

Abeygunawardana, A., Berizzi, A., Bovo, C. & Innorta, M. (2008). A conjectural supply function model for the italian electricity market. In *Proceedings of the 43rd IEEE International Universities Power Engineering Conference*, 1–5. 10, 11

Alikhanzadeh, A., Irving, M.R. & Taylor, G.A. (2011). Bilateral electricity market model using conjectural variation equilibria and hierarchical optimization. In *Proceedings of the 46th International Universities Power Engineering Conference*, 1–6. 10, 11

Ammeri, A., Chabchoub, H., Hachicha, W. & Masmoudi, F. (2010). A comprehensive literature classification of simulation–optimization methods. In *Proceedings of the 9th International Conference on Multi Objective Programming and Goal Programming*, 24–26. 53, 54

Anuta, O.H., Taylor, P., Jones, D., McEntee, T. & Wade, N. (2014). An international review of the implications of regulatory and electricity market structures on the emergence of grid scale electricity storage. *Renewable and Sustainable Energy Reviews*, **38**, 489–508. 7

Asif, M. & Muneer, T. (2007). Energy supply, its demand and security issues for developed and emerging economies. *Renewable and Sustainable Energy Reviews*, **11**, 1388–1413. 1

Azadivar, F. (1999). Simulation optimization methodologies. In *Proceedings of the 31st Conference on Winter Simulation: Simulation – a bridge to the future - Volume 1*, 93–100. 52

Baker, L. (2011). Governing electricity in South Africa: wind, coal and power struggles. *Governance of Clean Development Working Paper*, **15**, 1–27. 2, 18

Baldick, R. (2002). Electricity market equilibrium models: The effect of parametrization. *IEEE Transactions on Power Systems*, **17**, 1170–1176. 11

Banerjee, D., Hirani, M. & Sanyal, S. (2000). Coal-quality deterioration in a coal stack of a power station. *Applied Energy*, **66**, 267–275. 66

Behzadian, M., Otaghsara, S.K., Yazdani, M. & Ignatius, J. (2012). A state-of the-art survey of topsis applications. *Expert Systems with Applications*, **39**, 13051–13069. 96

Bekker, J. (2012). *Applying the cross-entropy method in multi-objective optimisation of dynamic stochastic systems*. Ph.D. thesis, Stellenbosch: Stellenbosch University. 51, 55, 56, 58, 76, 77, 79, 81, 83, 84, 86

Bekker, J. (2013). Multi-objective buffer space allocation with the cross-entropy method. *International Journal of Simulation Modelling*, **12**, 50–61. 83

Bekker, J. & Aldrich, C. (2010). The cross-entropy method in multi-objective optimisation: An assessment. *European Journal of Operational Research*, **211**, 112–121. 76, 77, 78, 79, 80, 81

Beltran, C. & Heredia, F.J. (1999). Short-term hydrothermal coordination by augmented lagrangian relaxation: a new multiplier updating. *Investigación Operativa*, **8**, 2. 10

Boom, A. (2003). Investments in electricity generating capacity under different market structures and with endogenously fixed demand. *WZB Markets and Political Economy Working Paper No. SP II*, **1**. 7, 8

Boussaïd, I., Lepagnot, J. & Siarry, P. (2013). A survey on optimization metaheuristics. *Information Sciences*, **237**, 82–117. 54, 55

Carson, Y. & Maria, A. (1997). Simulation optimization: methods and applications. In *Proceedings of the 29th Conference on Winter Simulation*, 118–126. 53

Castro-Gutierrez, J., Landa-Silva, D. & Pérez, J.M. (2011). Nature of real-world multi-objective vehicle routing with evolutionary algorithms. In *Proceedings of the 2011 IEEE International Conference on Systems, Man, and Cybernetics*, 257–264. 83

Coello, C.C., Lamont, G.B. & Van Veldhuizen, D.A. (2007). *Evolutionary algorithms for solving multi-objective problems*. Springer Science & Business Media. 55, 58, 59, 60, 96

Conradie, D.G., Morison, L.E. & Joubert, J.W. (2008). Scheduling at coal handling facilities using simulated annealing. *Mathematical Methods of Operations Research*, **68**, 277–293. 13

Corne, D.W., Knowles, J.D. & Oates, M.J. (2000). The pareto envelope-based selection algorithm for multiobjective optimization. In *Proceedings of the 6th International Conference on Parallel Problem Solving from Nature*, 839–848, Springer. 60

Curran, K., Droppo, I. & Irvine, K. (2002). Hydrology of stockpiled industrial coal exposed to rainfall. *Hydrological Processes*, **16**, 2781–2790. 66

David, A.K. & Wen, F. (2000). Strategic bidding in competitive electricity markets: a literature survey. In *Proceedings of the Power Engineering Society Summer Meeting*, vol. 4, 2168–2173, IEEE. 8, 9

Day, C.J. & Bunn, D.W. (2001). Divestiture of generation assets in the electricity pool of england and wales: A computational approach to analyzing market power. *Journal of Regulatory Economics*, **19**, 123–141. 12

De Weck, O.L. (2004). Multiobjective optimization: History and promise. In *Invited Keynote Paper, GL2-2, The Third China-Japan-Korea Joint Symposium on Optimization of Structural and Mechanical Systems*, vol. 2, 34. 57, 58

Deb, K., Pratap, A., Agarwal, S. & Meyarivan, T. (2002). A fast and elitist multiobjective genetic algorithm: NSGA-II. *IEEE Transactions on Evolutionary Computation*, **6**, 182–197. 60

Dogra, R., Gupta, N. & Saroa, H. (2014). Economic load dispatch problem and MATLAB programming of different methods. In *Proceedings of the International Conference of Advanced Research and Innovation*. 9, 10

Eberhard, A. (2011). The future of South African coal: market, investment, and policy challenges. Tech. rep., PESD Working Paper 100, Stanford. 20, 21, 22

Erickson, M., Mayer, A.S. & Horn, J. (1999). Development of a multi-objective optimization framework for groundwater remediation design using the niched-pareto genetic algorithm. *EOS: Transactions of American Geophysical Union. Am. Geophys. Union*, F840–F843. 60

Eskom Holdings SOC Ltd (2014a). Base and peak load electricity. Online, http://www.eskom.co.za/AboutElectricity/FactsFigures/Pages/Facts_Figures.aspx, accessed on 21 October 2014. 18, 19

Eskom Holdings SOC Ltd (2014b). Coal in South Africa. Online, http://www.eskom.co.za/AboutElectricity/FactsFigures/Pages/Facts_Figures.aspx, accessed on 21 October 2014. 18, 20, 21

Eskom Holdings SOC Ltd (2014c). Coal transport by road. Online, http://www.eskom.co.za/AboutElectricity/FactsFigures/Pages/Facts_Figures.aspx, accessed on 22 October 2014. 23

Eskom Holdings SOC Ltd (2014d). Generation plant mix. Online, http://www.eskom.co.za/AboutElectricity/FactsFigures/Pages/Facts_Figures.aspx, accessed on 21 October 2014. 1, 18, 19, 20

Eskom Holdings SOC Ltd (2014e). How electricity is produced at a coal fired power station. Online, http://www.eskom.co.za/AboutElectricity/FactsFigures/Pages/Facts_Figures.aspx, accessed on 22 October 2014. 6

Eskom Holdings SOC Ltd (2014f). Transmission and distribution of electricity. Online, http://www.eskom.co.za/AboutElectricity/FactsFigures/Pages/Facts_Figures.aspx, accessed on 22 October 2014. 7, 18

Eskom Holdings SOC Ltd (2015a). Generating electricity at a nuclear power station. Online, http://www.eskom.co.za/AboutElectricity/FactsFigures/Pages/Facts_Figures.aspx, accessed on 3 March 2015. 6

Eskom Holdings SOC Ltd (2015b). Pumped storage hydroelectric schemes and water transfer. Online, http://www.eskom.co.za/AboutElectricity/FactsFigures/Pages/Facts_Figures.aspx, accessed on 3 March 2015. 6

Eskom Holdings SOC Ltd (2015c). Solar Energy - Photovoltaic Solar power generation. Online, http://www.eskom.co.za/AboutElectricity/FactsFigures/Pages/Facts_Figures.aspx, accessed on 4 March 2015. 7

Fang, D., Zhang, M. & Wang, X. (2011). Power coal transportation and storage: A programming analysis of road and rail options. *Wuhan University Journal of Natural Sciences*, **16**, 469–474. 14

Farhat, I. & El-Hawary, M. (2009). Optimization methods applied for solving the short-term hydrothermal coordination problem. *Electric Power Systems Research*, **79**, 1308–1320. 10

Fleten, S.E. & Pettersen, E. (2005). Constructing bidding curves for a price-taking retailer in the norwegian electricity market. *IEEE Transactions on Power Systems*, **20**, 701–708. 9

Fonseca, C.M. & Fleming, P.J. (1993). Genetic algorithms for multiobjective optimization: Formulation, discussion and generalization. In *Proceedings of the Fifth International Conference on Genetic Algorithms*, vol. 423. 60

Fu, M.C., Glover, F.W. & April, J. (2005). Simulation optimization: a review, new developments, and applications. In *Proceedings of the 37th Conference on Winter Simulation*, 83–95. 54

Fu, M.C., Bayraksan, G., Henderson, S.G., Nelson, B.L., Powell, W.B., Ryzhov, I.O. & Thengvall, B. (2014). Simulation optimization: a panel on the state of the art in research and practice. In *Proceedings of the 2014 Winter Simulation Conference*, 3696–3706, IEEE. 50

García, J., Román, J., Barquín, J. & González, A. (1999). Strategic bidding in deregulated power systems. In *Proceedings of the 13th Power Systems Computation Conference*, vol. 1, 258–264. 9

Gendreau, M. & Potvin, J.Y. (2005). Metaheuristics in combinatorial optimization. *Annals of Operations Research*, **140**, 189–213. 54

Goldberg, D.E. (1989). Genetic algorithms in search, optimization and machine learning. *Addison-Wesley Publishing Company*. 60, 77

Hanoun, S., Khan, B., Johnstone, M., Nahavandi, S. & Creighton, D. (2013). An effective heuristic for stockyard planning and machinery scheduling at a coal handling facility. In *Proceedings of the 11th IEEE International Conference on Industrial Informatics*, 206–211. 13

Hao, S., Angelidis, G.A., Singh, H. & Papalexopoulos, A.D. (1997). Consumer payment minimization in power pool auctions. In *Proceedings of the 20th International Conference on Power Industry Computer Applications*, 368–373. 9

Hatton, M. (2015). *Requirements specification for the optimisation function of an electric utility's energy flow simulator*. Master's thesis, Stellenbosch: Stellenbosch University. ii, iii, 2, 67

Hauman, C. (2012). *The application of the cross-entropy method for multi-objective optimisation to combinatorial problems*. Master's thesis, Stellenbosch: Stellenbosch University. 84

Hwang, C.L. & Yoon, K. (1981). Methods for multiple attribute decision making. In *Multiple Attribute Decision Making*, 58–191, Springer. 96

Jian, Z. & Shi-xin, L. (2013). Models for coal blending with inventory in coal-fired power plant. In *Proceedings of the 25th Chinese Control and Decision Conference*, 1790–1793, IEEE. 13

Kazempour, S.J., Conejo, A.J. & Ruiz, C. (2015). Strategic bidding for a large consumer. *IEEE Transactions on Power Systems*, **30**, 848–856. 9

Kessides, I., Bogetic, Z. & Maurer, L. (2007). Current and forthcoming issues in the South African electricity sector. *Policy Research Working Paper, no WPS 4197, World Bank*. 2

Knowles, J.D. & Corne, D.W. (2000). Approximating the nondominated front using the pareto archived evolution strategy. *Evolutionary computation*, **8**, 149–172. 60

Kroese, D.P., Porotsky, S. & Rubinstein, R.Y. (2006). The cross-entropy method for continuous multi-extremal optimization. *Methodology and Computing in Applied Probability*, **8**, 383–407. 76

Kroese, D.P., Rubinstein, R.Y., Cohen, I., Porotsky, S. & Taimre, T. (2013). Cross-entropy method. In *Encyclopedia of Operations Research and Management Science*, 326–333, Springer. 76

Law, A.M. & Kelton, W.D. (2000). *Simulation modeling and analysis*. McGraw Hill Boston. 46

Li, Y. & Li, R. (2008). Simulation and optimization of the power station coal-fired logistics system based on witness simulation software. In *2008 Workshop on Power Electronics and Intelligent Transportation System*, 394–398, IEEE. 12

Lindner, B., Eygelaar, J., Lotter, D. & van Vuuren, J. (2015). Tri-objective generator maintenance scheduling for a national power utility. In *Proceedings of the 44th Annual Conference of the Operations Research Society of South Africa*, 112–122. 122

Ma, L. & Lin, M. (2008). Determination of safety stock for power enterprises under uncertainty. In *Proceedings of the 2008 International Symposium on Computer Science and Computational Technology*, vol. 1, 92–94, IEEE. 15, 16

Marcovecchio, M.G., Novais, A.Q. & Grossmann, I.E. (2014). Deterministic optimization of the thermal unit commitment problem: A branch and cut search. *Computers & Chemical Engineering*, **67**, 53–68. 9

Mercado, E.C. (2007). *Hands-on Inventory Management*. CRC Press. 63

Micali, V. & Heunis, S. (2011). Coal stock pile simulation. In *Proceedings of the 8th Conference on the Industrial and Commercial Use of Energy*, 198–203, IEEE. 32

Mielczarski, W., Michalik, G. & Widjaja, M. (1999). Bidding strategies in electricity markets. In *Proceedings of the 21st International Conference on Power Industry Computer Applications*, 71–76, IEEE. 9

Möst, D. & Keles, D. (2010). A survey of stochastic modelling approaches for liberalised electricity markets. *European Journal of Operational Research*, **207**, 543–556. 8

Muckstadt, J.A. & Sapra, A. (2010). *Principles of inventory management: When you are down to four, order more*. Springer Science & Business Media. 63

Muller, M. (2003). *Essentials of inventory management*. AMACOM. 64

Ólafsson, S. & Kim, J. (2002). Simulation optimization: simulation optimization. In *Proceedings of the 34th Conference on Winter Simulation: exploring new frontiers*, 79–84. 50, 51, 53, 54

Otero-Novas, I., Meseguer, C., Batlle, C. & Alba, J.J. (2000). A simulation model for a competitive generation market. *IEEE Transactions on Power Systems*, **15**, 250–256. 7, 11, 12

Ozdeniz, A., Corumluoglu, O., Kalayci, I. & Sensogut, C. (2008). 3.5 d temperature model of a coal stockpile. *Energy Sources, Part A*, **30**, 1085–1097. 65

Padhy, N.P. (2004). Unit commitment-a bibliographical survey. *IEEE Transactions on Power Systems*, **19**, 1196–1205. 9

Pone, J.D.N., Hein, K.A., Stracher, G.B., Annegarn, H.J., Finkleman, R.B., Blake, D.R., McCormack, J.K. & Schroeder, P. (2007).

The spontaneous combustion of coal and its by-products in the witbank and sasolburg coalfields of south africa. *International Journal of Coal Geology*, **72**, 124–140. 65, 66

Rahman, D.F., Viana, A. & Pedroso, J.P. (2014). Metaheuristic search based methods for unit commitment. *International Journal of Electrical Power & Energy Systems*, **59**, 14–22. 9

Ramirez, J.M. & Oñate, P.E. (2006). The short-term hydrothermal coordination via genetic algorithms. *Electric Power Components and Systems*, **34**, 1–19. 10

Rastegar, M.A., Guerci, E. & Cincotti, S. (2009). Agent-based model of the italian wholesale electricity market. In *Proceedings of the 6th International Conference on the European Energy Market*, 1–7, IEEE. 12

Rosen, S.L., Harmonosky, C.M. & Traband, M.T. (2007). A simulation optimization method that considers uncertainty and multiple performance measures. *European Journal of Operational Research*, **181**, 315–330. 51

Roy, P.K., Bhui, S. & Paul, C. (2014). Solution of economic load dispatch using hybrid chemical reaction optimization approach. *Applied Soft Computing*, **24**, 109–125. 9

Rubinstein, R. (1999). The cross-entropy method for combinatorial and continuous optimization. *Methodology and Computing in Applied Probability*, **1**, 127–190. 76, 81

Rubinstein, R. & Kroese, D. (2004). *The Cross Entropy Method: A Unified Approach to Combinatorial Optimization, Monte-Carlo Simulation, and Machine Learning*. Springer. 76, 77, 81

Rubinstein, R.Y. (1997). Optimization of computer simulation models with rare events. *European Journal of Operational Research*, **99**, 89–112. 76

Sarker, M., Chowdhury, D. & Hossain, I. (2014). Power generation from coal - A review. *Journal of Chemical Engineering*, **27**, 50–54. 6

Sarkhani, S., Soleymani, S. & Mozafari, B. (2014). Strategic bidding of an electricity distribution company with distributed generation and interruptible load in a day-ahead electricity market. *Arabian Journal for Science and Engineering*, **39**, 3925–3940. 9

Scholtz, E. (2014). *A comparative study on the value of accounting for possible relationships between decision variables when solving multi-objective problems*. Master's thesis, Stellenbosch: Stellenbosch University. 56, 57, 58, 76, 84

Simon, D. (2013). *Evolutionary optimization algorithms*. John Wiley & Sons. 55

Singh, S.P., Tyagi, R. & Goel, A. (2014). Genetic algorithm for solving the economic load dispatch. *International Journal of Electronic and Electrical Engineering, International Research Publication*, **7**, 523–528. 9

Stadler, J.G. (2012). *Multi-objective optimisation using the cross-entropy method in CO gas management at a South African ilmenite smelter*. Master's thesis, Stellenbosch: Stellenbosch University. 83, 84

Subathra, M., Selvan, S.E., Victoire, T.A.A., Christinal, A.H. & Amato, U. (2014). A hybrid with cross-entropy method and sequential quadratic programming to solve economic load dispatch problem. 9

Swisher, J.R., Hyden, P.D., Jacobson, S.H. & Schruben, L.W. (2000). A survey of simulation optimization techniques and procedures. In *Proceedings of the 2000 Winter Simulation Conference*, vol. 1, 119–128, IEEE. 53

Talbi, E.G. (2009). *Metaheuristics: from design to implementation*, vol. 74. John Wiley & Sons. 54, 55

Taraba, B., Michalec, Z., Michalcová, V., Blejchař, T., Bojko, M. & Kozubková, M. (2014). Cfd simulations of the effect of wind on the spontaneous heating of coal stockpiles. *Fuel*, **118**, 107–112. 65, 66

Tekin, E. & Sabuncuoglu, I. (2004). Simulation optimization: A comprehensive review on theory and applications. *IIE Transactions*, **36**, 1067–1081. 52, 53

Toomey, J.W. (2000). *Inventory management: principles, concepts and techniques*. Kluwer Academic Publishers. 63

van Harmelen, G., Phaswana, A., Dean, J., Bashe, M. & Matshalaga, D. (2014). Energy flow simulator – visually interactive financial strategic decision support, confidential report: Eskom Holdings Limited. 23

Van Veldhuizen, D.A. & Lamont, G.B. (2000). Multiobjective optimization with messy genetic algorithms. In *Proceedings of the 2000 ACM symposium on Applied computing - Volume 1*, 470–476, ACM. 60

Ventosa, M., Baillo, A., Ramos, A. & Rivier, M. (2005). Electricity market modeling trends. *Energy Policy*, **33**, 897–913. 7, 8, 10, 11, 12

West, J. (2011). Optimising coal stockpiles in a supply chain using a dynamic cost flow model. Tech. rep., Griffith University, Department of Accounting, Finance and Economics. 13

Winston, W.L. (2004). *Operations research: applications and algorithms*. Brooks/Cole. 63, 64, 96

Xi-jin, G., Ming, C. & Jia-wei, W. (2009). Coal blending optimization of coal preparation production process based on improved ga. *Procedia Earth and Planetary Science*, **1**, 654–660. 13

Yabin, L. (2010). Research on simulation and optimization of transshipment port operation in a power coal ocean shipping logistics system on the basis of witness. *Journal of Convergence Information Technology*, **5**, 84–87. 14

Yucekaya, A. (2013). Cost minimizing coal logistics for power plants considering transportation constraints. 13, 14

Zhang, D., Wang, Y. & Luh, P.B. (1999). Optimization based bidding strategies in the deregulated market. In *Proceedings of the 21st IEEE International Conference on Power Industry Computer Applications*, 63–68. 8

Zhang, L. & Xia, X. (2014). An optimization model for reducing energy usage of coal washing plants. *Energy Procedia*, **61**, 1017–1020. 13

Zhanwu, W., Xiao, Y., Zhonglei, F. & Xiongbiao, X. (2011). Research on improving the inventory management of coal in thermal power plants – take H Corporation as an example. In *Proceedings of the 2011 International Conference on Business Management and Electronic Information*, vol. 1, 321–324, IEEE. 15, 16

Zhou, Z., Zhao, F. & Wang, J. (2011). Agent-based electricity market simulation with demand response from commercial buildings. *IEEE Transactions on Smart Grid*, **2**, 580–588. 12

Zitzler, E. (1999). *Evolutionary algorithms for multiobjective optimization: Methods and applications*, vol. 63. Citeseer. 55, 59, 60

Zitzler, E. & Thiele, L. (1999). Multi-objective evolutionary algorithms: a comparative case study and the strength pareto approach. *IEEE Transactions on Evolutionary Computation*, **3**, 257–271. 60

Appendix A

Additional experimental results

This appendix presents additional results for three of the four experiments presented in Chapter 6.

For Experiment 1, plots for both *model 1* and *model 2* are given that show the progression of the parameter vectors of the decision variables. These are only for the closest first coal transfer policy. The progression plots for the most urgent transfer policy show similar patterns and are not included in this document. Also provided for Experiment 1 are matrices that show the coal transfers recorded for the solutions analysed in Subsection 6.4.2 (model 1 with the two transfer policies) and Subsection 6.4.3 (model 2 with the two transfer policies).

For each of Experiments 2.1 to 2.6 (Subsection 6.5.2) and Experiments 3.1 and 3.2 (Subsection 6.6.2), a solution that the author considers a good trade-off between f_1 and f_2 was selected and analysed. The objective function values, decision variable values and coal transfer matrix are provided for each of these solutions.

A.1 Experiment 1

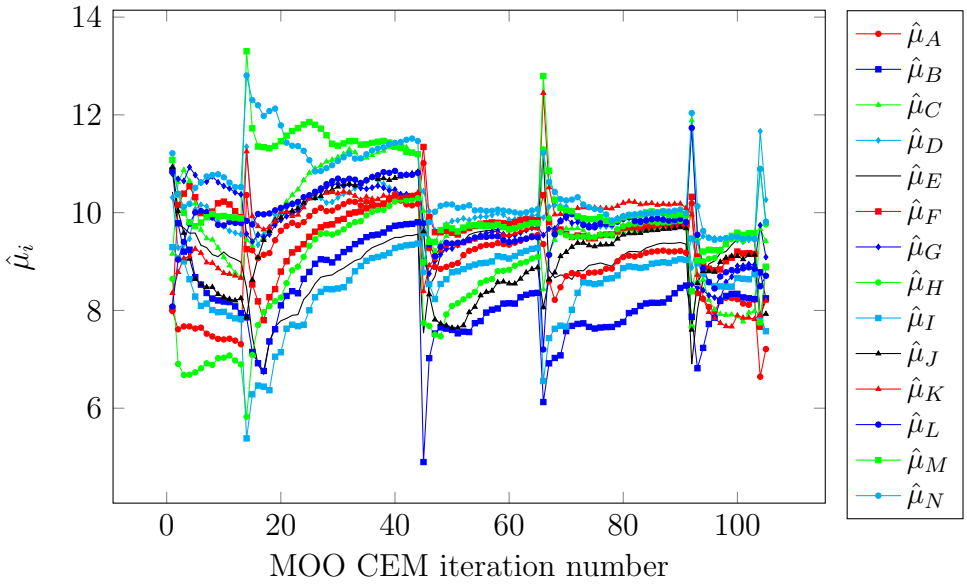

Figure A.1: Progression of the values of $\hat{\mu}_i$ for the variables $x_i = L_s$, model 1 with the closest first transfer policy.

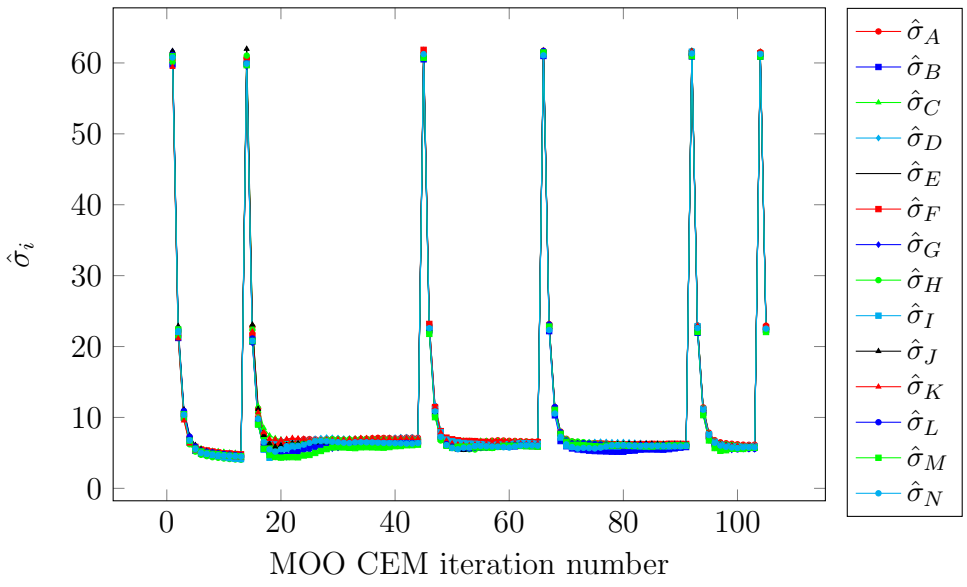

Figure A.2: Progression of the values of $\hat{\sigma}_i$ for the variables $x_i = L_s$, model 1 with the closest first transfer policy.

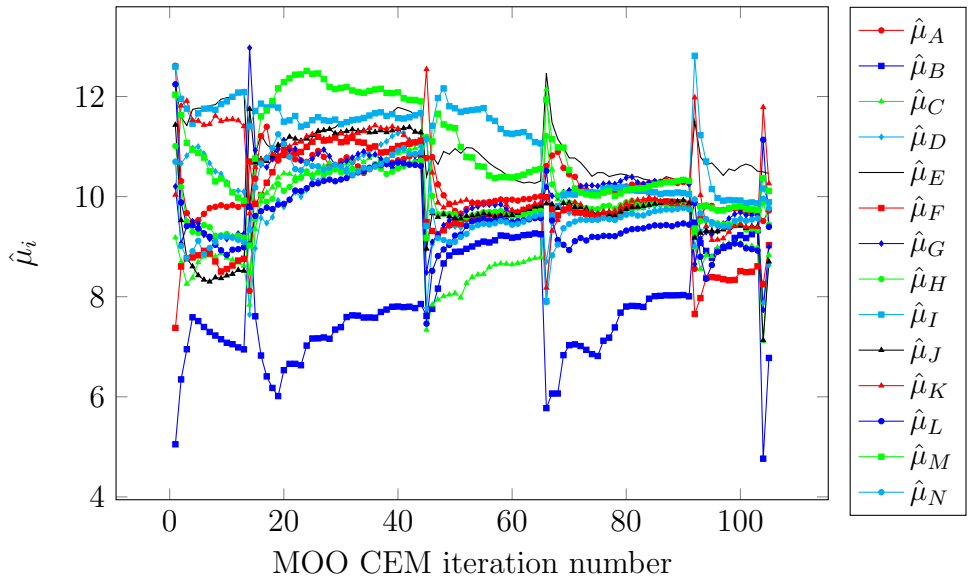

Figure A.3: Progression of the values of $\hat{\mu}_i$ for the variables $x_i = T_s - L_s$, model 1 with the closest first transfer policy.

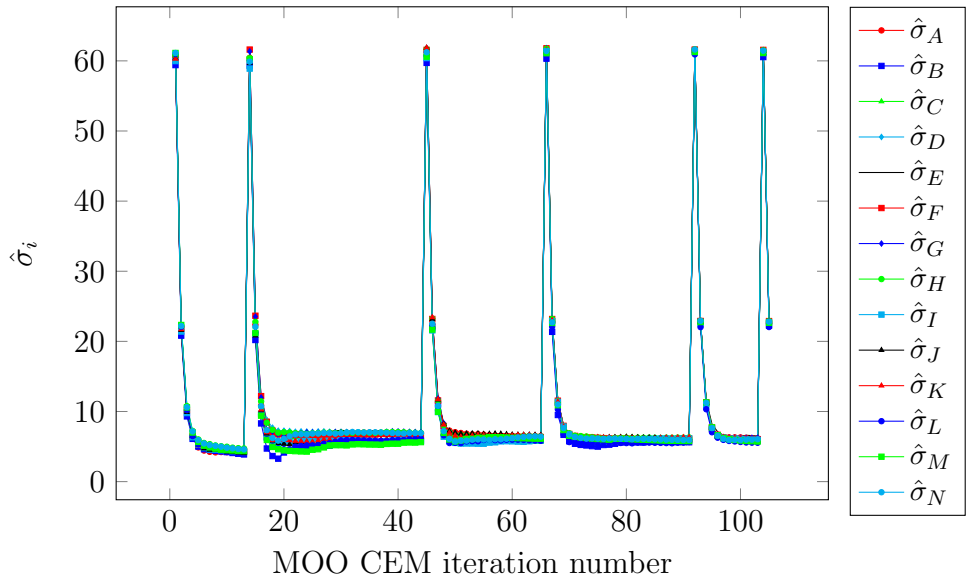

Figure A.4: Progression of the values of $\hat{\sigma}_i$ for the variables $x_i = T_s - L_s$, model 1 with the closest first transfer policy.

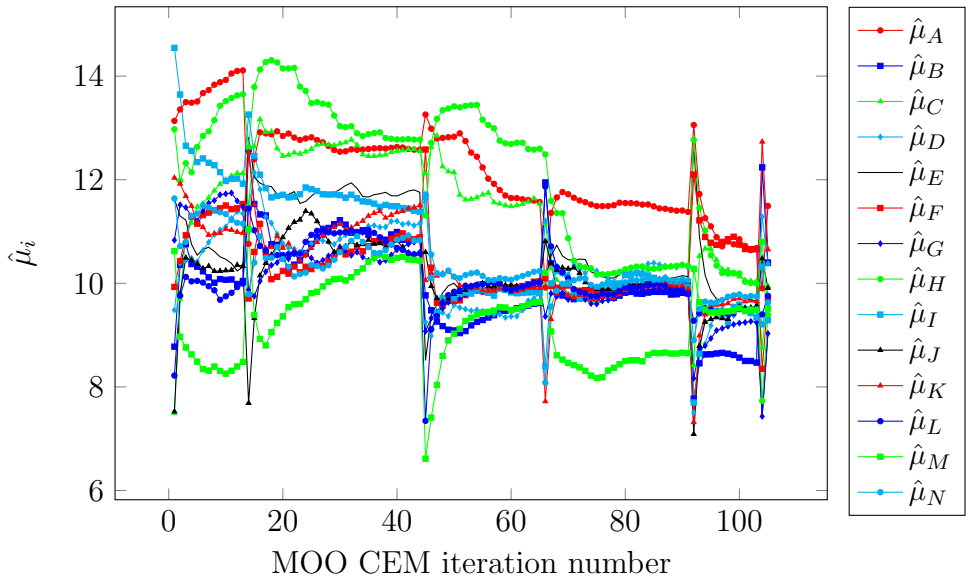

Figure A.5: Progression of the values of $\hat{\mu}_i$ for the variables $x_i = U_s - T_s$, model 1 with the closest first transfer policy.

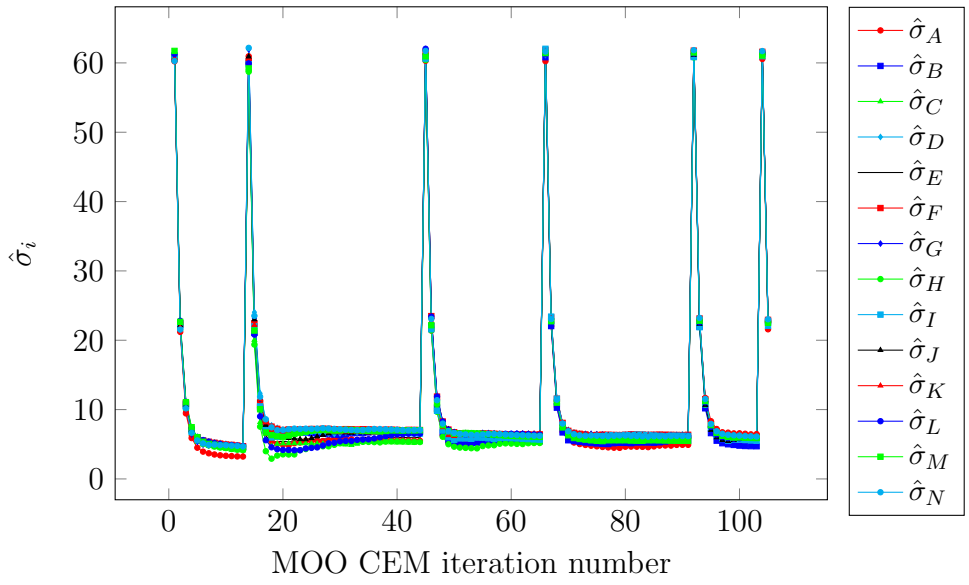

Figure A.6: Progression of the values of $\hat{\sigma}_i$ for the variables $x_i = U_s - T_s$, model 1 with the closest first transfer policy.

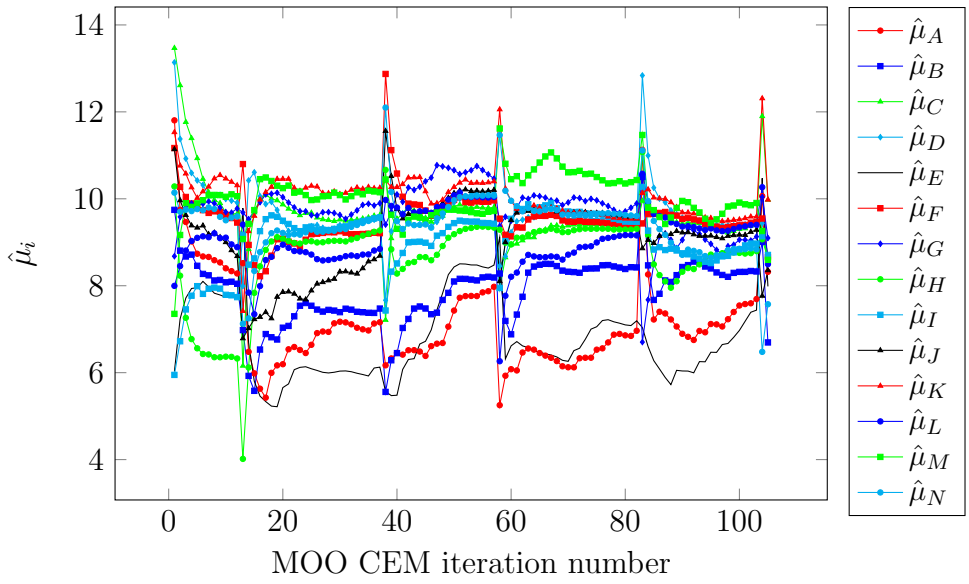

Figure A.7: Progression of the values of $\hat{\mu}_i$ for the variables $x_i = L_s$, model 2 with the closest first transfer policy.

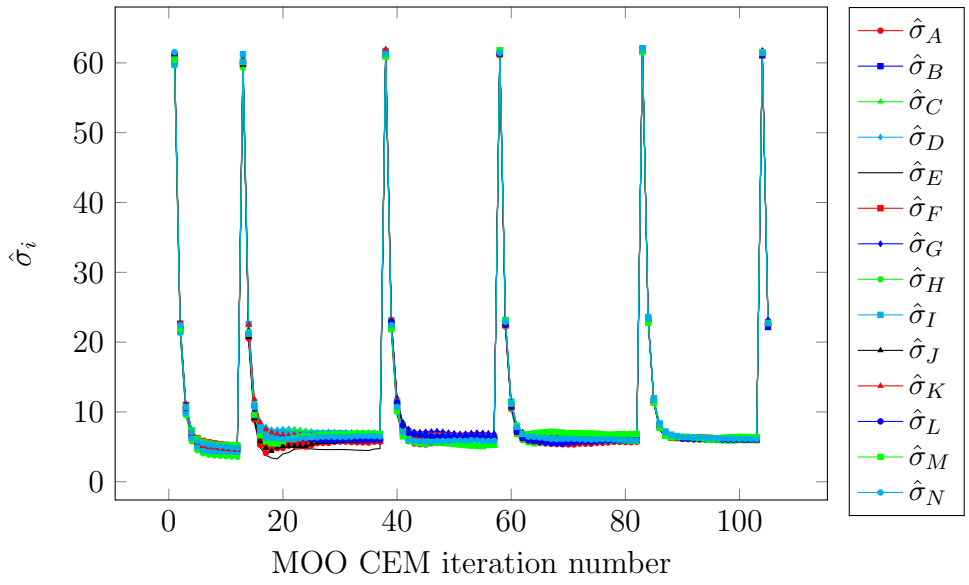

Figure A.8: Progression of the values of $\hat{\sigma}_i$ for the variables $x_i = L_s$, model 2 with the closest first transfer policy.

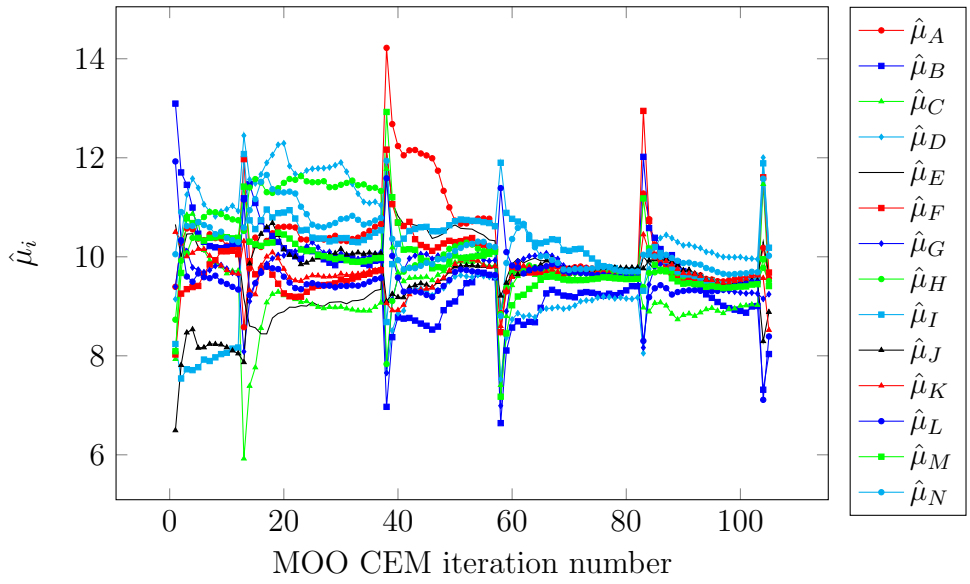

Figure A.9: Progression of the values of $\hat{\mu}_i$ for the variables $x_i = T_s - L_s$, model 2 with the closest first transfer policy.

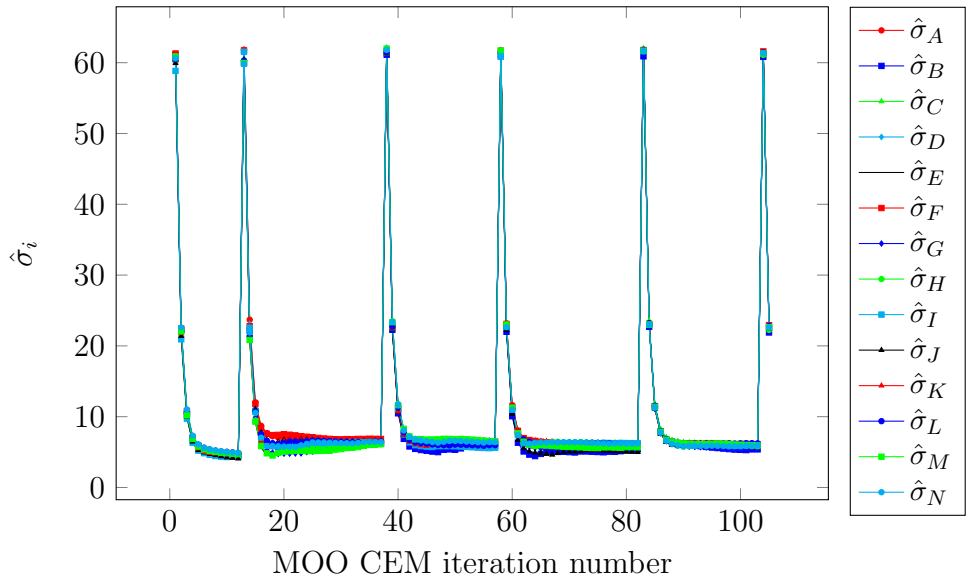

Figure A.10: Progression of the values of $\hat{\sigma}_i$ for the variables $x_i = T_s - L_s$, model 2 with the closest first transfer policy.

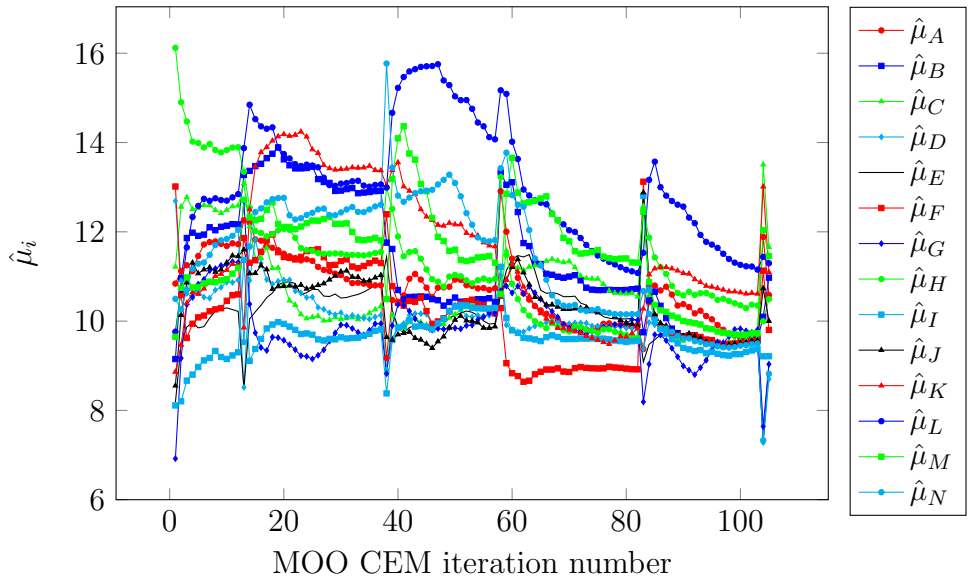

Figure A.11: Progression of the values of $\hat{\mu}_i$ for the variables $x_i = U_s - T_s$, model 2 with the closest first transfer policy.

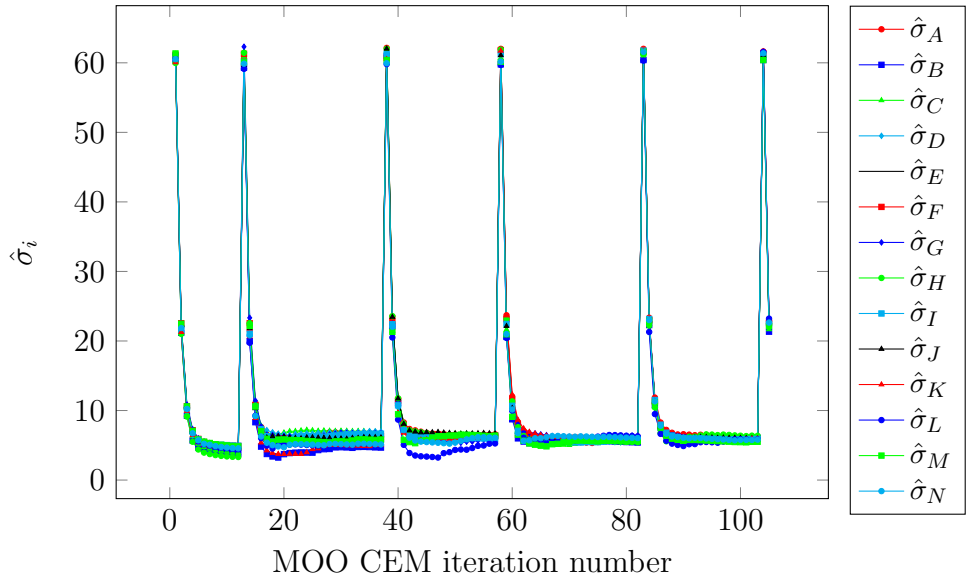

Figure A.12: Progression of the values of $\hat{\sigma}_i$ for the variables $x_i = U_s - T_s$, model 2 with the closest first transfer policy.

Table A.1: Coal transfers recorded for a good solution of model 1 with the closest first coal transfer policy, expected value as output statistic (ktonnes).

	A	B	C	D	E	F	G	H	I	J	K	L	M	N
A	-	0	0	0	9.97	0	0	0	0	0	0	0	0	0
B	-	-	0	0	0	0	0	0	0	0	0	0	0	0
C	-	-	-	0	0	69.49	3.79	0	0	3.08	0	0	0.03	25.83
D	-	-	-	-	0	0	7.68	0	0	0	5.49	0.59	14.59	100.3
E	-	-	-	-	-	0	0	0	0	0	0	0	0	0
F	-	-	-	-	-	-	34.08	0	0	0	45.06	81.58	0	25.73
G	-	-	-	-	-	-	-	0	0	65.37	0	0	78.01	105.1
H	-	-	-	-	-	-	-	-	0	0	0	0	0	0
I	-	-	-	-	-	-	-	-	-	0	0	0	0	0
J	-	-	-	-	-	-	-	-	-	-	7.01	0.17	57.74	77.76
K	-	-	-	-	-	-	-	-	-	-	-	0	0	0
L	-	-	-	-	-	-	-	-	-	-	-	-	3.99	78.29
M	-	-	-	-	-	-	-	-	-	-	-	-	-	0
N	-	-	-	-	-	-	-	-	-	-	-	-	-	-

Table A.2: Coal transfers recorded for a good solution of model 1 with the most urgent coal transfer policy, expected value as output statistic (ktonnes).

	A	B	C	D	E	F	G	H	I	J	K	L	M	N
A	-	0	0	0	57.72	0	0	0	79.48	0	0	0	0	0
B	-	-	0	0	0	0	0	0	0	0	0	0	0	0
C	-	-	-	32.95	0	117.3	129.6	0	0	53.73	162.9	26.51	174.8	10.23
D	-	-	-	-	0	18.31	77.95	0	0	25.51	20.29	95.96	76.80	7.79
E	-	-	-	-	-	0	0	0	4.35	0	0	0	0	0
F	-	-	-	-	-	-	77.72	0	0	0	43.27	71.65	67.16	37.31
G	-	-	-	-	-	-	-	0	0	0	5.97	32.51	75.72	75.12
H	-	-	-	-	-	-	-	-	52.82	0	0	0	0	0
I	-	-	-	-	-	-	-	-	-	0	0	0	0	0
J	-	-	-	-	-	-	-	-	-	-	0	101.1	0	27.94
K	-	-	-	-	-	-	-	-	-	-	-	0	0	0
L	-	-	-	-	-	-	-	-	-	-	-	-	0	0
M	-	-	-	-	-	-	-	-	-	-	-	-	-	0
N	-	-	-	-	-	-	-	-	-	-	-	-	-	-

Table A.3: Coal transfers recorded for a good solution of model 2 with the closest first coal transfer policy, expected value as output statistic (ktonnes).

	A	B	C	D	E	F	G	H	I	J	K	L	M	N
A	-	0	0	0	160.8	0	0	0	6.94	0	0	0	0	0
B	-	-	0	0	0	0	0	0	0	0	0	0	0	0
C	-	-	-	0	0	0	24.13	0	0	0	0	0	0	0
D	-	-	-	-	0	78.57	43.42	0	0	58.99	0	35.73	0	58.31
E	-	-	-	-	-	0	0	4.05	57.46	0	0	0	0	0
F	-	-	-	-	-	-	0	0	0	42.96	51.65	32.31	81.38	120.9
G	-	-	-	-	-	-	-	0	0	157.8	0	0	41.66	18.03
H	-	-	-	-	-	-	-	-	115.5	0	0	0	0	0
I	-	-	-	-	-	-	-	-	-	0	0	0	0	0
J	-	-	-	-	-	-	-	-	-	-	6.12	0	3.67	37.04
K	-	-	-	-	-	-	-	-	-	-	-	0	0	4.87
L	-	-	-	-	-	-	-	-	-	-	-	-	5.02	15.82
M	-	-	-	-	-	-	-	-	-	-	-	-	-	0
N	-	-	-	-	-	-	-	-	-	-	-	-	-	-

Table A.4: Coal transfers recorded for a good solution of model 2 with the most urgent coal transfer policy, expected value as output statistic (ktonnes).

	A	B	C	D	E	F	G	H	I	J	K	L	M	N
A	-	0	0	0	127.6	0	0	52.51	59.24	0	0	0	0	0
B	-	-	0	0	0	0	0	0	0	0	0	0	0	0
C	-	-	-	0	0	151.1	149.3	0	0	389.0	0	76.28	83.11	0
D	-	-	-	-	0	0	0	0	0	4.09	0	0	50.18	0
E	-	-	-	-	-	0	0	184.9	46.98	0	0	0	0	0
F	-	-	-	-	-	-	50.20	0	0	0	13.84	22.66	10.88	19.16
G	-	-	-	-	-	-	-	0	0	40.77	0	6.13	16.96	60.41
H	-	-	-	-	-	-	-	-	243.3	0	0	0	0	0
I	-	-	-	-	-	-	-	-	-	0	0	0	0	0
J	-	-	-	-	-	-	-	-	-	-	35.18	73.18	23.82	51.90
K	-	-	-	-	-	-	-	-	-	-	-	13.33	0	0
L	-	-	-	-	-	-	-	-	-	-	-	-	0	0
M	-	-	-	-	-	-	-	-	-	-	-	-	-	0
N	-	-	-	-	-	-	-	-	-	-	-	-	-	-

A.2 Experiment 2

Table A.5: Approximation of the objective function values for a good solution of Experiment 2.1.

f_1 (ktonnes)	5 205
f_2 (ktonnes·km)	150 257

Table A.6: Approximation of the decision variable values for a good solution of Experiment 2.1.

	Stockpile days			ktonnes		
Power station	L_s	T_s	U_s	L_s	T_s	U_s
A	5	13	31	231.5	601.9	1 435.2
B	10	11	20	545.4	600.0	1 090.9
C	5	13	25	179.6	467.0	898.0
D	11	12	19	215.7	235.3	372.5
E	8	12	15	334.2	501.3	626.6
F	10	14	31	149.7	209.5	464.0
G	5	9	22	74.8	134.7	329.3
H	6	9	23	286.5	429.8	1 098.4
I	5	10	17	238.4	476.9	810.7
J	5	14	15	182.3	510.4	546.9
K	9	10	21	135.6	150.7	316.4
L	6	7	20	140.8	164.3	469.4
M	5	12	16	46.9	112.6	150.1
N	8	23	35	95.8	275.4	419.1

Table A.7: Coal transfers recorded for a good solution of Experiment 2.1 (ktonnes).

	A	B	C	D	E	F	G	H	I	J	K	L	M	N
A	-	0	0	0	110.0	0	0	0	0	0	0	0	0	0
B	-	-	0	0	0	0	0	0	0	0	0	0	0	0
C	-	-	-	2.87	0	0	40.0	0	0	11.34	10.0	39.07	80.49	147.1
D	-	-	-	-	0	10.0	10.0	0	0	20.88	18.15	29.98	25.68	0
E	-	-	-	-	-	0	0	20.0	70.0	0	0	0	0	0
F	-	-	-	-	-	-	0	0	0	7.35	15.95	40.0	50.0	81.93
G	-	-	-	-	-	-	-	0	0	117.2	19.13	10.0	53.88	39.59
H	-	-	-	-	-	-	-	-	20.45	0	0	0	0	0
I	-	-	-	-	-	-	-	-	-	0	0	0	0	0
J	-	-	-	-	-	-	-	-	-	-	66.06	31.90	184.2	218.8
K	-	-	-	-	-	-	-	-	-	-	-	9.19	0	0
L	-	-	-	-	-	-	-	-	-	-	-	-	0	0
M	-	-	-	-	-	-	-	-	-	-	-	-	-	0
N	-	-	-	-	-	-	-	-	-	-	-	-	-	-

Table A.8: Approximation of the objective function values for a good solution of Experiment 2.2.

f_1 (ktonnes)	5 243
f_2 (ktonnes·km)	150 796

Table A.9: Approximation of the decision variable values for a good solution of Experiment 2.2.

	Stockpile days			ktonnes		
Power station	L_s	T_s	U_s	L_s	T_s	U_s
A	5	14	24	231.5	648.1	1 111.1
B	9	10	14	490.9	545.4	763.6
C	5	10	12	179.6	359.2	431.1
D	5	10	18	98.0	196.1	352.9
E	6	12	18	250.6	501.3	751.9
F	10	11	17	149.7	164.6	254.4
G	6	15	16	89.8	224.5	239.5
H	5	9	23	238.8	429.8	1 098.4
I	7	15	24	333.8	715.3	1 144.5
J	9	12	18	328.1	437.5	656.3
K	9	14	15	135.6	210.9	226.0
L	5	7	11	117.3	164.3	258.2
M	5	13	20	46.9	121.9	187.6
N	11	12	14	131.7	143.7	167.6

Table A.10: Coal transfers recorded for a good solution of Experiment 2.2 (ktonnes).

	A	B	C	D	E	F	G	H	I	J	K	L	M	N
A	-	0	0	0	80.49	0	0	0	0	0	0	0	0	0
B	-	-	0	0	0	0	0	0	0	0	0	0	0	0
C	-	-	-	4.55	0	0	243.4	0	0	56.20	94.78	283.2	45.83	162.0
D	-	-	-	-	0	22.82	4.37	0	0	15	41.25	12.49	0	2.15
E	-	-	-	-	-	0	0	30	0	0	0	0	0	0
F	-	-	-	-	-	-	53.43	0	0	7.94	59.20	33.53	37.94	90.81
G	-	-	-	-	-	-	-	0	0	44.64	65.44	49.57	27.96	24.41
H	-	-	-	-	-	-	-	-	0	0	0	0	0	0
I	-	-	-	-	-	-	-	-	-	0	0	0	0	0
J	-	-	-	-	-	-	-	-	-	-	22.18	15	72.52	188.4
K	-	-	-	-	-	-	-	-	-	-	-	0	4.46	19.91
L	-	-	-	-	-	-	-	-	-	-	-	-	15	18.12
M	-	-	-	-	-	-	-	-	-	-	-	-	-	0
N	-	-	-	-	-	-	-	-	-	-	-	-	-	-

Table A.11: Approximation of the objective function values for a good solution of Experiment 2.3.

f_1 (ktonnes)	6 340
f_2 (ktonnes·km)	146 267

Table A.12: Approximation of the decision variable values for a good solution of Experiment 2.3.

	Stockpile days			ktonnes		
Power station	L_s	T_s	U_s	L_s	T_s	U_s
A	7	13	23	324.1	601.9	1 064.8
B	7	9	19	381.8	490.9	1 036.3
C	10	15	23	359.2	538.8	826.2
D	8	21	26	156.9	411.7	509.8
E	11	19	25	459.5	793.6	1 044.3
F	14	16	25	209.5	239.5	374.2
G	10	18	20	149.7	269.4	299.3
H	7	8	18	334.3	382.1	859.6
I	5	14	24	238.4	667.6	1 144.5
J	5	7	18	182.3	255.2	656.3
K	8	17	24	120.5	256.1	361.6
L	11	20	25	258.2	469.4	586.7
M	13	20	27	121.9	187.6	253.2
N	14	25	39	167.6	299.3	467.0

Table A.13: Coal transfers recorded for a good solution of Experiment 2.3 (ktonnes).

	A	B	C	D	E	F	G	H	I	J	K	L	M	N
A	-	0	0	0	0	0	0	82.50	0	0	0	0	0	0
B	-	-	0	0	0	0	0	0	0	0	0	0	0	0
C	-	-	-	0	0	28.81	107.5	0	0	0	0	268.3	21.43	93.33
D	-	-	-	-	0	56.50	36.16	0	0	4.76	3.91	108.7	0	0
E	-	-	-	-	-	0	0	1.93	0	0	0	0	0	0
F	-	-	-	-	-	-	0	0	0	2.85	0	59.27	84.24	58.05
G	-	-	-	-	-	-	-	0	0	40.89	0	0	8.25	51.57
H	-	-	-	-	-	-	-	-	177.5	0	0	0	0	0
I	-	-	-	-	-	-	-	-	-	0	0	0	0	0
J	-	-	-	-	-	-	-	-	-	-	26.96	0	103.3	8.64
K	-	-	-	-	-	-	-	-	-	-	-	0	6.18	16.29
L	-	-	-	-	-	-	-	-	-	-	-	-	0	0
M	-	-	-	-	-	-	-	-	-	-	-	-	-	0
N	-	-	-	-	-	-	-	-	-	-	-	-	-	-

Table A.14: Approximation of the objective function values for a good solution of Experiment 2.4.

f_1 (ktonnes)	6 230
f_2 (ktonnes·km)	127 110

Table A.15: Approximation of the decision variable values for a good solution of Experiment 2.4.

	Stockpile days			ktonnes		
Power station	L_s	T_s	U_s	L_s	T_s	U_s
A	14	18	32	648.1	833.3	1 435.0
B	5	7	18	272.7	381.8	981.8
C	5	13	18	179.6	467.0	646.6
D	13	17	27	254.9	333.3	529.4
E	5	14	25	208.9	584.8	1 044.3
F	8	12	21	119.7	179.6	314.3
G	13	19	25	194.6	284.4	374.2
H	6	10	21	286.5	477.6	1 002.9
I	5	14	23	238.4	667.6	1 096.8
J	13	17	25	474.0	619.8	911.5
K	13	21	27	195.9	316.4	406.8
L	8	16	23	187.7	375.5	539.8
M	7	13	25	65.7	121.9	234.5
N	13	19	28	155.7	227.5	335.3

Table A.16: Coal transfers recorded for a good solution of Experiment 2.4 (ktonnes).

	A	B	C	D	E	F	G	H	I	J	K	L	M	N
A	-	0	0	0	0	0	0	0	0	0	0	0	0	0
B	-	-	0	0	0	0	0	0	0	0	0	0	0	0
C	-	-	-	34.85	0	16.36	130.1	0	0	0	18.68	190.6	0	112.2
D	-	-	-	-	0	0	25.06	0	0	0	0.68	0	0	38.88
E	-	-	-	-	-	0	0	0	0	0	0	0	0	0
F	-	-	-	-	-	-	80.89	0	0	0	44.81	98.49	133.5	78.81
G	-	-	-	-	-	-	-	0	0	10.52	2.49	0	23.92	140.3
H	-	-	-	-	-	-	-	-	0	0	0	0	0	0
I	-	-	-	-	-	-	-	-	-	0	0	0	0	0
J	-	-	-	-	-	-	-	-	-	-	41.60	0	0	0
K	-	-	-	-	-	-	-	-	-	-	-	0	0	1.24
L	-	-	-	-	-	-	-	-	-	-	-	-	0	19.18
M	-	-	-	-	-	-	-	-	-	-	-	-	-	0
N	-	-	-	-	-	-	-	-	-	-	-	-	-	-

Table A.17: Approximation of the objective function values for a good solution of Experiment 2.5.

f_1 (ktonnes)	5 538
f_2 (ktonnes·km)	137 895

Table A.18: Approximation of the decision variable values for a good solution of Experiment 2.5.

	Stockpile days			ktonnes		
Power station	L_s	T_s	U_s	L_s	T_s	U_s
A	5	7	19	231.5	324.1	1 342.6
B	5	6	12	272.7	327.3	654.5
C	7	12	22	251.4	431.1	790.3
D	10	16	25	196.1	313.7	490.2
E	8	15	22	334.2	626.6	919.0
F	8	14	22	119.7	209.5	419.1
G	13	16	24	194.6	239.5	359.2
H	6	12	23	286.5	573.1	1 098.4
I	6	15	25	286.1	715.3	1 192.2
J	5	13	20	182.3	474.0	729.2
K	6	13	22	90.4	195.9	331.5
L	13	18	26	305.1	422.4	610.2
M	10	15	26	93.8	140.7	243.9
N	12	18	33	143.7	215.5	395.1

Table A.19: Coal transfers recorded for a good solution of Experiment 2.5 (ktonnes).

	A	B	C	D	E	F	G	H	I	J	K	L	M	N
A	-	0	0	88.38	0	0	0	0	0	0	0	0	0	0
B	-	-	0	0	0	0	0	0	0	0	0	0	0	0
C	-	-	-	20.0	0	0	40.0	0	0	0	48.05	17.43	96.99	80.0
D	-	-	-	-	0	19.11	69.95	0	0	0	0	0	0	0
E	-	-	-	-	-	0	0	0	0	0	0	0	0	0
F	-	-	-	-	-	-	81.33	0	0	0	55.74	78.10	60.0	110.9
G	-	-	-	-	-	-	-	0	0	133.8	20.0	0	108.1	37.51
H	-	-	-	-	-	-	-	-	40.0	0	0	0	0	0
I	-	-	-	-	-	-	-	-	-	0	0	0	0	0
J	-	-	-	-	-	-	-	-	-	-	0	0	39.82	120.0
K	-	-	-	-	-	-	-	-	-	-	-	0	0	0
L	-	-	-	-	-	-	-	-	-	-	-	-	0	20.0
M	-	-	-	-	-	-	-	-	-	-	-	-	-	0
N	-	-	-	-	-	-	-	-	-	-	-	-	-	-

Table A.20: Approximation of the objective function values for a good solution of Experiment 2.6.

f_1 (ktonnes)	5 682
f_2 (ktonnes·km)	159 120

Table A.21: Approximation of the decision variable values for a good solution of Experiment 2.6.

	Stockpile days			ktonnes		
Power station	L_s	T_s	U_s	L_s	T_s	U_s
A	5	11	23	231.5	509.3	1 064.8
B	5	8	11	272.7	436.3	600.0
C	7	14	26	251.4	502.9	934.0
D	5	11	20	98.0	215.7	392.1
E	10	18	22	417.7	751.9	919.0
F	11	17	19	164.6	254.4	284.4
G	9	15	26	134.7	224.5	389.1
H	10	16	20	477.6	764.1	955.2
I	5	12	20	238.4	572.3	953.8
J	9	10	15	328.1	364.6	546.9
K	9	15	27	135.6	226.0	406.8
L	6	12	19	140.8	281.6	445.9
M	11	14	20	103.2	131.3	187.6
N	5	7	18	59.9	83.8	215.5

Table A.22: Coal transfers recorded for a good solution of Experiment 2.6 (ktonnes).

	A	B	C	D	E	F	G	H	I	J	K	L	M	N
A	-	0	0	0	7.15	0	0	81.34	0	0	0	0	0	0
B	-	-	0	0	0	0	0	0	0	0	0	0	0	0
C	-	-	-	0	0	69.52	165.0	0	0	12.83	25.0	26.98	50.0	101.85
D	-	-	-	-	0	32.29	69.57	0	0	0	0	18.83	38.62	51.69
E	-	-	-	-	-	0	0	75.0	0	0	0	0	0	0
F	-	-	-	-	-	-	0	0	0	80.63	53.17	29.56	92.45	108.7
G	-	-	-	-	-	-	-	0	0	33.69	22.04	46.15	29.02	27.36
H	-	-	-	-	-	-	-	-	128.2	0	0	0	0	0
I	-	-	-	-	-	-	-	-	-	0	0	0	0	0
J	-	-	-	-	-	-	-	-	-	-	58.33	0	45.82	190.5
K	-	-	-	-	-	-	-	-	-	-	-	0	0	0
L	-	-	-	-	-	-	-	-	-	-	-	-	36.35	0
M	-	-	-	-	-	-	-	-	-	-	-	-	-	0
N	-	-	-	-	-	-	-	-	-	-	-	-	-	-

A.3 Experiment 3

Table A.23: Approximation of the objective function values for a good solution of Experiment 3.1.

f_1 (ktonnes)	5 257
f_2 (ktonnes·km)	21 440

Table A.24: Approximation of the decision variable values for a good solution of Experiment 3.1.

	Stockpile days			ktonnes		
Power station	L_s	T_s	U_s	L_s	T_s	U_s
A	7	9	15	324.1	416.7	694.4
B	10	12	13	545.4	654.2	709.1
C	7	10	15	251.4	359.2	538.1
D	9	10	15	176.5	196.1	294.1
E	9	12	19	375.9	501.3	793.6
F	8	11	14	119.7	164.6	209.5
G	7	12	13	104.8	179.6	194.6
H	6	13	20	286.5	620.9	955.2
I	5	11	16	238.4	524.6	763.0
J	6	13	18	218.8	474.0	656.3
K	9	18	24	135.6	271.2	361.6
L	7	12	20	164.3	281.6	469.4
M	5	12	15	46.9	112.6	140.7
N	5	12	17	59.9	143.7	203.6

Table A.25: Coal transfers recorded for a good solution of Experiment 3.1 (ktonnes).

	A	B	C	D	E	F	G	H	I	J	K	L	M	N
A	-	0	0	0	0	0	0	0	0	0	0	0	0	0
B	-	-	0	0	0	0	0	0	0	0	0	0	0	0
C	-	-	-	62.45	0	0	0	0	0	0	0	0	186.5	0
D	-	-	-	-	0	0	0	0	0	0	0	0	11.10	0
E	-	-	-	-	-	0	0	0	29.66	0	0	0	0	0
F	-	-	-	-	-	-	264.3	0	0	0	0	0	0	0
G	-	-	-	-	-	-	-	0	0	0	0	0	0	0
H	-	-	-	-	-	-	-	-	0	0	0	0	0	0
I	-	-	-	-	-	-	-	-	-	0	0	0	0	0
J	-	-	-	-	-	-	-	-	-	-	10.0	0	0	0
K	-	-	-	-	-	-	-	-	-	-	-	0	0	0
L	-	-	-	-	-	-	-	-	-	-	-	-	0	110.4
M	-	-	-	-	-	-	-	-	-	-	-	-	-	0
N	-	-	-	-	-	-	-	-	-	-	-	-	-	-

Table A.26: Approximation of the objective function values for a good solution of Experiment 3.2.

f_1 (ktonnes)	5 858
f_2 (ktonnes·km)	21 809

Table A.27: Approximation of the decision variable values for a good solution of Experiment 3.2.

	Stockpile days			ktonnes		
Power station	L_s	T_s	U_s	L_s	T_s	U_s
A	8	10	17	370.4	463.0	787.0
B	8	11	15	436.3	600.0	818.2
C	5	14	21	179.6	502.9	754.3
D	5	14	20	98.0	274.5	392.1
E	9	16	23	375.9	668.3	960.7
F	10	19	25	149.7	284.4	374.2
G	6	7	11	89.8	104.8	164.6
H	6	9	16	286.5	429.8	764.1
I	11	17	28	524.6	810.7	1 335.3
J	6	9	18	218.8	328.1	656.3
K	9	20	27	135.6	301.3	406.8
L	7	16	29	164.3	375.5	680.6
M	10	20	26	93.8	187.6	243.9
N	5	11	24	59.9	131.7	287.4

Table A.28: Coal transfers recorded for a good solution of Experiment 3.2 (ktonnes).

	A	B	C	D	E	F	G	H	I	J	K	L	M	N
A	-	0	0	0	0	0	0	6.83	0	0	0	0	0	0
B	-	-	0	0	0	0	0	0	0	0	0	0	0	0
C	-	-	-	30.0	0	0	0	0	0	0	0	0	315.0	0
D	-	-	-	-	0	0	0	0	0	0	0	0	3.88	0
E	-	-	-	-	-	0	0	0	60.0	0	0	0	0	0
F	-	-	-	-	-	-	90.43	0	0	0	0	0	0	0
G	-	-	-	-	-	-	-	0	0	0	0	0	0	0
H	-	-	-	-	-	-	-	-	0	0	0	0	0	0
I	-	-	-	-	-	-	-	-	-	0	0	0	0	0
J	-	-	-	-	-	-	-	-	-	-	0	0	0	0
K	-	-	-	-	-	-	-	-	-	-	-	0	0	0
L	-	-	-	-	-	-	-	-	-	-	-	-	0	0
M	-	-	-	-	-	-	-	-	-	-	-	-	-	0
N	-	-	-	-	-	-	-	-	-	-	-	-	-	-